2D Model Parameterization of Porcupine River Training Structures:

Hydrodynamic and Morphological Impact Assessment

Meghan Irving

2D Model Parameterization of Porcupine River Training Structures:

Hydrodynamic and Morphological Impact Assessment

by

Meghan Irving

in partial fulfillment of the requirements for the degree of

Master of Science in Civil Engineering

at Delft University of Technology,
to be defended publicly on Monday November 30, 2020 at 13:00.

Committee members:	Dr. ir. A. Blom,	TU Delft
	Dr. ir. C. Sloff,	TU Delft & Deltares
	Dr. J. Bricker, PE	TU Delft
	Dr. F. Schuurman	Royal HaskoningDHV

An electronic version of this thesis is available at `http://repository.tudelft.nl/`.

Cover: Porcupine Field in Ayeyarwady River, Myanmar. Courtesy of H. Fredrikze, Royal HaskoningDHV.

Deltares TU Delft Delft University of Technology

Abstract

Flexible river training structures such as tetrahedron frames ('porcupines') can be attractive for control of braided river channel networks in regions where permanent control structures (e.g. groynes or dams) are too expensive or potentially inefficient, such as systems with highly dynamic flow regimes and morphology. Porcupines provide hydraulic resistance, generating energy loss and reducing velocities that may further encourage sediment deposition. Porcupine systems have seen increasing implementation, especially for bed or bank protection, but were also recently implemented in a channel-control pilot project on the Ayeyarwady River in Myanmar. Many porcupine systems to date are designed by trial and error due to lack of quantitative design criteria. The 2019 pilot project used large-scale numerical modelling of resistance areas to evaluate the potential impacts of porcupine structures; however, how to best incorporate the impacts of porcupine structures on flow and sediment transport in numerical models has not been systematically evaluated. Improved models or better estimates of uncertainties could facilitate future porcupine system design. Therefore, this study examines methods for incorporating porcupine fields into numerical models and interpreting those models to make informed design choices. Data and observations from the 2019 pilot project implementation, a 2018 porcupine flume experiment, and extensive literature review have been used to examine the expected hydrodynamic and morphodynamic impacts of porcupine systems that need to be accurately captured in large-scale numerical models. A 2DV model using two resistance formulations representing porcupines was elaborated and tested against experimental porcupine performance. The Uittenbogaard (2003) rigid cylinder model was found to replicate well porcupine behavior for less dense systems under limited flow conditions; however further verification is needed for more dense systems, variable flow regimes, wider boundary conditions and mobile beds. The 2DV model was collapsed to 1DH, using two different resistance formulations, to examine the strengths and weaknesses of large-scale models in predicting porcupine performance. The Baptist (2005) resistance model was found to best represent porcupines; however, parameterization was not straightforward from porcupine geometry, indicating that further studies will be needed to confidently translate porcupines into 'rigid cylinders' for input into the model. In addition, neither the 2DV nor 1DH models were able to capture the hydrodynamics at the leading and trailing edges of porcupine fields, which were found to be critical for design considerations from the pilot study data. Therefore, these important limitations need to be taken into account when interpreting model results and examining how to improve them in the future.

Summary

Flexible river training structures such as tetrahedron frames ('porcupines') can be attractive for control of braided river channel networks in regions where permanent control structures (e.g. groynes or dams) are too expensive or potentially inefficient, such as systems with highly dynamic flow regimes and morphology. Porcupines provide hydraulic resistance, generating energy loss and reducing velocities that may further encourage sediment deposition. Porcupine systems have seen increasing implementation, especially for bed or bank protection, but were also recently implemented in a channel-control pilot project on the Ayeyarwady River in Myanmar. Many porcupine systems to date are designed by trial and error due to a lack of quantitative design criteria. The 2019 pilot project used large-scale numerical modelling of resistance areas to evaluate the potential impacts of porcupine structures; however, how to best incorporate the impacts of porcupine structures on flow and sediment transport in numerical models has not been systematically evaluated. Improved models or better estimates of uncertainties could facilitate future porcupine system design. Therefore, this study examines methods for incorporating porcupine fields into numerical models and interpreting those models to make informed design choices. Data and observations from the 2019 pilot project implementation, a 2018 porcupine flume experiment, and extensive literature review have been used to examine the expected hydrodynamic and morphodynamic impacts of porcupine systems that need to be accurately captured in large-scale numerical models.

First, the physics of porcupines was examined. The existing literature on porcupines is sparse, particularly for detailed measurements of the flow field. Therefore, porcupines were hypothesized to be a special kind of vegetation, and use was made of an analogy between how resistance elements like vegetation (often represented as rigid cylinder) impacts hydrodynamics and morphology and how that response might differ for porcupines. The most important finding is that the velocity profile and turbulence characteristics can be very different for 'sparse' or 'dense' resistance fields, where dense fields generally reduce velocities and shear stresses inducing sedimentation; and sparse fields may experience erosion. In addition, the leading, trailing and lateral edges of a field or patch can have a different response than the center (fully-developed) flow area, where increased shear stresses are generally observed at the edges, before velocities can be reduced. Therefore the density and location of the field or patch is critical in estimating its influence on the flow field and in turn velocities and shear stresses near the bed, which dictate morphological responses.

The Ayeyarwady River pilot study was analyzed for the short-term local morphological response of the porcupine fields over their first wet season. While a lack of site data makes it difficult to distinguish between what changes were induced by porcupines versus local morphological influences, several observations could be hypothesized. It was observed that the design porcupines likely exhibit transitional or sparse behavior of the flow field, where significant scour at the leading and lateral edges was not evident; however porcupines located in high-energy areas did show significant scour and sinking, where the porcupines were not able to reduce flow velocities sufficiently. In addition, it seems likely that transverse resistance gradients have helped to push the flow in Sagaing and Middle channels towards the outer bend. This analysis demonstrated that understanding the behavior of porcupines at the field edges, the range of hydrodynamic conditions the porcupines might experience, and in particular the burial of porcupines over time through scour or deposition are critical aspects that need to be understood and captured in short- and long-term numerical models of porcupine systems.

Next, a 2DV and 1DH model were created to examine how porcupine resistance can be incorporated into numerical models. The best frameworks were found to be those developed for modelling resistance as rigid cylinders (often used for modelling vegetation). Limited experiment data was available for calibration. Therefore, these preliminary results can be used to guide future research, but we cannot draw definitive conclusions. In 2DV the Uittenbogaard rigid cylinder model represented a less-dense porcupine field reasonably well. Further studies will be required if the model can work for more-dense porcupine systems and for a wider range of hydrodynamic conditions. The 2DV model was collapsed to 1DH to gain an understanding of the strengths and weaknesses of large-scale models in predicting porcupine performance. The 1DH model was able to predict reasonably well changes in water level and the general trends in shear stress development; however parameterization of porcupines into rigid cylinders for input into the model was not straightforward.

The results of this research indicate that numerical modeling of long-term performance of porcupine sys-

tems will require some special considerations. The models must take into account burial of porcupines, either through scour or deposition. In addition, parameterization of porcupines needs careful consideration. Finally, the models developed in this thesis were not able to capture the details of the flow response to the porcupine fields in transition areas. Therefore, caution needs to be taken when interpreting model results for potential local morphological responses. Further studies are needed to examine the validity of these models in representing porcupines over a wider range of design and flow conditions.

Contents

List of Symbols

Symbol	Definition	Unit
a	frontal area	m^2
A	frontal cross-sectional resistance area	m^2
A_p	horizontal cross-sectional plant area	m^2
b	porcupine beam width	m
B	1. river width	m
	2. flume width	m
B_k	buoyancy turbulence production term	m^2/s^3
B_ϵ	buoyancy turbulence production term	m^2/s^3
c_D	constant	-
c_f	friction factor	-
c_{loss}	energy loss coefficient	-
$c_{loss\ up}$	energy loss coefficient of upper plate	-
$c_{loss\ down}$	energy loss coefficient of lower plate	-
$c_{2\epsilon}$	constant	-
c_μ	constant	-
C	Chéezy coefficient	$m^{1/2}/s$
C_b	Chézy bed coefficient	$m^{1/2}/s$
$C_{b,porc}$	Chézy bed coefficient in area of porcupine field	$m^{1/2}/s$
C_d	drag coefficient	-
C_l	length scale conversion coefficient	-
C_r	representative Chézy coefficient	$m^{1/2}/s$
D	element (cylinder) diameter	m
d	river depth	m
d_{50}	average grain diameter	m
D	1. diameter	m
	2. characteristic element length scale	m
f	Darcy–Weisbach friction factor	-
F	drag force	N/m^2
Fr	Froude number	-
g	gravity	m/s^2
h_0	roughness element height	m
h_{bw}	height of backwater curve	m
h_v	roughness element height	m
H	head elevation	m
i	water slope	-

Symbol	Definition	Unit
i_b	bed slope	-
k	1. vegetation height	m
	2. turbulent kinetic energy	m^2/s^2
k_{max}	number of vertical layers	-
k_s	Nikurades roughness length	m
$< \bar{k} >$	time and spatially-averaged turbulent kinetic energy	m^2/s^2
k_b	bare-bed turbulent kinetic energy (same forcing without resistance elements)	m^2/s^2
l	characteristic length	m
ℓ	turbulence length scale	m
L	1. eddy length scale	m
	2. porcupine field length	m
	2. Lengths scale	m
L_f	flume length	m
L_p	porcupine beam length	m
n	1. canopy porosity	-
	2. Manning's n	$s/m^{1/3}$
	3. vegetation density	-
	4. number of stems per unit area	m^-2
	5. number of elements	-
m	number of stems per square meter	-
M_ζ	source or sink of momentum in the ζ-direction	m/s^2
P_k	turbulence shear production term	m^2/s^3
P_ϵ	dissipation production term	m^2/s^4
Q	discharge	m^3/s
R	hydraulic radius	m
Re	Reynolds number	-
Rou_*	Rousse number	-
s	effective porcupine height	m
S_n	average distance to the nearest neighboring cylinder element	m
t_η	time scale for vertical bed movement	s
T	vegetation turbulence source term	m^2/s^3
T_τ	vegetation dissipation source term	m^2/s^4
u	velocity	m/s
u_0	upstream velocity	m/s
u_b	bare-bed velocity (velocity for same forcing without resistance elements)	m/s
$\vec{u}_b$	horizontal bed velocity	m/s
u_c	velocity in the canopy	m/s
u_m	velocity averaged up to measurement height	m/s

Symbol	Definition	Unit
u_p	velocity averaged up to porcupine height	m/s
u_u	overflow velocity	m/s
u_*	shear velocity	m/s
$\bar{u}$	experiment velocity (Q/hB)	m/s
$< \bar{u} >$	time and spatially-averaged velocity	m/s
u'	u velocity fluctuations	m/s
U	depth-averaged velocity in η-direction	m/s
$\vec{v}\,\vert$	magnitude of depth-averaged horizontal velocity vector	m/s
x_{fi}	flume element value	-
x_{mi}	model element prediction	-
x, y, z	cartesian co-ordinates	m
z	elevation	m
z_0	bed roughness length	m
δ	thickness of the viscous sub-layer	m
δ_e	penetration depth of canopy-scale turbulence into the canopy	m
δz_b	thickness of bed layer	m
ΔE	change in energy	m
ΔS	average spacing between cylindrical elements	m
ΔS_x	longitudinal spacing from center to center of porcupine elements	m
ΔS_y	cross-sectional spacing from center to center of porcupine elements	m
Δx	cell width in x-direction	m
ϵ	dissipation	m^2/s^3
ϵ_ϵ	dissipation term	m^2/s^3
η	water level	m
η_0	upstream water level	m
κ	Von K*árm*án constant	-
λ	non-dimensional roughness density	-
μ	dynamic viscosity	N/m^2s
ν	kinematic viscosity	m^2/s
$\nu_{background}$	background horizontal kinematic viscosity	m^2/s
ν_h	horizontal eddy viscosity	m^2/s
ν_m	molecular kinematic viscosity	m^2/s
$\nu_{molecular}$	molecular kinematic viscosity	m^2/s
ν_t	turbulent eddy viscosity	m^2/s
ν_{total}	total turbulent eddy viscosity	m^2/s
ϕ	solid volume fraction	-
ρ_w	water density	kg/m^3
ρ_s	sediment density	kg/m^3

Symbol	Definition	Unit
σ_k	closure coefficient	-
σ_ϵ	closure coefficient	-
τ	1. shear stress	N/m^2
	2. dissipation time scale	s
τ_b	bed shear stress	N/m^2
$\tau_b 0$	upstream bed shear stress	N/m^2
$\vec{\tau}_{b_{3D}}$	bed shear stress 3D computation	N/m^2
τ_{free}	dissipation time scale of free turbulence	s
τ_t	total shear stress	N/m^2
τ_v	shear stress contributed to resistance elements	N/m^2
τ_{veg}	dissipation time scale of eddies between stems	s
$\tau_x y$	Reynolds stress s	N/m^2
ζ_u	upstream water level	m
ζ_d	downstream water level	m

Chapter 1

Introduction

1.1 Overview

Flexible river training structures such as tetrahedron frames ('porcupines') can be attractive for control of braided river channel networks in regions where permanent control structures (e.g. groynes or dams) are too expensive or potentially inefficient, such as systems with highly dynamic flow regimes and morphology. Porcupines provide hydraulic resistance, generating energy loss and reducing velocities that may further encourage sediment deposition. Porcupine systems have seen increasing implementation, especially for bed or bank protection, but were also recently implemented in a channel-control pilot project on the Ayeyarwady River in Myanmar. Many porcupine systems to date are designed by trial and error due to a lack of quantitative design criteria. The 2019 pilot project used large-scale numerical modelling of resistance areas to evaluate the potential impacts of porcupine structures; however, how to best incorporate the impacts of porcupine structures on flow and sediment transport in numerical models has not been systematically evaluated. Improved models or better estimates of model uncertainties could facilitate future porcupine system design. Therefore, this thesis examines methods for incorporating porcupine fields into 2D numerical models and interpreting those models to make informed design choices.

This thesis is organized into six chapters. First, the basic concepts related to porcupines, the porcupine pilot study in Myanmar, flow through resistance elements and numerical modelling of resistance is introduced with their data gaps, along with the research questions and methodology driving this thesis. Next, Chapter 2 is dedicated to developing a conceptual model of the hydrodynamic impacts of porcupine fields. Chapter 3 presents expected impacts of porcupines on local morphology. Then Chapter 4 discusses the 2019 pilot study and analyzes how porcupines have influenced the local morphology over the first 10 months of implementation (one wet season). Incorporating hydrodynamic impacts of porcupines into 2D numerical models is the focus of Chapter 5, where several models are developed and calibrated against flume data to gain insights into the strengths and weaknesses of (simplified) numerical models used to evaluate configuration designs and long-term morphological impacts. Chapter 5 combines the insights gained from the literature review, modelling analysis and pilot study analysis to present recommendations for the design of porcupine systems, numerical modelling of porcupine system performance and the design of future experimental setups. Finally, the last chapter presents conclusions and outlines data gaps needing to be addressed to further our ability to design and implement porcupine systems for braided river channel control.

This introduction is organised as follows. First, an overview is given of the Ayeyarwady River in Myanmar with a focus on the site location of the pilot project implementation. Next, a summary of the history and current research on porcupine structures is elaborated. Then an overview of modeling resistance elements is discussed. The data gaps presented in these sections drive the primary and secondary research questions of the thesis, which are presented at the end of the chapter.

1.2 Background and Motivation

Controlling erosion in river systems can be accomplished with a variety of river training works. Certain structures, such as weirs or groynes, are designed with a longer life-span in mind and are generally more expensive. Their effectiveness in highly dynamic braided river systems, such as the Ayeyarwady River, is questioned due to the large-scale and dynamic nature of the system. In addition, the costs are likely prohibitive [40], [16]. In these locations, permeable control works such as bandal structures, pile dikes, jack-jetties or porcupines are considered attractive alternatives due to the low-cost and flexible implementation [1], [56], [2]. While this research could be applicable to other forms of permeable control structures, the evaluation will only consider porcupine structures since they are the focus of the pilot study. The following sections will elaborate on the current research around the hydrodynamic and morphological impacts of porcupines and their applications to river training, as well as introduce the pilot project carried out in Myanmar- the motivation for this research.

1.2.1 Porcupine Structures

Porcupines are tetrahedron open-pyramid structures (see Figure 1.1a). Porcupines are made out of wood or reinforced concrete beams 2 to 4 meters (m) in length held together with bolts or wire cables. Wooden porcupines are generally weighed down with rocks [10]. Beams can be round or square. 'Porcupine' and 'tetrahedron frame' will be used interchangeably, although for tetrahedron frames the member beams may come together without the ends of the beams sticking out (compare Figure 1.1a with Figure 2.3 which show a porcupine and a tetrahedron frame respectively).

(a) (b)

Figure 1.1: (a) Individual porcupine structure and (b) field or porcupines (Taken from [28])

Porcupines are typically implemented grouped in a field or in rows along the area to be protected (see Figure 1.1b). In designing porcupine systems, both the individual porcupine elements (e.g. slenderness, size, beam shape) and the field configurations (e.g. density, staggering) can be adjusted. When placed in or along a river bed, the structures increase the resistance to the flow. This leads to reduced local flow velocities and increased energy dissipation due to turbulence, which can reduce boundary shear stress and encourage sediment deposition. For this reason porcupines have been implemented along reaches of the Brahmaputra River in India [1], in Bangladesh and in China to protect bridge piers from scour [61], or to protect the toe of dams ("root stones") [58]. However, porcupine fields can also be placed in multi-channel systems for the purpose of channel configuration control. In addition to encouraging sediment deposition, the increased resistance can create a backwater curve that raises the water level upstream of the porcupine field compared to normal flow conditions. In this way porcupine fields placed in channels downstream of bifurcations can be used to control discharge distributions through the bifurcation and maintain channel configurations in a braided river. This is the goal of the 2019 pilot project implementation in the Ayeyarwady River.

1.2.2 Pilot Project Ayeyarwady River, Myanmar

Ayeyarwady River Basin Description

The Ayeyarwady (Irrawaddy) River is the largest in Myanmar and 70% of the population lives within its basin. The river is vitally important for freshwater resources, biodiversity, navigation and the local economy. Much of Myanmar's water, energy and food security can be linked to the well-functioning of the Ayeyarwady river basin. The Ayeyarwady, in this area, is a highly dynamic braided river that experiences hydrological variations up to a factor of 10 difference between low and peak discharge (up to 12 m difference between low and peak flow water levels) and has an abundance of fine but non-cohesive sediment (the 5th highest sediment load of any major world rivers) [76]. The variable water levels and velocities combined with large sediment loads lead to rapidly shifting river planforms including channel, bank, island and thalweg migration, as well as significant local changes to bed slope. As a result, navigation pathways can be hard to predict from year to year and the abundant populations living near the river for transportation, agricultural and other benefits are at severe risk for flooding. Every year many villages are destroyed and up to several million Myanmar citizens are affected by flooding [30].

Much of the future opportunities for growth in Myanmar can be directly linked to water. In this context, the World Bank approved 100 million (USD) in funding to improve water usage, river transport, and disaster risk management in the river basin in 2014. Multiple projects have been spurred by this initiative, implemented between 2017 and 2020. The projects aim to improve lives of the population living along the river in the context of an integrated Ayeyawardy River Basin Management Initiative [76], [17]. One project explores river training (control structures) to improve the reliability of navigational channels next for the city of Mandalay, including a pilot project implemented in 2019 using porcupines for secondary-channel control, as described below.

Pilot Project Implementation

The pilot project was implemented in a section of the Ayeyarwady River next to the city of Mandalay in Myanmar (the 'Site'), as shown in Figure 4.1. In this location the river consists of five distinct channels separated by islands - a primary channel to the east (the Mandalay Channel), and four secondary channels located in the center and western edge of the braid plain. At the Site the river is geologically bounded to the west by a mountain ridge and a bedrock outcrop, and the city of Mandalay is developed along the eastern bank [30].

In 2019 a pilot project was implemented in this section of the Ayeyarwady River with the primary objective of maintaining a least available depth (LAD) of 2 meters (m) for a 1,000 deadweight tonnage (DWT) vessel in this section of the river. The project should improve access to the Port of Mandalay, deepen and stabilize the main (Mandalay) channel and reduce the risk that navigation is hindered by one of the secondary channels taking over as the primary channel, which naturally occurs approximately every 10 to 30 years [30]. To achieve this, porcupine structures were placed in two secondary channels to increase local resistance. This helps to maintain the current discharge distributions, ensuring that the Mandalay channel remains the primary channel. In addition, the porcupines should encourage sediment deposition in the secondary channels, further discouraging a primary channel shift. Porcupine field placement options were initially evaluated with a hydrodynamic numerical model and further refined after discussions with stakeholders. The porcupines were constructed and implemented during the dry season in 2019 and have currently experienced one flood season. Therefore a preliminary evaluation can be made of the actual versus predicted porcupine performance.

1.3 Summary of Current Research

Existing data and literature on porcupine fields is sparse; however many studies have been performed for vegetation, often represented as rigid cylinders, which conceptually should behave similar to porcupine structures, as described in Chapter 2. Therefore, this thesis uses patterns observed in vegetation studies to estimate the behavior of porcupine fields.

Goa et al. in [21] developed a 3D hydrodynamic model to examine the flow field around an individual porcupine structure. For a submerged porcupine, the flow is generally pushed up above the porcupine, and it is pushed down again immediately downstream of the porcupine. This phenomenon was confirmed with experimental flume measurements [46, 34]. Flume studies have examined the impact of single porcupines on flow fields [34] and show that flow velocities downstream of the element were reduced. Several flume studies have examined the impact of a field of porcupines hydrodynamics and morphodynamics [1,

Figure 1.2: Ayeyarwardy River near Mandalay. Red Box indicates approximate location of the pilot project implementation. Landsat aerial imagery from 11/03/2020 (apps.sentinel-hub.com)

46, 82]. These studies found that flow velocities were reduced within the porcupine field and for a certain distance downstream of the field (the flow retardation zone). Morphodynamic effects were more variable from different experiments. Certain conditions, such as high flow velocities, emergent porcupines and low field density encouraged scour within the field. However, the opposite conditions encouraged sediment deposition. The majority of studies have evaluated the performance of porcupine configurations by finding configurations that give the maximum reduction in flow velocities or maximum sediment deposition. Neither modelling nor flume experiments have not been carried out to systematically evaluate the use of porcupines in controlling channel configurations in a multi-channel system.

1.4 Modelling of Porcupine Fields

Models of the impacts of porcupine fields can be physical or numerical. Numerical models can be further divided into detailed 3D models able to capture all of the nuances of the 3D flow structure, and large-scale 2D models able to capture the larger details of porcupines influence on hydro- and morphodynamics.

Flow through an individual porcupine or porcupine field is 3D and highly dynamic. While many aspects of porcupine physics at this level are not completely understood, there is a lack of experimental data to justify implementation of a complex 3D model. In addition, modelling the impact of porcupines in a large river system, such as the Ayeyarwady River, for design purposes is infeasible at this scale. Experimental studies have been eliminated from consideration due to time constraints. Therefore, this thesis focuses on improving our understanding of 2D numerical modelling of porcupine fields, rather than 3D modelling of individual porcupine structures. The measurements taken from the 2018 Nientker ([46])

flume experiment will be used for validation of model results.

Porcupine structures impact the hydrodynamics of flow by altering the flow resistance. This can be taken into account in a numerical model in several ways. First, a very simplified approach would be to change the bed roughness parameter (e.g. Chezy, Manning's n or White-Colebrook) to take into account increased bed roughness; however, more sophisticated methods are available. In Delft3D, three additional options are considered, including two resistance models that mimic vegetation as rigid cylinders at the sub-grid level: Baptist (2005) and Uittenbogaard (2003). Cylinders can be applied in multiple layers, to take into account density differences in vegetation (or porcupines) that extend to different heights above the bed. In these formulations the roughness impacting flow resistance and the roughness impacting sediment transport need to be separated since increased roughness will lead to flow resistance; however it can also lead to increased sediment transport which is not necessarily the case. Delft3D also has an option to model permeable structures that induce energy losses. All of these options are explored in Chapter 5.

1.5 Objectives and Research Questions

The research objectives of this thesis are motivated by the data gaps presented above and explore three main categories: understanding of porcupine physics, morphological impacts and the important data gaps, incorporating impacts of porcupines into 2D numerical models and understanding the limitations of those models; and evaluating potential porcupine performance from analysis of pilot study data and through simplified modelling. The primary research question is:

How can the hydrodynamic impacts of porcupine structures be incorporated into and evaluated with numerical models?

A number of secondary research questions (RQs) can be evaluated to answer the primary question:

RQ1: What do we know, and not know, about porcupines' hydrodynamic impacts? (Chapter 2)

RQ2: What do we know, and not know, about porcupines' morphological impacts? (Chapter 3)

RQ2: How can the subgrid impacts of porcupine fields be incorporated into 2DV and 1DH numerical models, and what are the model limitations? (Chapter 4)

RQ3: What can the 2019 pilot study tell us about (modelling) porcupine impacts? (Chapter 5)

RQ4: What recommendations can be given for designing, modelling and analyzing the performance of porcupine systems? (Chapter 6)

Chapter 2

Porcupine Field Hydrodynamics

This chapter discusses the impacts of porcupine structures on flow hydrodynamics including the velocity profile and turbulence generation. Understanding the detailed impacts to the velocity profile and turbulence properties are essential to understanding impacts to bed shear stress and flow properties near the bed, which dictate morphological responses that highly influence porcupine performance. The goal of this chapter is to clarify what is, and is not, understood about how porcupines influence hydrodynamics, and which of those impacts can, or cannot, be incorporated into large-scale (2D) numerical models. Our understanding of porcupine physics influences both the choice of numerical parameters and the potential limitations of the model output.

Three elements are considered: (1) flow around a single porcupine beam, (2) flow through an individual porcupine and (3) flow through a field of porcupines. For each element a theoretical discussion is followed by current evidence from laboratory experiments, where available. Studies of flow through porcupine fields are limited; therefore, this section focuses on an analogy of flow through vegetation, which are conceptually similar and have been the subject of considerably more investigations. The analysis of these three elements leads to a conceptual model for how porcupine fields influence hydrodynamics. Finally, implications for numerical modelling of porcupine fields is discussed.

Throughout the chapter 'vegetation field' and 'porcupine field' will be used when properties of each can be distinguished. 'Resistance field' will be used for discussion that could (theoretically) apply to both vegetation or porcupine fields. 'Field' refers to a configuration of uniform elements (equal height and equal spacing between elements), that is sufficiently wide and long so that the flow described can be considered both fully developed and two-dimensional. Boundary layer development over or along short or narrow fields (now called 'patches') is discussed at the end of the chapter.

2.1 Flow Field around a Porcupine

This sections describes the theoretical flow field development around an individual porcupine. We imagine a porcupine in the middle of a river channel, and neglect interference from the banks, wind or atmospheric forcing. The flow is sub-critical and fully turbulent. Upstream of the porcupine the flow is fully-developed with the boundary layer taking up the entire water depth and the velocity has a typical logarithmic profile. The ultimate question is, how do porcupines influence this logarithmic velocity profile with the associated impacts to turbulence, bed shear stress and sediment transport? First we will consider the impact of the flow by one single porcupine beam, and then by one individual porcupine element.

2.1.1 Individual Beam

The porcupine structure influences the flow in several ways. First, beams block the flow causing the streamlines to curve around them. The water will move around the vertical beams of the tetrahedron frame in a similar manner to how flow moves around a bridge pier column (see Figure 2.1).

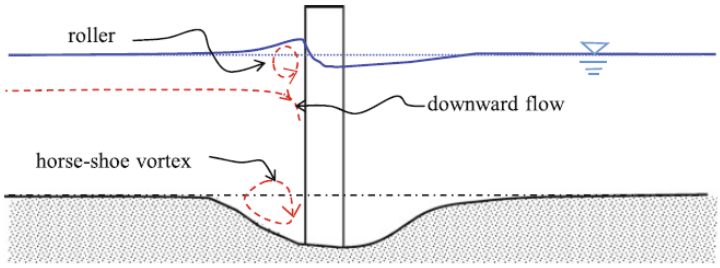

Figure 2.1: Flow around a circular bridge pier (taken from [3]).

Higher in the water column (not next to the bed), in front of the beam, the flow decelerates. The flow accelerates along the sides of the beams, and decelerates on the downstream-side of the beam as the flow separates from the beam and expands. This causes the water level to rise just upstream of the beam, lower at the sides of the beams, and rise again behind the beam. This change in velocity head leads to a negative pressure gradient that directs the vertical flow downward toward the bed and can induce scour. Behind the beam, as the flow separates, turbulence is greatly enhanced [3, 38, 55].

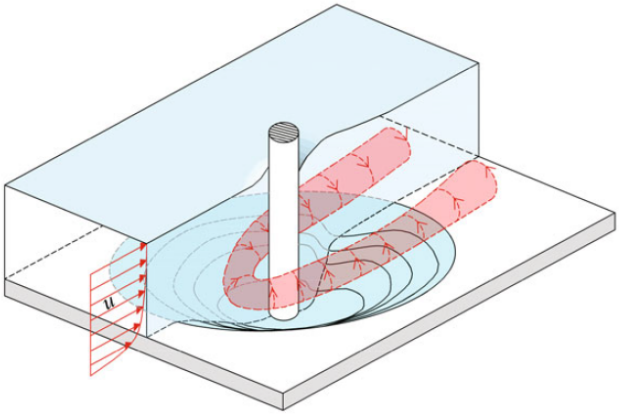

Figure 2.2: Horseshoe vortex around bridge pier column (taken from [3]).

The flow field around an individual beam is complex and highly three-dimensional. This 3D flow induces scour at the base and sides of the beam, generating a horseshoe vortex around the beam (Figure 2.2) and enhances turbulence in the wake of the structure leading to energy dissipation and velocity reductions. For a porcupine structure, scour around the base of the beam can cause the structure to sink into the bed, reducing its projection in the water column and its ability to generate turbulence and reduce velocities. Understanding potential scour will be shown to be an important factor for porcupine design.

While many parameters influence potential scour around a bridge pier, the diameter of the pier, and grain size are important factors, where the scour depth generally decreases for decreasing diameter and decreases when grain sizes are relatively coarse or relatively fine [3, 37]. Therefore the local conditions and porcupine beam design can be expected to influence potential scour.

The figure above described flow around a vertical, cylindrical beam; however, porcupine beams are both angled, and (often) square, and have additional horizontal beams. Square bridge piers will produce larger scour holes than circular bridge piers for the same forcing [3]. Compared to a vertical cylinder, upstream-inclined cylinders can increase the scour depth due to enhanced down-flow in front of the cylinder, where downstream-inclined cylinders can have reduced scour depths due to diminished down-flow [73]. Porcupines consist of multiple beams in close proximity that will result in a complex interactions of wakes that may enhance or lessen scour. While the behavior of bridge piers with similar characteristics may give some hypotheses of porcupine scour behavior, understanding scour around an individual or group of porcupines will require targeted studies.

2.1.2 Individual Porcupine

As demonstrated above, the flow field around an individual beam is highly three-dimensional. For a single porcupine element, complex 3D flow interactions occur between the wakes and mixing layers generated by multiple beams in close proximity. Limited measurements of velocity or turbulence within a porcupine element have been made, therefore the exact flow patterns are not known; however Goa et al. in [21] developed a 3D hydrodynamic model to examine the flow field in and around an individual porcupine structure. They found that, for a submerged porcupine, the upstream flow is pushed up above the porcupine, and it is pushed down again immediately downstream of the porcupine, as shown in Figure 2.3a. This phenomenon was confirmed with experimental flume measurements [46, 34], as will be discussed below. The deceleration of the flow by the beams, leading to flow separation and increased turbulence along the downstream-side of the beam, was also confirmed in the 3D modelling study, shown in Figure 2.3b.

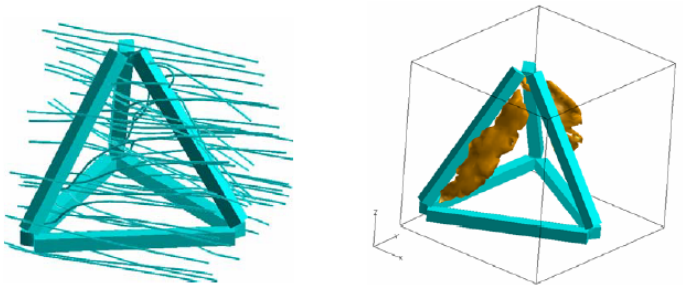

(a) (b)

Figure 2.3: (a) Flow field around an individual porcupine structure (note that flow is from left (two vertical beams) to right (vertex of tetrahedron frame), and (b) Area of maximum turbulence generation in flow around an individual porcupine structure (taken from [21]).

Several flume experiments have analyzed the hydrodynamic impact of a single porcupine structure. Lu et al. in [34] carried out a fixed-bed flume experiment for a single porcupine structure measuring velocity with an acoustic doppler velocimeter (ADV). Figure 2.4 shows the evolution of the velocity profile as the flow moves past the single tetrahedron frame. As the flow enters the frame, the flow through core of the frame accelerates while the flow above the frame remains largely unchanged (location B). Past the frame, a zone is observed with retarded velocities which gradually diminishes downstream (C to D). Further downstream still, the velocity has recovered to the equilibrium approach profile (location E). This study has found that the flow directly through the porcupine element accelerates, when flow

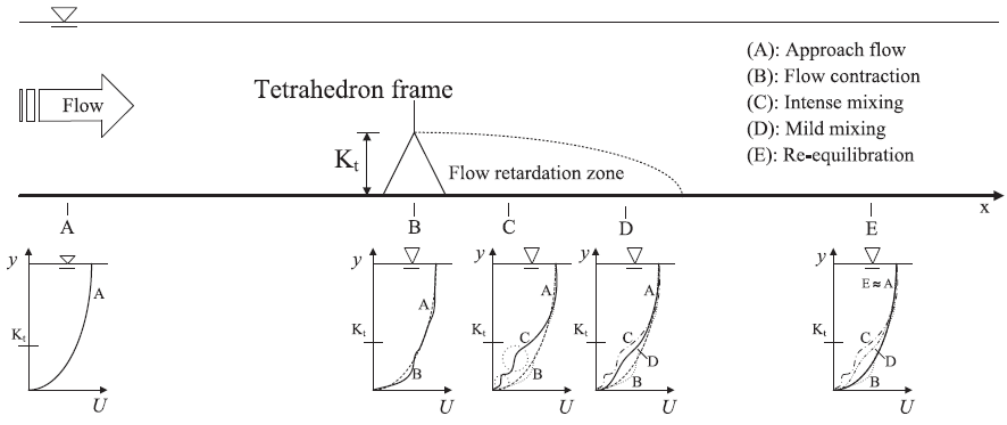

Figure 2.4: Flow field evolution through a tetrahedron frame (taken from [34]).

through porcupine fields is expected to decelerate and even flatten due to the energy dissipation by increased turbulence. This finding could partly be due to the exact placement or measurement device

used, and partly due to the fact that only one porcupine element was placed in the flow, as opposed to a field of porcupines. This is evidence that the first row or rows of porcupines may require special consideration when designing porcupine fields since they could be at additional risk for scour from increased bed shear stresses due to accelerating flow. In addition, this finding can imply that while porcupines on average might induce turbulence, energy loss and an overall reduction in velocities, local accelerations and turbulent fluctuations within individual porcupine elements can still be important and may influence local scour. Yang et al., in [81] examined the flow field around a single porcupine structure in a fixed-bed flume with a vertex facing upstream or downstream using particle image velocimetry (PIV) measurements. Porcupines placed in the flow with the vertex facing downstream were found to reduce the flow more strongly and had a longer retardation length downstream of the porcupine (see Figure 2.5); however the angle of the beams could partly explain this phenomenon. This orientation was also found to be more stable.

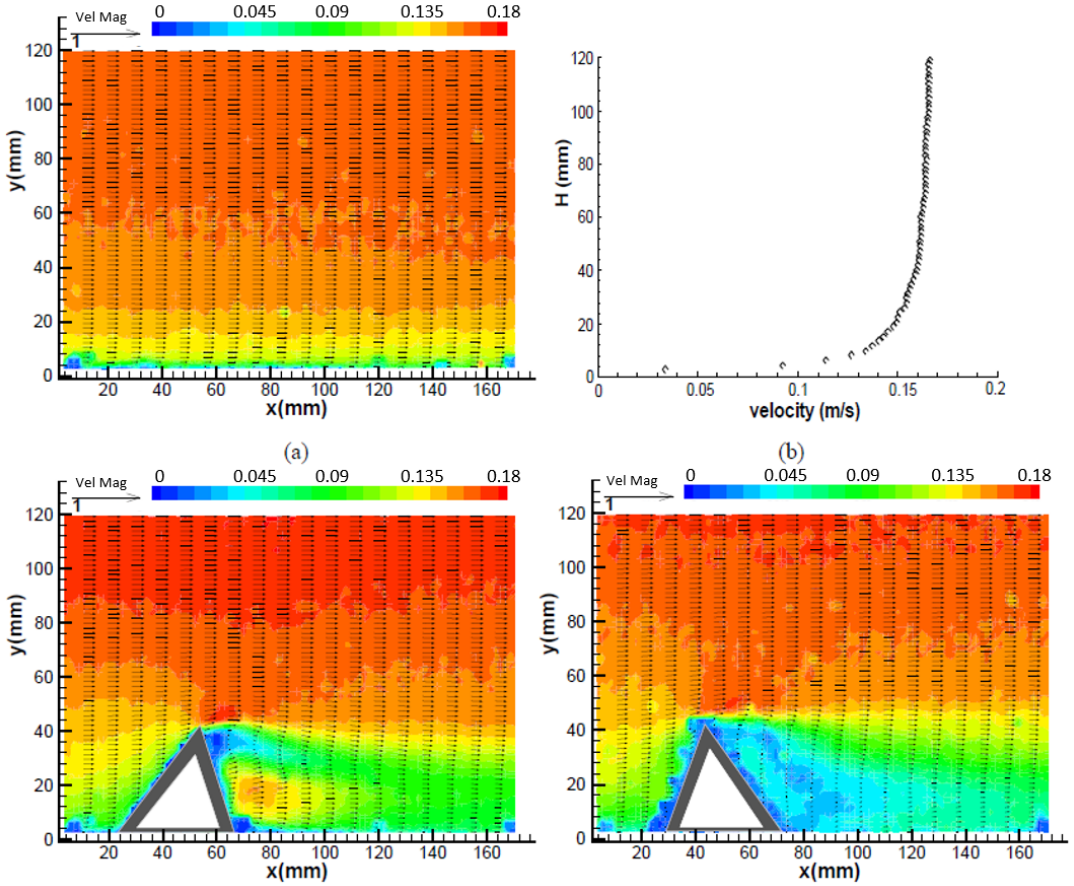

Figure 2.5: Time-averaged velocity vector diagram (Re=10,400) (a) no tetrahedron frame, (b) vertical velocity profile without tetrahedron frame (c) velocity field with tetrahedron frame vertex pointing upstream (d) velocity field with tetrahedron frame vertex pointing downstream. Vel mag = velocity magnitude (m/s). Reference vector is 1 m/s (taken from [81]).

2.2 Flow through a Porcupine Field

As demonstrated in the introduction, studies of flow patterns through porcupine fields are very limited; however, conceptually porcupine elements and vegetation are very similar since they both induce hydraulic resistance to the flow. In addition, analytical, conceptual and laboratory studies of vegetation often schematize vegetation as rigid cylinders [5, 43, 66, 67], which further fits with the analogy of porcupine beams acting as rigid cylinders in the flow. Therefore, we will discuss the flow field through

vegetation, and how it might differ for porcupines, before reviewing the current understanding of how fields of porcupines influence the flow based on existing laboratory flume studies.

2.2.1 Fully-Developed Flow through a Vegetation Field

Flow through vegetation will be discussed for two cases: emergent vegetation (water depth below the top of the vegetation) and submerged vegetation (water depth above the top of the vegetation). The turbulence and velocity profiles for these two cases can be quite different, which in turn can impact the bed shear stress [36]. The following sections consider fully-developed flow through vegetation fields, as opposed to boundary-layer development along field edges or through patches.

First, some definitions are introduced, as discussed in [45]. The geometry of resistance elements in flow (e.g. vegetation, porcupines) plays an important role in the resistance offered. A vegetation field represented by a set of uniform-height, uniformly-spaced rigid cylinders, is characterized by the size of individual elements (diameter [D] and frontal area per canopy volume [a, a = $D/\Delta S^2$, where ΔS is the average spacing between elements, see Figure 2.6]) and the height (h_v) of the vegetation canopy (individual cylinder).

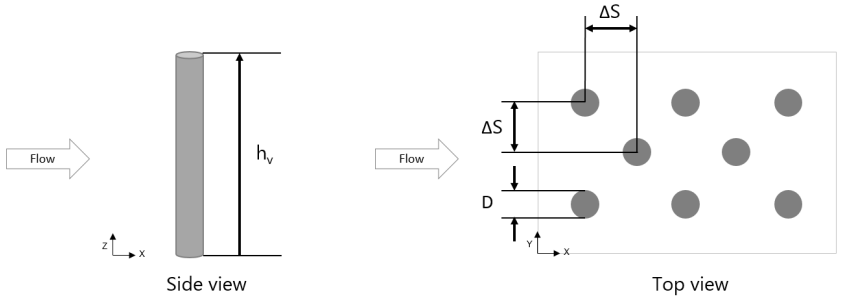

Figure 2.6: Visualization of parameters for a single cylinder from the side and for a uniform, staggered grid of cylinders from the top. Top view adapted from [66].

The non-dimensional roughness density (frontal area per bed area) can be defined as:

$$\lambda = \int_{z=0}^{h_v} a dz \tag{2.1}$$

This is equivalent to the terrestrial leaf area index (LAI). For vegetation represented by rigid cylinders Equation 2.1 becomes ah_v. This roughness density can be used to define the difference between sparse (ah_vC_d«0.1) and dense (ah_vC_d»0.1) beds, where C_d is the drag coefficient, often assumed to be one [45].

For a porcupine as designed for the pilot study (the horizontal beams are attached a distance of $L_p/3$ from the bottom of the vertical beam), with a length L_p, a width b, a longitudinal spacing ΔS_x, a cross-sectional spacing ΔS_y (see Figure 2.7), the total a (frontal area per canopy volume) can be calculated as:

$$a = \frac{6b + 3L_p}{\Delta S_x \Delta S_y} \tag{2.2}$$

For the design porcupines, this gives an a of 0.57 m$^-$1. And the porcupine roughness density (λ_p), taking into account the variation in a with height can be defined as:

$$\lambda_p = \int_{z=0}^{s} a dz = \frac{12bL_p}{\Delta S_x \Delta S_y} \tag{2.3}$$

Where s is the effective height of the porcupine ($s = L_p\sqrt{6}/3$), as the beams of length L_p are slanted when assembled. This gives the pilot study porcupines an "ah_vC_d" value of 0.21, assuming C_d=1, which places them in the transition between sparse and dense beds.

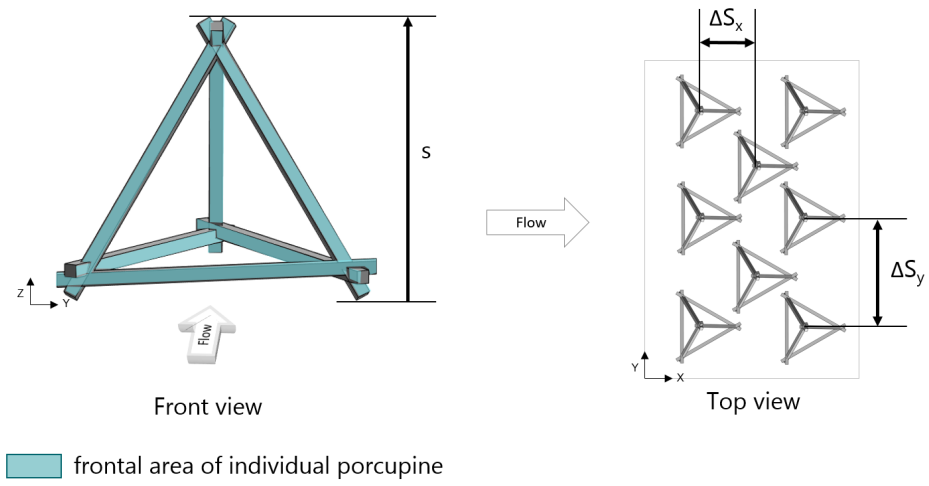

Figure 2.7: Visualization of parameters for a single porcupine from the front and for a uniform, staggered grid of porcupines from the top. Not to scale.

Figure 2.8 below shows a comparison of rigid cylinders and porcupines for varying λ. As we will see later, λ is an important parameter in estimating how the velocity profile and turbulence characteristics evolve through a resistance field and the implication for sediment transport (erosion or deposition) within the field.

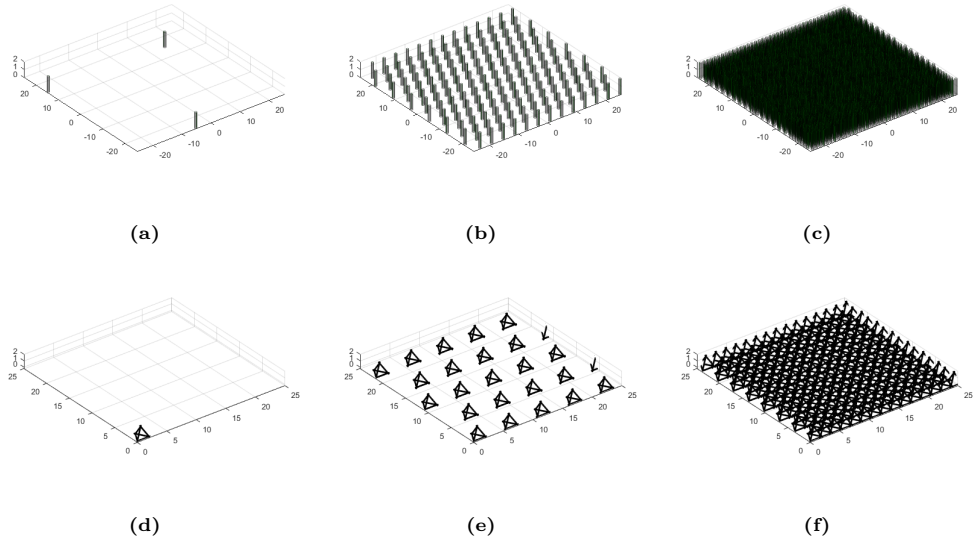

Figure 2.8: Fields with varying roughness density (λ), for rigid cylinders: (a) $\lambda = 0.001$; (b) $\lambda = 0.1$, (c) $\lambda = 1$; and for porcupines: (d) $\lambda_p = 0.001$; (e) $\lambda_p = 0.1$, (f) $\lambda_p = 1$. All axes show length in meters.

Emergent Vegetation

As flow passes through an emergent vegetation bed (water depth (h at or below the canopy height (h_v), the turbulent length scales associated with the flow will depend on the density described above. Turbulence length scales (ℓ) will be controlled by the smaller of the diameter of cylinder elements (d) or the spacing between elements (ΔS), as shown in Figure 2.9a. Larger-scale eddies in the approach flow will be dissipated and additional turbulence will be created at the smaller length scale. Even in very sparse beds, turbulence production within the vegetation field exceeds the turbulence produced by the no-slip condition at the bed for most of the water depth [45]. Therefore, the turbulence must be predicted

as a function of the vegetation-induced drag force as opposed to the friction velocity of the bed. For submerged canopies, as will be discussed later, turbulent length scales can be much larger but may not necessarily reach the bed. For emergent canopies, when the diameter of the stems is less than the stem

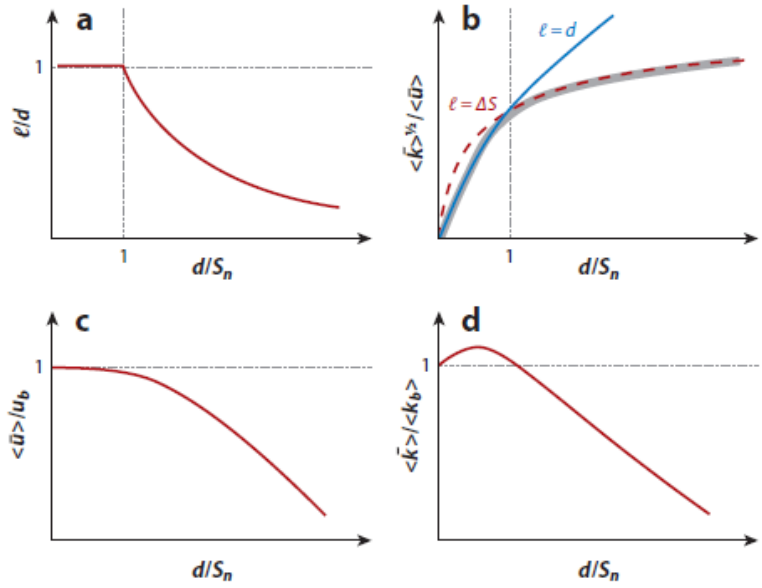

Figure 2.9: The density of a resistance element controls velocity and turbulence characteristics. (a) As density increases the integral turbulence length scale, ℓ, shifts from the stem diameter (d) to the spacing between stems (S_n). (b) the turbulence intensity increases with increasing stem density; however turbulence intensity increases more slowly once the spacing between stems gets smaller. The velocity decreases as canopy density increases (c) which leads to (d) turbulent kinetic energy increasing initially, then decreasing as the canopy density increases further. Subscript b indicates bare bed (normalizing parameter), assuming the same hydrodynamic forcing (taken from [43]).

spacing (as is the case for porcupines), the turbulence intensity increases rapidly for increased vegetation density (see Figure 2.9b). At the same time, the velocity through the bed decreases (Figure 2.9c). The turbulent kinetic energy (tke) is both negatively influenced by the reduced velocity and positively influenced by increasing density (more wakes produced behind more stems), resulting in a non-monotonic tke function which increases initially with increasing vegetation density, and then decreases (Figure 2.9d). This indicates that an emergent porcupine field that is too sparse could encourage erosion within the field rather than deposition. This has indeed been found to be the case for vegetation [33, 41, 78].

Submerged Vegetation

Now we will consider submerged vegetation (cylinders). The level of submergence will be defined as the ratio of the water depth (h) to vegetation height (h_v). The level of submergence controls the driving force for flow through the vegetation field. At high levels of submergence, the flow is driven by turbulent stresses at the top of the canopy, where momentum is transferred from the overflow to the flow within the canopy. As the level of submergence decreases, the pressure gradients and gravitational potential become more important. For emergent vegetation, the flow is entirely driven by potential gradients [43]. The ratio of these two driving forces can be approximated by Equation 2.4.

$$\frac{\text{turbulent stress}}{\text{pressure gradient}} \sim \frac{h}{h_v} - 1 \tag{2.4}$$

The three levels can be given as: deep submergence (h/h_v >10), shallow submergence (h/h_v <5) and emergent (h/h_v =1). For submerged vegetation, the vegetation density plays a key role in the behavior of the fully-developed flow field. For sparse beds (Figure 2.8a), the canopy drag is small compared

to the bed drag, whereas canopy drag dominates for dense beds (Figure 2.8c). Therefore sparse beds maintain a turbulent boundary layer velocity profile (see Figure 2.10c), whereas dense beds will generate a velocity profile with an inflection point near the top of the canopy, creating a shear flow between the overflow and the canopy flow (see Figure 2.10e). The transition from a sparse to a dense canopy and the associated velocity profiles and turbulence scales vary as a function of $C_d a h_v$ where C_d is the canopy drag coefficient. For vegetation, the drag coefficient is often assumed to be one [43, 6]. The transition from sparse to dense beds has been found to occurs at approximately ah_vC_d =0.1, for C_d =1, in studies of vegetation [43].

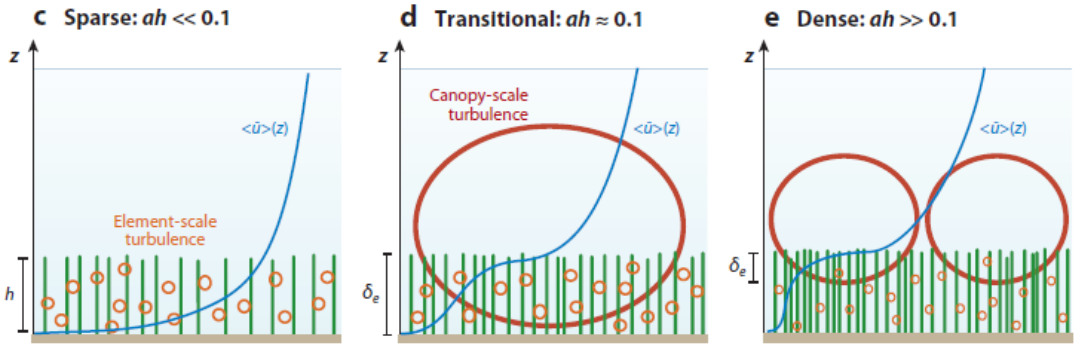

Figure 2.10: Longitudinal velocity profiles and turbulent length scales for sparse (c), transition (d) and dense (e) canopies (taken from [43]).

As ah_vC_d goes to 1, the canopy is cut off from the overflow, whereas for ah_vC_d <0.1, the velocity profile does not exhibit an inflection point and the turbulent stresses penetrate to the bed. If ah_vC_d is calculated for porcupine structures as designed for the 2018 pilot study in the Ayeyarwady river, assuming a drag coefficient of one, the porcupine field will be transitional (ah_vC_d = 0.21); however, the drag coefficient for porcupine fields have been found to vary between one and five for numerical and experimental studies with fixed beds [34, 46], and to be about one for an experimental study with a mobile bed [46] (this result is discussed further in Chapter 5).

The ah_vC_d factor for porcupines will evolve with time. Vegetation has roots, which help to stabilize the bed, and can grow when deposition occurs within a vegetation field. Porcupines, without roots, have no additional capacity to help stabilize the bed, and when they sink into the bed they will not get taller again. Therefore, over time the ah_vC_d factor for porcupines will reduce. Porcupines, particularly when buried past the horizontal bars, will significantly reduce their frontal area. In addition, as they become buried the effective spacing between porcupines will increase, increasing the turbulent length scale between individual porcupines and potentially allowing for higher shear stresses to penetrate to the bed.

The 'sparse' and 'dense' classifications defined above have been derived empirically for specific flow regimes and vegetation properties (rigid cylinders, fake and real vegetation). There is not sufficient data for porcupines to determine the equivalent value of ah_vC_d where the velocity profile transitions. In addition, local flow or morphology conditions may influence this transition point as they can influence the drag coefficient. Even though our current understanding indicates that porcupines are unlikely to be classified as 'dense', this cannot be excluded from future design options. Therefore, the potential implications of 'sparse' or 'dense' porcupine fields are discussed, based on knowledge of 'sparse' or 'dense' vegetation fields.

For submerged flow over dense vegetation fields, two turbulence length scales above the bed can be distinguished: 1) The canopy-scale turbulence related to Kelvin-Helmholtz instabilities induced by the free shear layer of the inflected velocity profile at the top of the canopy, and 2) boundary-layer turbulence that occupies the entire water depth above the canopy. For deeply submerged canopies, both turbulence scales are present. For shallow submergence only the canopy-scale turbulence is present. Due to the large size of porcupine structures, deep submergence is unlikely and shallow submergence can be considered the typical state. In both cases it is the canopy-scale turbulence that dominates the momentum transfer

from the overflow the the canopy flow [43]. For the canopy-scale turbulence , the vortices grow until canopy transport is in balance with the vegetation drag force. This results in a fixed penetration depth of canopy-scale turbulence into the canopy (δ_e in Figure 2.10), which has been found to depend on vegetation density and the level of submergence [43]. The end result is that for sparse beds the canopy-scale turbulence extends all the way to the bed and as the density increases the penetration depth decreases until it reaches a constant value, dependent on bed and flow properties. For dense beds the turbulence within the canopy has a zone of high turbulence at the top of the canopy, and a zone of lower turbulence closer to the bed, whose length scale depends on the stem diameters and spacing. Dense beds are therefore more protected from strong turbulence and shear stress, and encourage more sediment deposition than sparse beds under the same hydrodynamic conditions [43]. Therefore dense porcupine fields under submerged flow would likely encourage more sediment deposition within the field than sparse porcupine fields.

Figure 2.11 shows the shear stress profile found to correspond to the 'sparse' and 'dense' velocity profiles. For 'sparse' fields the shear stress decreases within the canopy, but does not get close to zero near the bed, allowing for re-suspension within the field. Dense fields, on the other hand, are expected to show reduced shear stress a short distance from the top of the canopy, and be very low through the majority of the canopy depth. This further corroborates the story given above that porcupine field designs that 'sparse' can experience erosion within the field, when sedimentation is often the desired outcome. At the same time, if increased roughness is the primary design objective, erosion within the field may not lead to poor performance.

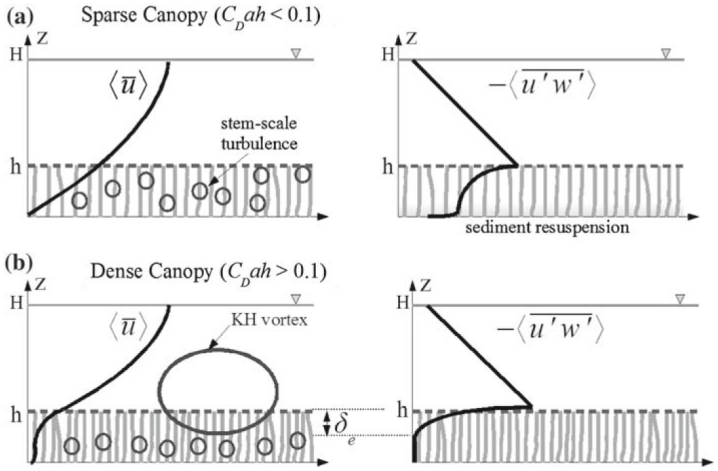

Figure 2.11: Velocity and shear stress profiles for (a) sparse vegetation and (b) dense vegetation. H is the water depth; h the height of the vegetation. δ_e is the depth of penetration of the canopy-scale vortices into the canopy. Taken from [36].

All of the discussion above related to the velocity profile has focused on the average velocity profile within the vegetation field. Within the canopy, the velocities are highly heterogeneous, as the flow moves through and around individual stems. Therefore, to define this average profile, spatial averaging of velocities in the cross-sectional direction is necessary [42, 47, 79]. Without spatial averaging, the velocities measured can be biased, and the measured profile will not reflect the actual 'behavior' of the field (e.g. sparse or dense). It can be assumed that porcupine fields would also require spatial averaging to obtain a representative average velocity profile. This consideration will come up again when examining flume data of porcupine studies in Chapter 5.

2.2.2 Non-Uniform Flow through Resistance Patches

Fully-developed flow through emergent or submerged vegetation fields were discussed above. However, before the boundary layer is fully developed, the flow approaching, moving over, moving around or moving past a resistance field will need to adjust. Remember a patch is defined here as a resistance area that it

too short or narrow for flow to be fully developed, therefore the following section focuses on resistance patches. Following the vegetation analogy, the next sections discuss results from vegetation experiments where flow development around the sides, at the start or at the end of the patches was analyzed. These experiments include flume or field experiments using rigid cylinders to represent vegetation as well as field data measurements from real vegetation patches. The implications for porcupine fields or patches are then discussed, including data for porcupine systems when available.

Flow along Lateral Edges of Resistance Patches

When one or both sides of a patch are exposed to flow, lateral shear layers can develop similar to the vertical shear layers discussed earlier, as shown in Figure 2.12. These shear layers act in a similar manner, transferring momentum from the side channel into the canopy. The strength of the lateral shear has been found to be a function of the patch blockage, defined through the solid volume fraction (ϕ), where ϕ is the volume of solid elements within in the canopy, or 1-n, where n is the canopy porosity [54]. Higher blockage leads to stronger shear layers.

This shear layers lead to increased shear stresses along the lateral edges of patches [83, 7]. In addition, the higher the blockage of the patch, the stronger the flow will be diverted around rather than through the patch. This can lead to higher velocities and shear stresses, and potentially scour in the adjacent channel[84]. This behavior was also observed in a porcupine flume experiment when the porcupines did not block the entire channel [46]. Finally, if the patch is thin enough, the vortices generated on either side are able to communicate with each other, and they can align themselves in a way that amplifies the vortices and further increases the shear stresses at the bed along the lateral edges [54]; however, this has only been demonstrated for dense arrays of emergent, rigid cylinders. It is not clear what the behavior will be for 'sparse' or transitional arrays, since lateral shear layers are either absent or weak. In addition, for submerged conditions, complex interactions between lateral and vertical shear layers may occur. These interactions have not been studied in detail.

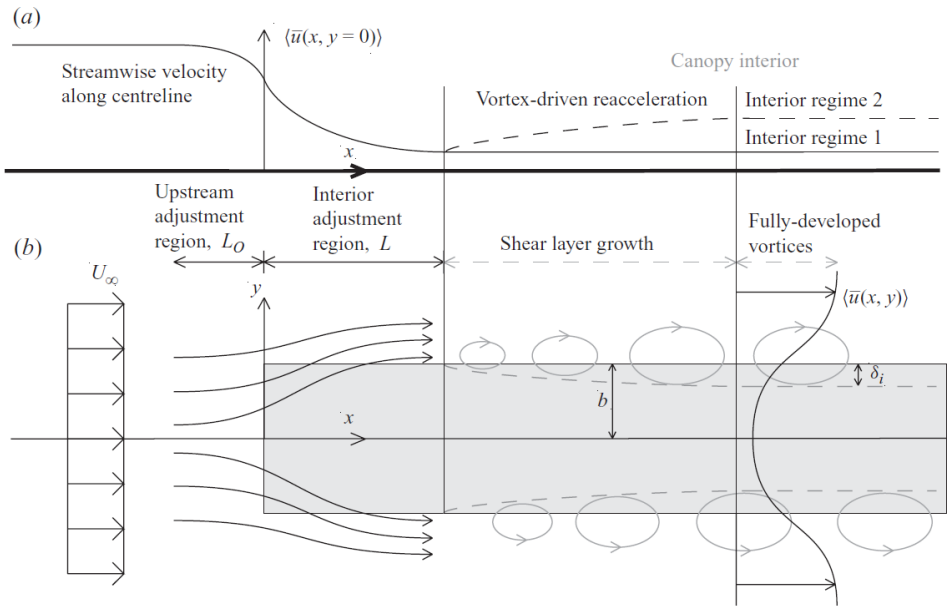

Figure 2.12: (a) Streamwise centerline velocity profile and (b) top view of vortex development along a vegetation patch with both lateral edges exposed to flow. δ_i is the depth of penetration of turbulent eddies into the canopy. b is the half-width of the canopy in the cross-sectional direction. Taken from [54].

Studies of lateral shear effects of porcupine patches are limited; however, the above observations allow us to identify three concerns that may require attention if porcupine systems have one or both sides exposed to flow. First, increased shear stresses along lateral edges may increase scour for the outer-

most porcupines, inducing them to sink. Second, porcupines areas, if dense enough, may divert flow and encourage scour in adjacent channels. Third, narrow patches may experience higher rates of shear compared to wider patches due to vortex communication across the patch.

Flow at Leading and Trailing Edges of Resistance Patches

The undisturbed approach flow will start to adjust to a resistance patch a certain distance upstream of the patch (L_0), and will continue to adjust for a certain distance inside the patch (L), see Figure 2.12. Studies of flow development at the leading edge of a patch of rigid cylinders has shown that the two length scales are a function of the patch blockage. For high blockages ($C_d ab \geq 2$), where b is the half-width of the patch, the interior adjustment length scales with b. For low flow blockages ($C_d ab < 2$), this adjustment scales with the inverse of the canopy drag length scale ($C_d a^{-1}$) [54]. In addition, at the leading edge of this boundary layer, shear stresses are higher [55, 54], and can lead to erosion at the leading edge of a resistance patch [8, 7].

For porcupine fields, this implies that at the upstream edge the first porcupines will still be exposed to high velocities, which can increase scour around the beams and encourage sinking of the porcupines. This phenomenon was observed in the 2018 porcupine flume experiment for a porcupine field with λ_p=0.8. As the first porcupines sink, they will be become less effective at 'protecting' the porcupines behind them. This could indicate that in designing porcupine systems the leading edge will need special consideration, or that care should be take in interpreting numerical modelling results for the start of the porcupine field.

Assuming the velocity adjustment is similar for the pilot study porcupine fields as the array of rigid cylinders studied above, we can make a rough estimate of what the interior adjustment length might be. The pilot study design porcupines have a low blockage factor, implying that L scales with the inverse of the canopy drag length scale ($C_d a^{-1}$). a for the design porcupines is 0.57 m^{-}1. Assuming C_d=1, the design porcupines would have a $C_d a^{-1}$ of approximately 2. Therefore the interior adjustment length of the velocity would be a certain factor times about 2 meters. The porcupines are approximately 2 m long in the longitudinal direction and have a longitudinal spacing of 3.4 m. If the above assumptions hold, it would be reasonable to expect velocities to be reduced within a few rows of porcupines. Experimental studies of velocity adjustment in porcupine fields would be needed to confirm this, and determine the appropriate scaling factor.

In addition to flow adjusting at the start of resistance patch, the end of the resistance patch will also induce an adjustment to the undisturbed flow velocities. After the initial adjustment flows within resistance areas are generally reduced [8, 42, 46, 66]. Lower flow velocities can encourage sediment deposition, especially if combined with low bed shear stress and low turbulent fluctuations [78]. As the flow exits the patch a certain adjustment length is required for the velocity to return to an undisturbed velocity. The 2018 porcupine flume experiment found adjustment lengths of approximately 4 to 8 times the field length for higher-density fields (λ_p = 0.8) and approximately 7 times the field length for a lower-density field (λ_p=0.2) [46]. Limited flow conditions, field densities and field lengths were tested (0.5 and 0.7 m); therefore it not clear how important this downstream retardation zone is for overall performance of porcupine systems. If the retardation zone does not increase significantly for very long fields, the total length of the field may be more important than adjusting the design to maximize the downstream retardation length.

Another consideration of the downstream adjustment area is that as velocities increase, sediment transport could increase leading to a zone of erosion where velocities are increasing. If sediment is trapped within and just downstream of a porcupine field, this erosion could be further exacerbated due to low sediment supply. The flume used in the 2018 porcupine flume study was not long enough to observe increased velocities downstream of the field, therefore the potential importance of this phenomena for porcupine fields has not been studied.

Configuration of Resistance Patches

When vegetation is present in a stream channel as a series of patches, rather than a continuous field, the arrangement of patches adjacent to each other can influence the flow in ways that initiates feedback mech-

anisms between the local morphology and the flow fields [63, 78]. Temmerman et al in [63] found that under emergent conditions, resistance differences between adjacent vegetated and un-vegetated zones led to perpendicular flow gradients into the vegetated area that led to sedimentation along vegetated patch edges, where the un-vegetated patches generally experienced erosion; however, under submerged conditions the differences between flow conditions in the vegetated and un-vegetated areas was significantly reduced.

For porcupines not placed along the full channel width or when navigation channels are placed in porcupine fields, the difference in resistance between the porcupined and un-porcupined areas can create secondary flows that will influence sedimentation and erosion patterns. In addition, even if the field is continuous, porcupines can offer different resistances depending on their location in the channel. For example, for the same water level, porcupines placed at higher elevations, such as the inner bend of a curve, will have a lower submergence ratio than porcupines at a lower elevation (outer bed). The transverse resistance differences can influence both the local flow field and the upstream backwater curve that the resistance may generate, and the subsequent erosion or depositional patterns.

As the water level rises, the effect of porcupines at different elevations (different submergence levels) will likely diminish; however, the differences (and influence) will return as the water level drops. The duration of these high and low flows, in combination with the porcupine design height, can significantly influence the long-term morphological influence, and feedback mechanisms between morphological development and flow-field development, of the porcupines. These impacts will vary with the nature of the sediment load in the porcupine implementation area (bed load versus suspended load).

Finally, a study by Luhar and Nepf [35] found that many patches of vegetation in a stream channel could increase the total resistance offered compared to a continuous field of vegetation across the full channel width due to the additional shear generated by the interfacial areas during flow conditions. In other words, under submerged conditions the patches offered lateral and horizontal shear layers where the continuous vegetation only offered a horizontal shear layer. This implies that to offer maximum resistance it may be more efficient to break a large porcupine field into smaller patches. More studies would be needed to determine what optimal configurations would be. In addition, the potential adverse effects of additional lateral shear for erosion and scour would need be evaluated.

2.2.3 Porcupine Laboratory Experiments

The above section gave a theoretical view of how porcupine fields should impact flow fields based on how vegetation fields and patches impact flow fields. These hypotheses cannot be confirmed due to limited laboratory or field experiments with porcupine fields. Some porcupine results were already presented. This section further discusses the studies to date examining hydrodynamic impacts of porcupine fields.

Studies have estimated the change in sediment transport capacity after placing tetrahedron frames [72], examined the capacity of porcupine fields to trap sediment based on before and after bathymetry measurements [2, 1], or examined porcupine performance in bed stabilization of a gravel bed river [70, 71]; however, for flow through a porcupine field the only detailed velocity profile measurements available are from the flume experiment carried out at TU Delft by Nientker in 2018 [46]. In this study, porcupines were placed across the width of a flume and detailed velocity (ADV) and water level measurements were taken in the streamwise direction at locations upstream, within and downstream of the porcupine field.

Similar to Lu's findings for a single porcupine element [34], Nientker found that the flow was pushed up just upstream of the porcupines, and was slightly downward directed as it left the porcupine field (see Figure 2.13). This figure also shows a reduced velocity profile with a flattened velocity gradient within the porcupine field, followed by a largely undisturbed velocity profile above the porcupines (green velocity vectors located within the red porcupine area from approximately 2.7 to 3.4 meters), similar to the expected behavior of a transitional vegetation bed (Figure 2.10d). Nientker did not collect measurements inside a porcupine element or at the first row of elements; however, the flow just upstream of the porcupines is accelerating compared to the approach flow, which could indicate agreement with the flow acceleration through an individual element observed by [34]. Nientker also found that the velocity was retarded for a certain distance downstream of the porcupine field, in agreement with the behavior of single porcupine frame observed by [34] and [81]. Upstream, the resistance of the field induces a

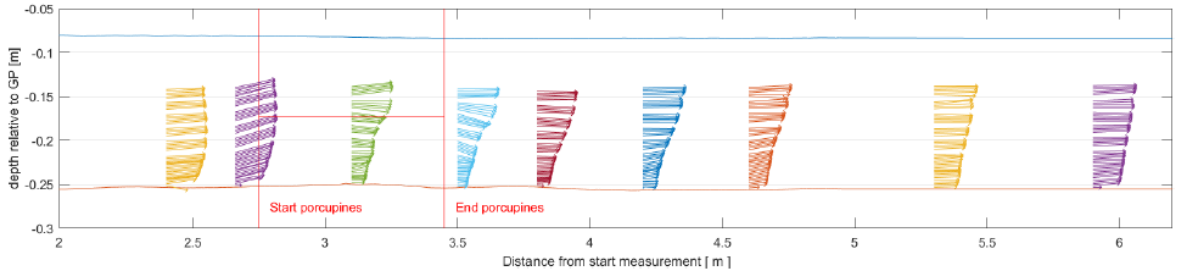

Figure 2.13: Velocity profile vector plot (h = 0.13 m, Q = 32.5 l/s, L = 0.7 m), Experiment 13.Taken from [46].

backwater curve, raising the water level. In addition, the near-bed shear stress was reduced within and downstream of the field for experiments run over a fixed-bed, indicating the potential for sedimentation at the downstream end of porcupine fields under certain flow conditions. Finally, the experiment shows that a shear layer developed along the top of the porcupine field under submerged flow conditions (as will be shown further in Chapter 5). Overall, the flume experiment results support the conclusion that the impact of porcupine beams on flow is similar to how rigid cylinders impact flow, which was the basis for many studies analyzing vegetation hydrodynamics.

2.3 Conceptual Model of Flow through a Porcupine Field

Conceptually, the hydrodynamic impact of a porcupine field likely shows strong resemblance to the impact a vegetation field has on the flow. As shown above, limited studies have been carried out on porcupine fields with detailed velocity measurements; however the 2018 flume experiment demonstrated many similarities. Therefore, initially, studies of vegetation can be used to hypothesise what the expected response of a porcupine field would be. A key finding from this chapter is that understanding if a porcupine field design would be likely to exhibit 'sparse' or 'dense' behavior can be very important for estimating system performance. The velocity profiles shown in the conceptual model in Figure 2.10 were derived from a variety of vegetation studies including experiments where vegetation is represented as rigid cylinders. For simplicity, this section will compare the velocity profiles through a porcupine field and a field of rigid cylinders. Figure 2.14 presents a hypothesized conceptual model for (fully-developed) velocity profiles through a porcupine field (dotted line), based on estimated difference between porcupine field behavior and the behavior of resistance fields made up of rigid cylinders (solid line), such as those used to develop the original model.

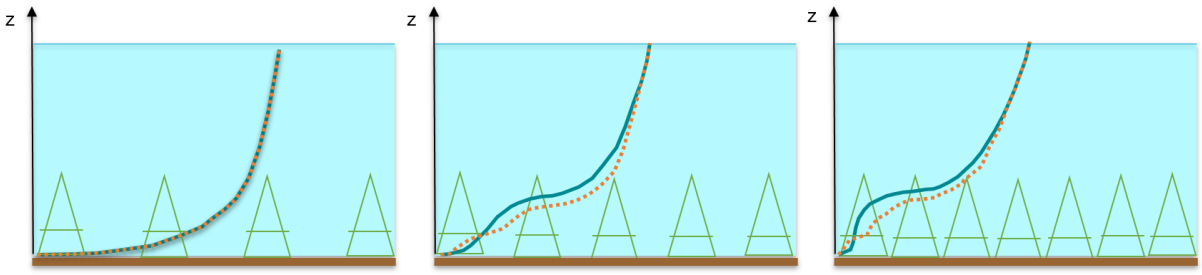

Figure 2.14: Conceptual model of a fully-developed, spatially- and temporally-averaged velocity profile through a porcupine field. Solid line indicates the velocity profile through a similar density field of rigid cylinders, dotted line indicates hypothesized velocity profile through a porcupine field.

The primary difference between the resistance elements used for the original conceptual model and porcupines is that due to the slanted beams, the lateral spacing between beams of adjacent porcupines increases as depth increases, allowing turbulent eddies to grow, where in cylinder or vegetation arrays the spacing controlling turbulent vortices is generally uniform, or decreases over depth. In addition, since

the porcupines have a higher flow blockage lower in the water column, velocities through the porcupine field will be reduced more strongly near the bed than near the top of the porcupine canopy. Therefore, I postulate that, for a porcupine field dense enough to generate a shear layer at the canopy top, the higher velocities towards the top of the porcupine canopy will weaken the strength of the shear layer and allow turbulence to penetrate further in to the canopy than for an array of rigid cylinders.

Indeed, the turbulence penetrates into the canopy until it is balanced by the drag force of the porcupines. The drag force, as will be discussed in Chapter 5, depends on both the drag coefficient (which can vary with depth), and the velocity. For porcupines, the drag coefficient should be larger at the base where there is higher flow blockage. The net effect will be a balance between the drag coefficient and the velocity; however I postulate that the horizontal beams, which offer a significant increase in density at the bottom of the porcupine field, will lead to a second (small) inflection point around the height of the horizontal beams.

Therefore, the porcupine conceptual model shows that for fields of porcupines the velocities within the canopy will not be reduced as much as for the same density (λ) array of rigid cylinders, the shear layer will penetrate further into the canopy, and the the strength of the shear layer will be weaker for the porcupine field than for the array of rigid cylinders; however the horizontal beams may help in reducing velocities near the bed. This can also imply that as porcupines are buried and 'loose' their horizontal beams, they will transition towards a 'sparse' field behavior.

The available data on porcupines is not sufficient to test this hypothesis; however, future experimental studies of porcupine fields with measurements from fully-developed flow at the center of the field can be used to validate this theory. For this thesis, the potential for increased turbulence penetration into a porcupine field, compared to a vegetation field, can be kept in mind when examining the performance of porcupines in the pilot study analysis, and when considering recommendations for future porcupine field designs.

2.4 Conclusions

This chapter has examined the expected hydrodynamic impacts of porcupine fields and patches, using existing porcupine laboratory data as well as estimating impacts assuming that porcupines can be represented as a special kind of vegetation resistance element. Porcupines can be expected to reduce flows within and downstream of a porcupine field. The behavior of the velocity profile and turbulence within the field will vary if it can be considered 'sparse' or 'dense'. This also has implications for the shear stress profile, where sediment can be re-suspended in sparse canopies, as opposed to deposition that is expected in dense canopies.

The behavior of velocity and shear stress profiles within and adjacent to porcupine fields will be examined further in Chapter 5. In the next chapter, these hydrodynamic impacts will be translated to potential impacts to sediment transport and local morphology, for the purpose of analyzing porcupine performance in the Ayeyarwady River pilot study.

Chapter 3

Porcupines' Influence on Morphology

Porcupines can be expected to influence the local flow field by altering velocities, turbulence patterns and Reynolds stresses. Alterations to the flow field in turn influence the local sediment transport which in turn affects the local morphology. Changes in morphology, in turn, re-impact the local flow field. These influences are felt at varying spatial and temporal scales, and will be different for different areas of the resistance patch.

This section first summarizes how porcupine patches can be expected to influence the local hydrodynamics, as elaborated in Chapter 2. Next, the potential impacts to sediment transport are discussed for three regions of a resistance patch: the center, the leading and trailing edges, and the lateral edges. Then boundary conditions (e.g discharge, sediment supply) that can influence the morphological response are discussed. The discussion remains general to any porcupine installation; however, evidence of interest for the pilot study analysis will be highlighted. The time scale considered is one to a few wet seasons and only local changes are considered.

3.1 Expected Morphological Influence of Porcupine Fields

Due to limited studies of porcupines' influence on morphology, this section continues the vegetation-porcupine analogy, making references to studies of how vegetation fields or patches (generally schematized as rigid cylinders) have influenced sediment transport and local morphology, and presenting hypotheses for where deviations from this behavior might be expected for porcupines. This section focuses on the porcupines' potential to induce sedimentation or erosion, compared to a bed without resistance elements.

3.1.1 Flow Field Impacts

The potential impacts of porcupines on the flow field was discussed in detail in Chapter 2. This paragraph summarizes the hypothesized theoretical model. Porcupines can influence the flow field by altering local velocities, turbulence characteristics and flow direction. Porcupines will be expected to reduce velocities just upstream, within, and downstream of the field. They are expected to raise water levels upstream of the porcupine field, and consequently increase the total shear stress over the porcupined reach, but will likely reduce the bed shear stress within the field. The density of the porcupine field will determine exact behavior within the field. For 'sparse' fields ($C_d\lambda << 0.1$) velocities are expected to be reduced. Turbulence intensity at the bed could increase or decrease. The bed shear stress will likely be reduced compared to a non-porcupined channel with similar flow conditions; however resuspension can still occur within the field. For 'dense' fields ($C_d\lambda >> 0.1$), as density increases, the turbulence length scales are expected to become smaller, but the total production of turbulence and subsequent energy dissipation within the canopy will increase, reducing velocities. Reynolds stresses should decrease significantly as the bed is approached, and should remain sufficiently low at the bed to minimize resuspsenion. The flow

can be expected to be diverted slightly upward at the upstream end of the field and slightly downward at the downstream end. If the field is exposed to flow on one or both sides, diversion of flow to the sides can also be expected. Higher density fields will show stronger diversions.

Therefore, the density ($C_d\lambda$) of the designed porcupine field can have a significant impact on the expected behavior. $C_d\lambda$ for the design porcupines is 0.2; which places them in regime that would be considered 'transitional' for vegetation; however, the value of $C_d\lambda$ indicating a 'sparse' versus 'dense' transition could be different for porcupines than vegetation. As discussed in Chapter 2, the C_d of the design porcupines will vary with flow conditions (velocity and submergence), and while widely assumed to be one for vegetation, could be higher for porcupines, giving them a higher density for an equivalent λ. 'Sparse' versus 'dense' fields can be defined by both the behavior of the velocity profile and the relative contribution of turbulent stress versus canopy drag in the momentum balance. Detailed velocity measurements are not available for the design porcupines, therefore their behavior cannot be characterized as 'sparse' or 'dense' from direct measurements. One configuration of porcupines used in the 2018 flume study had a λ of 0.17; however velocity measurements were not well captured for the mobile-bed experiment, and only one flow regime was evaluated. Therefore, the design porcupine behavior cannot be confidently inferred from the porcupines used in the flume study. Finally, when porcupines sink into the bed, their frontal area is reduced, reducing λ, and pushing the porcupine field behavior closer to 'sparse' if it was not sparse already. The behavior of both sparse and dense fields will be considered below, as the effective λ of the pilot study porcupines is not known; future porcupine designs could be either dense or sparse; and porcupine fields might exhibit both dense and sparse behavior as flow conditions change, depending on their exact placement within the channel, and as they sink into the bed or become buried. Without further evidence, the assumed behavior of the pilot study porcupines is transitional to dense when unburied, and sparse if the horizontal beams have been buried.

3.1.2 Sediment Transport in Resistance Patches

The potential sediment transport within a resistance patch will vary depending on the location within the patch (flow inside the patch versus along the leading or trailing edges or patch edges), the development stage (fully-developed or developing), the local flow conditions (which can vary temporally as well as spatially, if the patch is located along the center or the edges of a channel, for example), and the upstream sediment supply (including grain size fraction and distribution of bedload versus suspended material load). The ability of the field to influence the local flow conditions in a way that favors sediment deposition or reduces sediment suspension depends on the characteristics of the resistance elements including density and emergent or submerged conditions. This section will first discuss how resistance elements can alter sediment transport for three regions of patches: center, leading and trailing edge, and lateral edges. Then external factors that can influence the net morphological response, including hydrology and sediment supply are discussed.

Patch Center

First, we will consider sediment transport within the fully-developed portion of a resistance patch, far from the edges (Figure 3.1a). For 'dense' fields, sediment transport within the canopy can be expected to decrease inside a resistance field as velocities decrease resulting in near-bed shear stress decreases [36, 7, 78]. For 'sparse' fields local turbulence intensities can increase or decrease, and turbulent shear stresses may not be sufficiently suppressed near the bed to encourage deposition and sediment re-suspension could occur [36, 78]. Numerous studies of vegetation have shown enhanced deposition by vegetation [32, 83, 8]; however, deposition or erosion within the field depends on field placement and the local flow conditions. Yager et al. in [78] studied rigid cylinders representing vegetation in a flume (scaling to the size of small trees up to 0.1 m diameter, similar to the design porcupine beam width), and found that sedimentation within the field could increase or decrease depending on the local flow conditions (e.g. velocity and turbulence levels). They therefore concluded that the local conditions can influence whether a resistance field is able to induce a depositional environment. For example, flows at the edges of channels will have lower velocities than flows in the center of the channel, and may be more conducive to creating depositional areas. Porcupines placed in ares with high velocities may not be able to sufficiently reduce velocities to create a depositional environment.

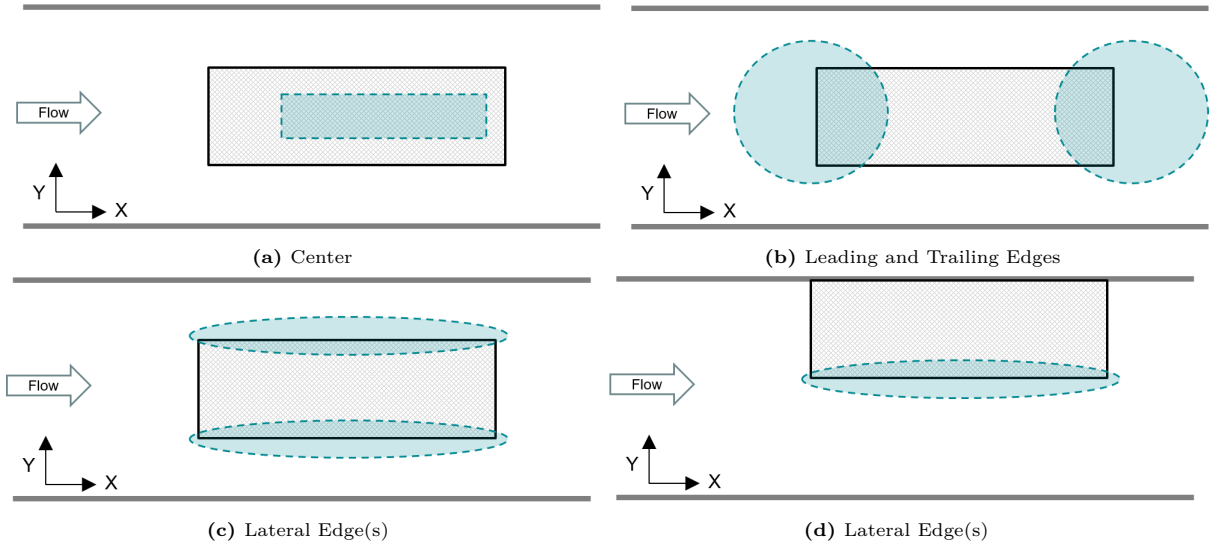

(a) Center

(b) Leading and Trailing Edges

(c) Lateral Edge(s)

(d) Lateral Edge(s)

Figure 3.1: Top view of channel. Resistance patch (grey box) will alter the flow field and sediment transport differently at different areas within and around the patch. Blue shapes indicate location specified in the caption. Note that a patch can have two lateral edges, if flow can move around both sides (c), or just one (d), if flow on one side is restricted.

Lateral Edges

The behavior of turbulence and shear stresses, and corresponding sediment transport, at the edges of patches can be different than inside the canopy. First, let us consider the lateral edges of resistance patches (Figure 3.1c,d). For patches (limited width or length), under emergent conditions for dense fields, strong shear layers can form along the edges between the vegetation (resistance element) edge and the non-vegetated channel ('main channel'), as described in Chapter 2. These shear layers both increase the local turbulence intensity along the edge of the patch and increase turbulent diffusivity into the patch. The increased turbulence generated can dissipate energy and reduce velocities; however locally turbulence intensities can be increased [53, 35]. If the patch is not closed on one side (non-vegetated channels are present on both sides, Figure 3.1c), and it is sufficiently narrow, vortices generated by the shear layers on both sides can communicate through the canopy and self-organize such that the shear stress and turbulence intensities at the patch edges are even more enhanced [35]. This enhanced turbulence can further reduce the potential for deposition within or adjacent to the patch and potentially encourage local erosion.

Zong and Nepf, in [83] found that the increased turbulent diffusivity could carry sediment from the main flow into the velocity patch where it settled due reduced velocities within the patch, in agreement with [29, 57, 26]. At the very edge of the patch, where local turbulence was increased, sedimentation was reduced, but still remained higher than within the main channel. Low and higher-density fields were examined ($\lambda = 0.6$ versus $\lambda = 2.8$, therefore still both 'dense'). The Reynolds stresses and turbulence intensity were lower at the patch edge for the less dense field; however the turbulence was able to penetrate further into the patch. Upstream flow was diverted away from the resistance path to the main channel, but this diversion was not as strong for the less dense field. Therefore velocities in the main channel were lower and more sedimentation was observed in the main channel for the less dense field than the higher density field. This is in agreement with findings from Kim et al. in [26]. Bouma et al. in [8] found that cylindrical bamboo sticks placed in tidal flat over two years (experiencing emergent and submerged conditions) tended to show bed level decreases (erosion) along the lateral edges of the patch (Note that the authors presumed that tidal currents, rather than waves, were the dominant flow mechanisms in the study area, although influence of waves could not be excluded).

Therefore, porcupine patches that do not cover the full channel width, but are, for example, aligned along a bank, could expect to experience erosion and sinking of porcupine at the edge due to scour,

and deposition a short distance into the porcupine field. This effect can be stronger for porcupine fields that are very dense, because the shear layer generated will be stronger, and because less flow (with suspended material) will be advected into the patch from the upstream direction, as the high resistance will encourage the flow to divert to the side. However, this behavior depends on the upstream sediment supply, as this deposition is primary suspended sediment carried into the field from the sides. This mechanism may change behavior entirely under submerged flow conditions, when additional shear vortices are able to penetrate into the canopy from above. Finally, this behavior was only studied for 'dense' patches ($\lambda <= 0.6$). For 'sparse' beds the behavior could be different.

Leading and Trailing Edge

Sediment transport can also be influenced by flow conditions at the leading and trailing edge of a patch or field. Flow upstream of a resistance field should show a certain adaptation length, where the water depth is increased (due to the upstream backwater curve), and flow velocities are reduced. Alternatively, flow encountering a step-change in resistance (and hence a step-change in velocity) as it enters the porcupines field can deposit suspended material at the interface. However, the extent of this impact depends upon the flow conditions and vegetation properties. Several authors have found increased shear stresses and erosion at the upstream edge of a resistance patch [8, 63, 53, 26]. On the other hand, the downstream edge of the patch showed aggradation. The study by Bouma et al., described in the previous section, also examined bamboo cylinders in a mobile-bed flume setup, in addition to the field experiment. Dense resistance patches were shown to have much higher shear stresses and erosion at the leading edge, and much higher aggradation at the trailing edge, than less-dense beds (both still "dense", considering λ). From their field data the bed elevation of the less-dense beds in some locations showed almost no net change over the two-year study period.

Erosion at the leading edge and aggradation at the trailing edge was observed for porcupine patches in the 2018 porcupine flume study [46]. Nientker found that higher flow velocities increased the erosion at the front edge of the patch, but also increased aggradation at the trailing edge and downstream of the patch. For a less dense porcupine patch, the erosion at the front edge was reduced, but the sedimentation at the trailing edge and downstream was also reduced, consistent with the results from [8]. As porcupines sink, their ability to reduce the flow, 'protecting' the porcupines behind them, decreases. In the long-term, this could hamper the effectiveness of porcupine fields in reducing velocities and encouraging depositional environments, as well as transition the porcupine field from 'dense' to 'sparse' behaviors, depending on how the frontal area of the leading porcupines are altered. This can indicate that special care needs to be taken at the leading edge of a porcupine field, to prevent sinking of the porcupines, or regular maintenance may be required.

The direction of the flow field can be important for impacts to suspended sediment. Flow directed away from the bed can carry sediment further into the water column, where flow directed towards the bed can carry suspended sediment towards the bed. In submerged conditions porcupines have been observed to push flow up at the upstream end of the field and direct flow downwards at the downstream end of the field [34, 46]. This could encourage deposition of suspended material downstream of the porcupine field.

3.1.3 Morphological Impacts by Spatial Scale

The morphological impacts of porcupines will vary with the spatial scale. The potential morphological impacts of porcupines are discussed at two spatial scales: the footprint of an individual porcupine, and the footprint of the entire porcupine field. Potential larger-scale impacts at a reach scale are outside the scope of this thesis.

Individual Porcupine

At the scale of a single porcupine, the local flow field and turbulence generated by the individual beams will lead to scour holes around the porcupine 'legs' contrasted with adjacent depositional areas. Figure 3.2, shows two images of porcupines from the pilot study discussed in the next chapter. Scour is observed around each of the vertical beams and a small depositional area in the center. This is more clear in Figure

3.2b. As discussed in Chapter 2, the size of the scour hole will be a function of beam width, sediment size, local velocity and beam angle to the flow direction.

(a) (b)

Figure 3.2: Scour and deposition patterns around partially-buried porcupines at two locations in Sagaing Channel (a) facing east (flow from right to left), and (b) facing west (flow from left to right)

Porcupine Fields

At the level of a porcupine field, scour and depositional patterns will arise between the individual porcupines. Going back to Figure 3.2, zones of scour are observed around the tops of the partially-buried porcupines and depositional zones are observed between them. Yager et al. (2013), in [78] using a mobile bed in a flume with rigid dowels representing vegetation, found a similar (stable) morphological evolution of the bed around the individual cylinders (see [78], Figure 10). Larger bedforms were found for larger spacing between cylinders. Therefore as porcupines become buried, and the effective distance between porcupines decreases, larger bedforms might be expected for the same hydrodynamic conditions. These bedforms between porcupines can influence the flow field approaching downstream porcupines. Yager et al. (2013) also found that while the depositional areas did not migrate this morphology was a function of locally-generated turbulence and the bed around and between cylinders was in continuous movement. Therefore, at the scale of a field of porcupines, the variability of the upstream sediment supply becomes critical in determining the stability of this pattern and the net results of erosion or deposition within the field.

3.1.4 Influence of Site Characteristics

Local flow, existing morphology and sediment load conditions will be critical in influencing the behavior and performance of porcupine fields. In addition, changing system dynamics, such as the opening or migration of channels or changing channel widths can also change their expected impact. The placement of porcupines in the channel influences the local flow conditions they are exposed to. In addition, changing flow conditions, including water level rising and falling over the course of the wet season, alters both local flow conditions and pushes porcupines to or from emergent and submerged conditions, for which their impact on the flow field differs. Finally, the upstream sediment supply, including division of sediment load between bedload and suspended load as well as the grain size fraction can influence how the porcupines influence sediment transport and the local morphology.

The exact location of the porcupine patch in the channel can influence how it impacts sediment transport. If deposition is an objective in placing porcupine patches, placing those patches in depositional areas (the edges of channels, inner bars, the downstream end of mid-channel bars), all create more favorable conditions for the porcupines to reduce velocities and bed shear stress, encouraging deposition, than placing porcupines in areas with high flow velocities.

The resistance offered by porcupines is largely governed by the local flow conditions and will be different for submerged or emergent conditions. If velocities and turbulence are high enough erosion may be observed in 'sparse' beds under emergent or submerged conditions; however they could be more susceptible under submerged conditions when velocities are higher and turbulent eddies have space to grow. This suggests that 'sparse' porcupine fields could be more susceptible to erosion (and sinking from scour)

under submerged than emergent conditions. Porcupines placed at lower elevations (e.g. outer bends), will be more susceptible to higher water levels (velocities), and 'sparse' fields in those locations will be the most vulnerable. For dense beds, velocities are generally reduced sufficiently within the field to inhibit sediment transport. Under submerged conditions the strong shear layers that forms above the canopy can further help to protect the bed. Therefore 'dense' porcupine fields might be expected to show depositional behavior under both emergent or submerged conditions.

The second consideration for emergent versus submerged behavior, is that the resistance of the porcupines can be expected to increase as water levels come from the bed to the top of the porcupine. Then, the resistance decreases as the depth of the overlayer increases. Porcupines installed at different elevations across a channel will experience different submergence ratios for the same water levels. The transverse resistance gradients can induce secondary flows to areas of less resistance; however, the effect will diminish at high submergence ratios.

These transverse gradients can carry suspended sediment in the direction of least resistance. Alternatively, if flow is pushed in a certain direction due to lower resistance (e.g. around a central bar with porcupines), this can lead to increased erosion of the channels around the resistance area. These transverse resistance gradients can also influence upstream areas, by creating uneven backwater curves that push flow to the outer bend. Care might need to be taken in designing systems where 'protection' of the outer bank from erosion is desired.

For porcupine fields placed in secondary channels, the bifurcation angle in relation to a main channel can influence how flow (and sediment) enter the porcupine field. At low flows, channels with high or low bifurcation angles can expect to direct flow directly into the porcupine field. At high flows, channels with a high bifurcation angle might find that flow is directed across the channel, which can turn the channel into a kind of sediment trap. where channels with low bifurcation angles will still direct the flow directly through the porcupine field.

Finally, the net morphological response is highly influenced by the lack (or abundance) of sediment entering the system. Sediment within the porcupine field will be consistently in motion due to local turbulence produced by the wakes of porcupine beams. The upstream sediment supply can determine if this consistent (but stable) movement could lead to a net erosion within the field. Once eroded, the porcupines will not regain their original elevation. An erosion wave travelling through the system could potentially lower the elevation of all porcupines in the field. At the same time, a deposition front could pass through, burying the porcupines. The exact impact of these processes will depend on what the design objectives were for the system. Neither may necessarily be good or bad, although erosion and sinking of porcupines is more likely to have negative consequences on foreseeable design objectives.

Feedbacks exist between each of these mechanisms. Deposition or erosion alters the water depth, which affects the total shear stress. Fonseca et al. in [19] hypothesize that sedimentation grows in eelgrass meadow mounds until the additional bed shear stress created by the reduced water depth is balanced by the bed shear stress reduction from the increased vegetation resistance. A similar mechanism can exist for porcupines. Erosion or deposition influences the flow field but also can either reduce or increase the effective density of the field. For example, deposition that occurs within the porcupine field can partially bury the porcupines, effectively reducing porcupine field density, and decreasing the water depth which can lead to increased velocities and scour, increasing the frontal area and density of the porcupine field again.

As these conditions change with time they will influence the future response. A field that has already experienced erosion will offer even less resistance when the water levels rise. The interactions between flow and morphology over a range of flow conditions is not well understood. Most laboratory studies of how resistance elements influence sediment transport and morphology focus on a narrow range of velocities, total shear stress or submergence rations. In addition, studies are limited to only looking at impacts to bedload or suspended material. These studies may have looked at short-term response rather than long term 'equilibrium' results. Studies are not available that can give better insights into how resistance elements, including porcupines, influence morphology over changing flow conditions and sediment loads, considering that the previous response to the initial conditions will influence the future response to changing conditions.

3.2 Conclusions

The potential local morphological influence of porcupine fields have been examined using limited porcupine experimental data and more extensive studies of vegetation's impact on sediment transport. The expected sedimentation or erosion patterns vary depending on the location with a resistance patch. For porcupines with an initial 'transitional' or 'dense' behavior, we might expect deposition just inside the lateral edges of the field, downstream from the leading edge, and downstream of the field. Deposition or erosion could be present at the leading edge depending on the effective field density and flow conditions; however, as porcupines are buried and their behavior transitions to 'sparse' net erosion or deposition within the field is possible. Erosion is more likely in deep areas of the channel, where velocities will be highest, and lower at higher elevations such as the edges of the channel or along the downstream end of mid-channel bars. Finally, under emergent conditions transverse resistance gradients can be expected to push the water towards areas of lower resistance (the outer bend), but this effect will be diminished as water levels rise and all porcupines become submerged. In the patch center, where flow is fully-developed, 'sparse' fields may experience erosion or deposition depending on velocities and bed shear stress for emergent or submerged conditions. 'Dense' fields are likely to experience deposition regardless of submergence. At the individual porcupine level or between individual porcupines in field, the presence of the porcupines generates turbulence that induces scour around the base of the beams and deposition inside and between porcupines. The bed may be stable but can be in continuous movement. Therefore the upstream sediment supply can be critical in determining if net erosion or deposition occurs within a field. In addition, the exact morphological response will vary as discharge (and hence submergence ratios) vary and the dynamics of the system (new channels forming, channels widening, entrance of erosion or deposition waves) change.

Chapter 4

Pilot Study Analysis

This chapter examines the pilot project implementation of porcupines in the Ayeyarwady River in Myanmar for the purposes of braided river channel control. First, the pilot project activities are summarized. Then, the expected morphological response is described based on the conceptual model of hydrodynamic impacts developed previously and the review of morphological impacts presented in the previous chapter. The results of the pilot project implementation are described from available bathymetry, photographs and aerial imagery. Finally, the expected and actual results are discussed, with their limitations.

4.1 Pilot Project Implementation

4.1.1 Site Description and Background

The pilot project was implemented in a section of the Ayeyarwady River next to the city of Mandalay in Myanmar (the 'Site'), as shown in Figure 4.1. In this location the river consists of four distinct channels separated by islands - a primary channel to the east (the Mandalay Channel), and three secondary channels located in the center and western edge of the braid plain. From west to east: Momeik, New, Sagaing and Middle Channel. New channel did not exist at the start of the design process - it was added in January 2019 after being discovered. Flow in the channels is from north to south.

The primary objective of the pilot project was to maintain a least available depth (LAD) of 2 meters (m) for a 1,000 deadweight tonnage (DWT) vessel in this section of the river. This effort is Sub-Project-1 of the larger AIRBM (Ayeyarwady River Basin Management) Project targeting the Mingun – Sagaing stretch of the Ayeyarwady River. The project should improve access to the Port of Mandalay, deepen and stabilize the main (Mandalay) channel and reduce the risk that navigation is hindered by one of the secondary channels taking over as the primary channel (which naturally occurs approximately every 10 to 30 years) [30]. The final design proposed to implement porcupine structures in the secondary channels to increase local roughness, as well as strategic dredging, as required, near the port of Mandalay and in the downstream 'bottleneck area' (geological constriction in the river near Sagaing). These efforts aim to maintain the current discharge distributions, ensuring that the Mandalay channel remains the primary channel. In addition, the porcupines were expected to encourage sediment deposition in the secondary channels, increasing the bed elevation and further discouraging a primary channel shift [28].

4.1.2 Porcupine Design and Installation

The porcupines installed in the pilot project were made of square reinforced concrete beams 2.4 m long and 10 cm thick, with an effective height when assembled of 2 m. Porcupines were placed along rows in a staggered configuration with 3.5 m distance between the center of the porcupines between rows (longitudinal direction, ΔS_x) and 4 m distance between the center of porcupines along the same row (cross-sectional direction ΔS_y), as shown in Figure 4.2. For this Chapter, the longitudinal and cross-sectional (transverse) directions are defined as parallel and normal to the primary flow direction, respectively.

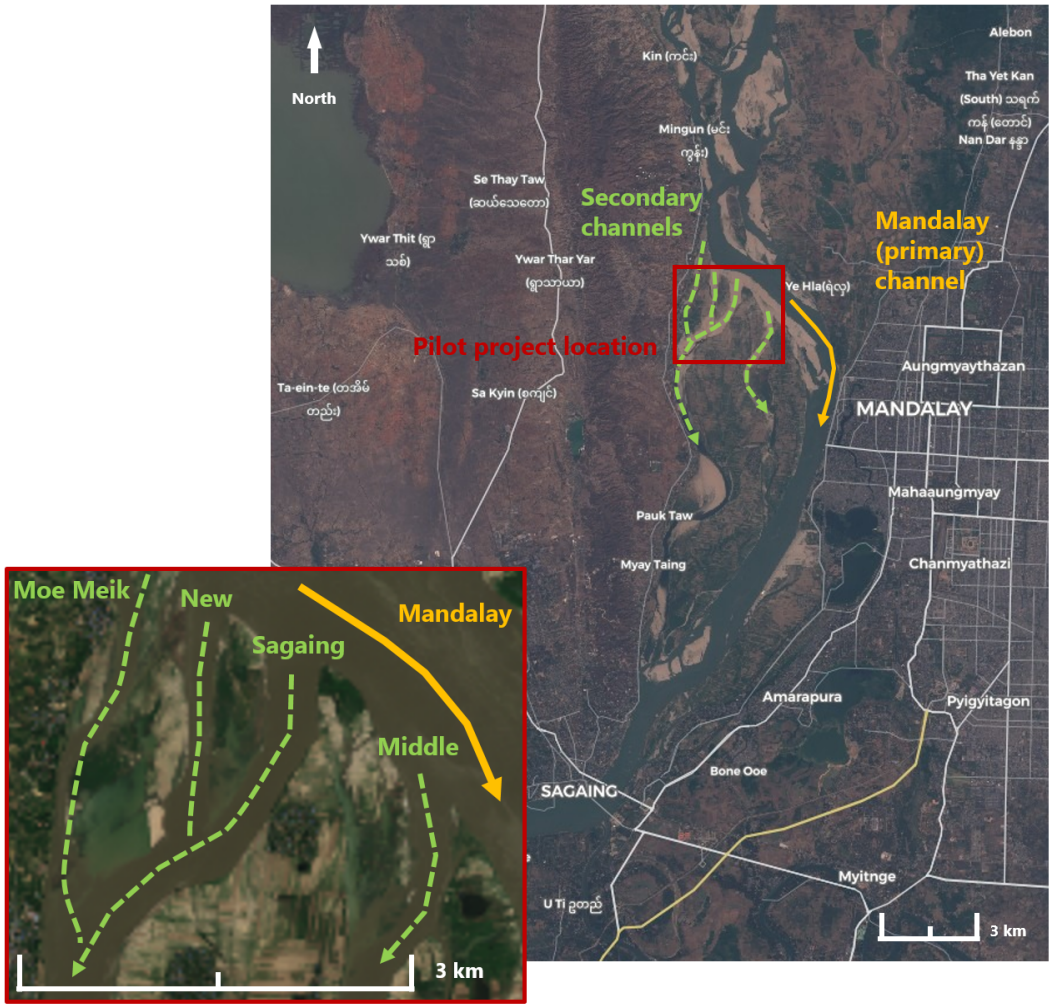

Figure 4.1: Ayeyarwardy River near Mandalay with pilot project location. Aerial imagery: Landsat 11/03/2020 (overview), 18/09/2020 (inset); (apps.sentinel-hub.com)

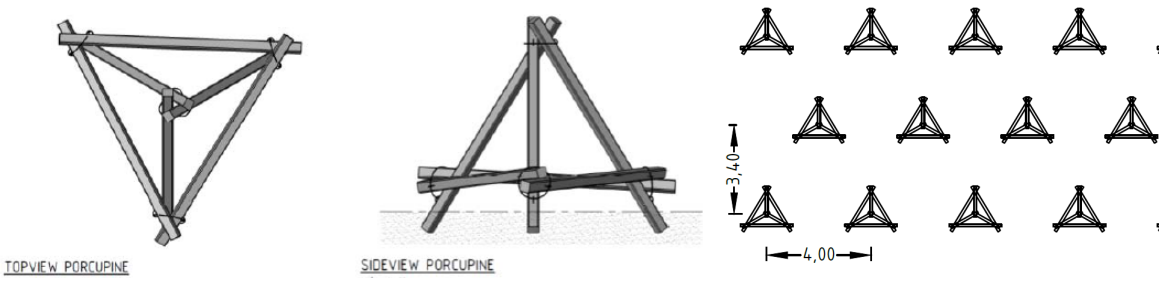

(a) (b)

Figure 4.2: Installed porcupine specifications (a) side and top view (b) layout, taken from [28].

Porcupine field placement options were initially evaluated with a hydrodynamic numerical model and further refined after discussions with stakeholders [28]. The porcupines were constructed and implemented during the two dry seasons in 2019. March to May ('1st dry season') and November to February ('2nd dry season'). During the 1st dry season a portion of the total design area of porcupines was placed in Middle and Sagaing Channels. During the second dry season the remaining porcupines were placed in Middle and Sagaing Channels, and the full amount of designed porcupines were placed in Moe Meik and

New Channels [18]. Figure 4.3 shows the extent of the 1st dry season installation (purple dashed line) and the combined 1st and 2nd dry season installation (red dashed line). The pilot study area generally experiences one wet and dry season each 12 months, from approximately May to October and November to May, respectively. The porcupines placed during the first dry season have currently experienced one flood season (May to November 2019 - the 'study period'). Only the impact of these porcupines on the local morphology, during the study period will be analyzed in this chapter.

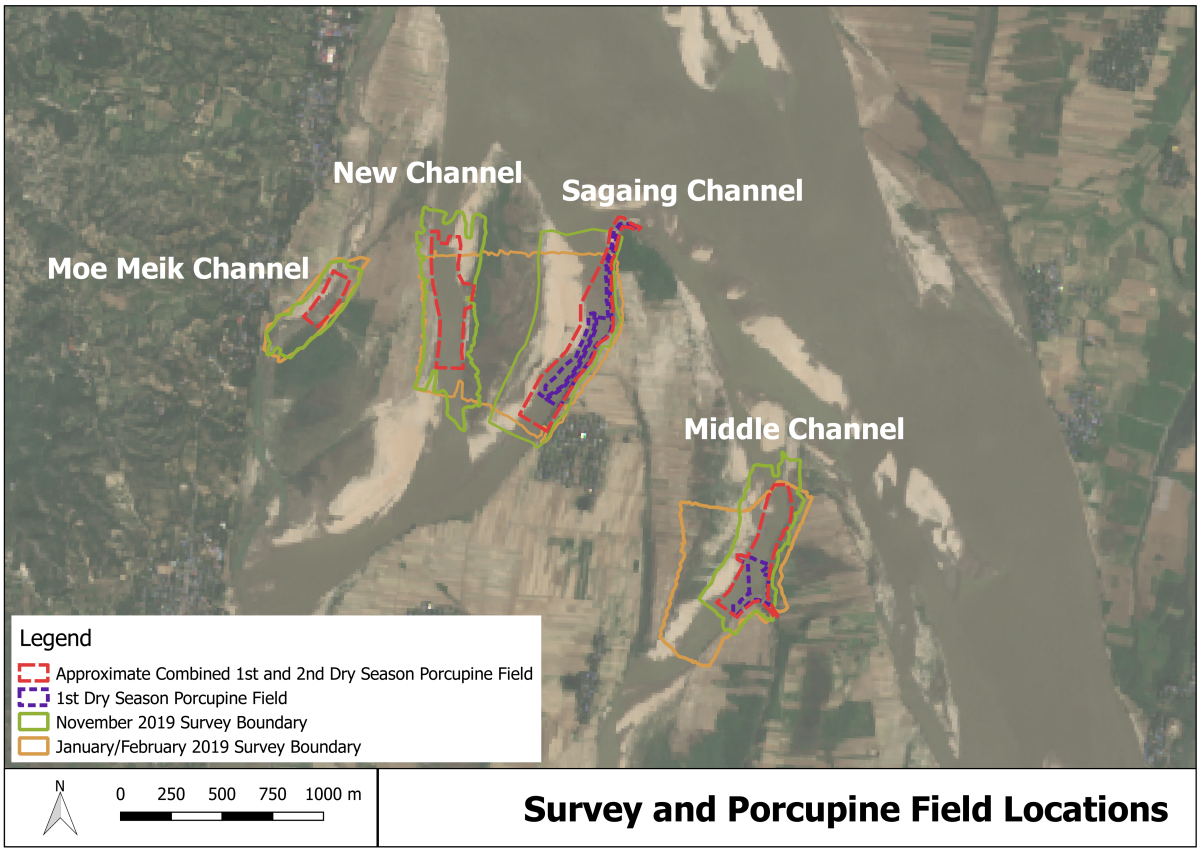

Figure 4.3: Overview of Porcupine Field and Survey Locations. Aerial Imagery: Landsat 23/10/2020 (https://apps.sentinel-hub.com)

Bathymetry and land surface measurements (survey points) were collected in January 2019 for Moe Meik, Sagaing and Middle Channels; in New Channel in February 2019; and in all four channels in November 2019 (see Figure 4.3). The accuracy of the measurements is not know; however it is assumed that a high quality GPS was used with good field practices, that should result in measurements with an accuracy of approximately $\pm$ 10 cm. In addition Landsat aerial imagery has been collected from between April 2019 and December 2020, and photographs of porcupine placement were taken in each channel in February 2020.

4.2 Hydrological Conditions and Physical Site Characteristics

The site hydrology and physical characteristics can have an important influence on porcupine performance. The water levels through the channels determine the submergence ratio of the porcupines which impacts their effective roughness, and control maximum velocities. The physical site characteristics, including the sediment load, can have a strong impact of how the porcupines are able to influence the local morphology. Each is discussed in more detail below.

4.2.1 Hydrological Conditions

Detailed hydrological information is not available for the period from January 2019 to November 2019; however an analysis of gauge data from the Mandalay port area from 1994 to 2014 indicates that the least available depth (LAD - depth that can be expected to be available no less than 20 days out of each two years) is approximately 62.25 m + MSL (mean sea level), while the high water period discharge elevation is approximately 70 m + MSL [28]. Figure 4.4 shows the typical water level variations near Mandalay derived from this 10-year period. These water levels appear to be high, given that the lowest elevation of the secondary channels was found to be just over just over 61 m + MSL in January 2019 (± 10 cm) and Landsat aerial imagery shows they were largely dry during the 2019 dry season. Improved rating curves for this area could improve the confidence in these water level estimates (see [28], pp. 17-18).

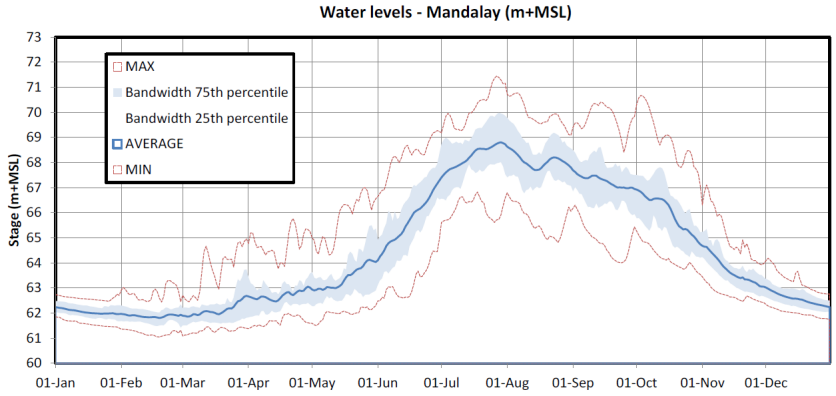

Figure 4.4: Water level statistics over a 10-year period (1994-2014). Taken from [28], Figure 2.8, using data from DMH (Department of meteorology and hydrology)

Nevertheless, this data can give us an idea of, for an average season, how long the porcupines installed in Middle and Sagaing Channel can be expected to be emergent or submerged. Figure 4.5 shows the installation elevation ranges for the 1st dry season porcupines in Middle and Sagaing Channels, as well as an estimate of how many months of each wet season the porcupines are emergent or submerged. At installation, the porcupine base elevation ranged from 61 to 65 m. With an effective height of 2 m, porcupines will start being submerged when the water level reaches 63 m.

Based on the average water stage, the majority of the porcupines installed during the 1st dry season were likely submerged at least 5 out of the 6 month wet season, assuming that there is no flow in the secondary channels except during the wet season (mid-May to mid-November). The maximum submergence ratio (h/s) for the porcupines varied between 1.75 and 3.5.

This analysis is not taking into account potential sinking of porcupines into the bed, or bed level changes over the course of the wet season. In addition, the estimates are for the average water level. There is a wide range of possible low and high water levels in any given year; however, it demonstrates that while, on average, nearly all porcupines will be submerged most of the wet season, the submergence ratio should remain low.

The behavior of porcupines during emergent and submerged conditions is important for two reasons. First, emergent versus submerged conditions control the shape of the velocity profile and the turbulence characteristics through the porcupine field, as described in Chapter 2, which in turn can influence the local sediment transport. Second, the flow resistance offered by porcupines will vary depending on the flow conditions. The bed without porcupines will offer the least resistance. Emergent porcupines will offer the most resistance. As the porcupines become submerged, and then more deeply submerged, resistance decreases. Since the porcupines are installed at varying elevations in both the lateral and cross-sectional (transverse) directions, this will lead to gradients in the resistance that can induce transverse gradients, impacting flow fields and sediment transport. As all areas become submerged and the level of submergence increases, the differences in resistance will reduced, as was shown to the case for vegetation [63].

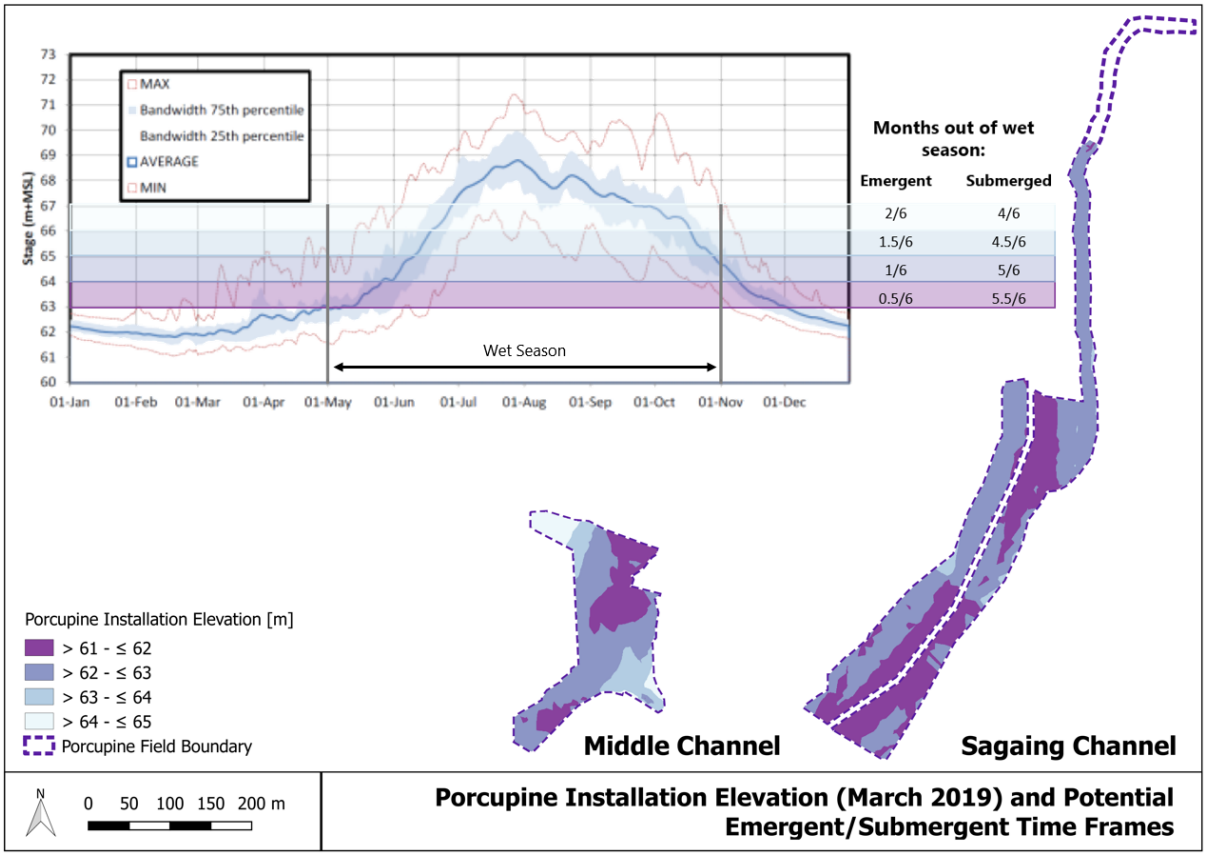

Figure 4.5: Porcupine installation elevations (March 2019), and potential time emergent or submerged during wet season. The majority of porcupines are submerged at least 5 out of the 6-month wet season. Note that porcupines are submerged at the stage equal to their installation elevation plus their effective height (2m). Stage diagram adapted from [28], Figure 2.8, using data from DMH (Department of meteorology and hydrology). Installation elevations were not available for the northern portion of the Sagaing porcupine field.

In addition, if the bed level lowers (due to erosion), or the porcupines scour and sink, their submergence ratio can increase. This can increase their resistance (if they are emergent) or decrease their resistance if they are already submerged. If the bed level rises (aggradation), the porcupine submergence ratio could increase or decrease depending on how the water level is changing.

For both Middle and Sagaing channels, the lowest porcupines are generally located towards to the center of the low flow channel, as shown in Figure 4.5. Sagaing channel has an additional navigation channel that approximately follows the channel thalweg. Therefore we could expect that the porcupine placement will attract flow towards the center of the channel and away from the banks; however, as discussed further below, the upstream backwater curve created by a transverse resistance gradient (less resistance downstream along the inner bend) can push flow upstream towards the outer bend.

4.2.2 Sediment Load and Geological Conditions

The Ayeyarwady River has the 5th largest sediment load of any major world rivers with an abundance of fine but non-cohesive sediment [76]. The bed material is primarily sand with up to 5% silt and 2% gravel [30]. The exact sediment load and distribution of sediment loads between the channels during the study period is not known; however both bedload and suspended sediment, including washload, can be expected. The porcupines may influence both bedload transportation and suspended sediment transportation in different ways, as discussed below.

4.3 Pilot Study Performance Criteria

The primary objective of the porcupine implementation in the pilot study was to increase the roughness in the side channels to maintain the current discharge distributions between the primary and secondary channels and prevent a main channel shift to one of the secondary channels. The increased roughness of the channels can raise the upstream water level attracting flow to the main (Mandalay) channel. While increased sedimentation (raising the bed level of the secondary channel) can also contribute to maintaining discharge distributions in the main channel in the long term (by attracting less flow to the secondary channels), sedimentation within the porcupine field was not the main objective. Unfortunately, water level information for the primary or secondary channels is not available during the study period. Therefore, it is not possible to estimate how the porcupines may have influenced the discharge distribution during this time period. The following analysis focuses on the potential impacts of porcupines on the local morphology, rather than addressing if the porcupine fields achieved this objective.

4.4 Expected Morphological Impact of Pilot Study Porcupines

From the results of the previous chapter, areas of the pilot study porcupine fields where we might expect erosion or deposition are discussed; however, it is important to remember that flow conditions and likely the upstream sediment load have been changing over the course of the wet season. The expected patterns can change as feedback mechanism translate morphological impacts back to flow-field impacts, back to morphological impacts.

As seen in the previous chapter, sedimentation or erosion patterns can be different at the edges of a porcupine field versus far from the boundaries. For the pilot study porcupines, with an initial 'transitional' or 'dense' behavior, we might expect deposition just inside the lateral edges of the field, downstream from the leading edge, and downstream of the field. Deposition or erosion could be present at the leading edge depending on the effective field density and flow conditions; however, as porcupines are buried and the behavior transitions to 'sparse' net erosion or deposition within the field is possible. Erosion is more likely in deep areas of the channel, where velocities will be highest, and lower at higher elevations such as the edges of the channel or along the downstream end of mid-channel bars. Finally, under emergent conditions transverse resistance gradients can be expected to push the water towards areas of lower resistance (the outer bend or the bare channel without porcupines), but this effect will be diminished as water levels rise and all porcupines become submerged.

4.5 Analysis of Morphological Changes

4.5.1 Topographic Evidence

Figure 4.3 gives an overview of the location of the topographic (survey) measurements for Sagaing and Middle Channels in January and November 2019. The combined location of the two sets of porcupines is shown for reference because the site photographs presented in Section 4.5.2 show the combined field. The elevation changes of each channel and the potential influence of porcupines on local morphology is discussed in the following section.

Middle Channel

Figures 4.6 and 4.7 show the results of the survey measurements for each month, and the resulting elevation differences (in m above MSL) respectively, for Middle Channel. For orientation, the outline of the November 2019 bathymetry is provided on top of the January 2019 survey results (green outline). Upstream of the porcupines three trends are observed. First the low-flow channel along the eastern side (outer bend) of the channel narrows and deepens, shifting the thalweg closer to the outer bank. Second, a zone of light accretion (approximately 1 m) is observed in the center of the channel. Finally, from 0 to 200 m upstream of the porcupines a large scour hole has developed with up to 6 m of elevation loss. Within the porcupine field the elevation remained relatively stable with localized areas of erosion or accretion. Downstream of the porcupines some accretion has occurred on the western edge (inner bend) of the channel, while in the center of the channel some erosion has taken place. In the small side-channel

to the west of the porcupine placement accretion has occurred on the northern side and erosion on the southern inside, indicating that the channel entrance is likely shifting to the south.

Sagaing Channel

A similar phenomenon is observed in Sagaing Channel as Middle Channel upstream of the porcupines: the low-flow channel is narrowed and deepened, shifting the thalwag closer to the outer (eastern) bank (Figure 4.8). The thalweg now follows the path of the porcupines. A portion of the inner sand bar is eroded and deposition has occurred in the channel center, adjacent to the placed porcupines. This sedimentation area extends from the upstream extent of the bathymetry to the porcupine field, and extends a certain distance into the field along the inner bend. The low-flow channel extends almost the entire length of the porcupine field along the outer bend, with the highest levels of erosion found at the furthest upstream end of the bathymetry measurements. The bank along the outer channel bend shows accretion. Overall, Sagaing channel shows lower extreme values of sedimentation or erosion than Middle channel (Figure 4.9).

New Channel

No porcupines were placed in New Channel during the 1st dry season; however, we can examine the morphological changes and compare them to the channels without porcupines. Figure 4.10 shows the morphology in January and November, and Figure 4.11 shows the elevation change. In the study area, the channel meanders from a western outer bend in the north to an eastern outer bend in the south. The general shape of New Channel did not and the thalweg follows the same line from January to November; however, the channel had deepened significantly, and some bank erosion has occurred in outer bed areas of the channel indicated by 4.5 to 6 meters of elevation lost. The elevation remained neutral or lost up to 2 meters in the center of the channel, and on the outer banks remained neutral or gained up to half a meter of elevation. New Channel appears to be attracting discharge and growing.

Moe Meik Channel

Like New Channel, Moe Meik Channel did not have any porcupines installed during the first dry season. Figure 4.12 shows the morphology in January and November, and Figure 4.13 shows the elevation change between the two surveys. Moe Meik Channel shows very little change. The form has remained the same, with small amounts (0.5 to 1 m) of erosion in the deeper parts of the channel, and small amounts of accretion in the elevated portions of the channel bed, with with exception of a portion of a central bar in the channel center that was partially eroded.

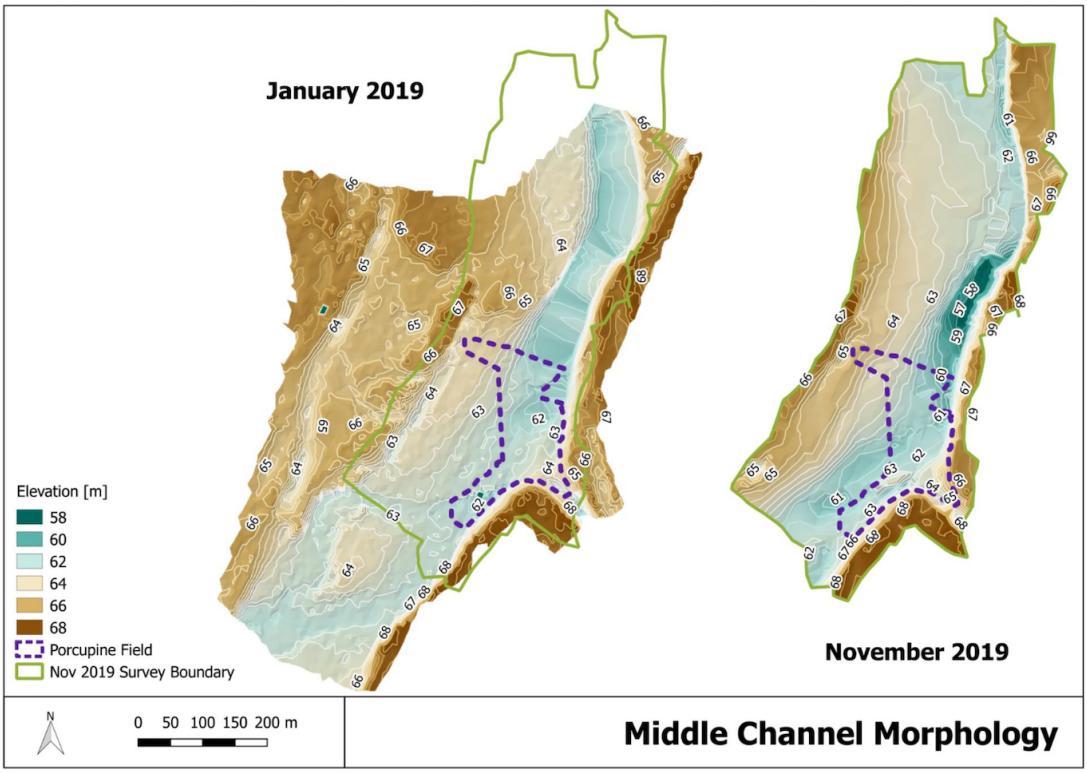

Figure 4.6: Morphology evolution of Middle Channel: January 2019 versus November 2019

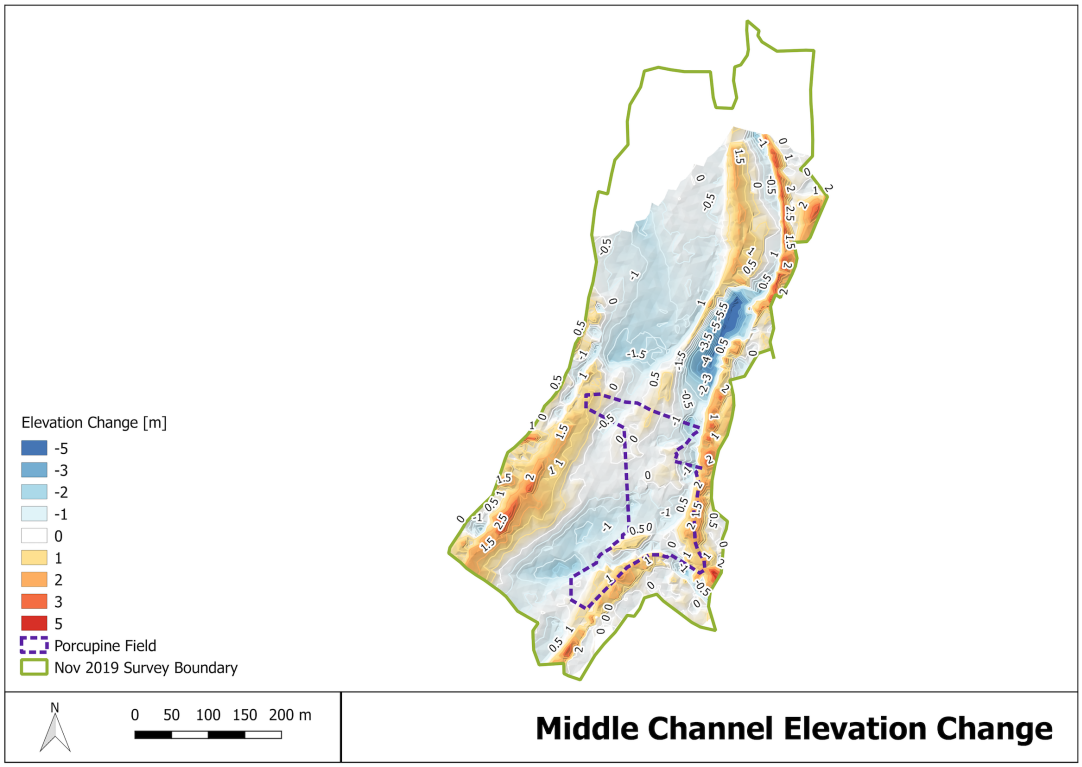

Figure 4.7: Differential Topography of Middle Channel: Elevation changes from January 2019 to November 2019

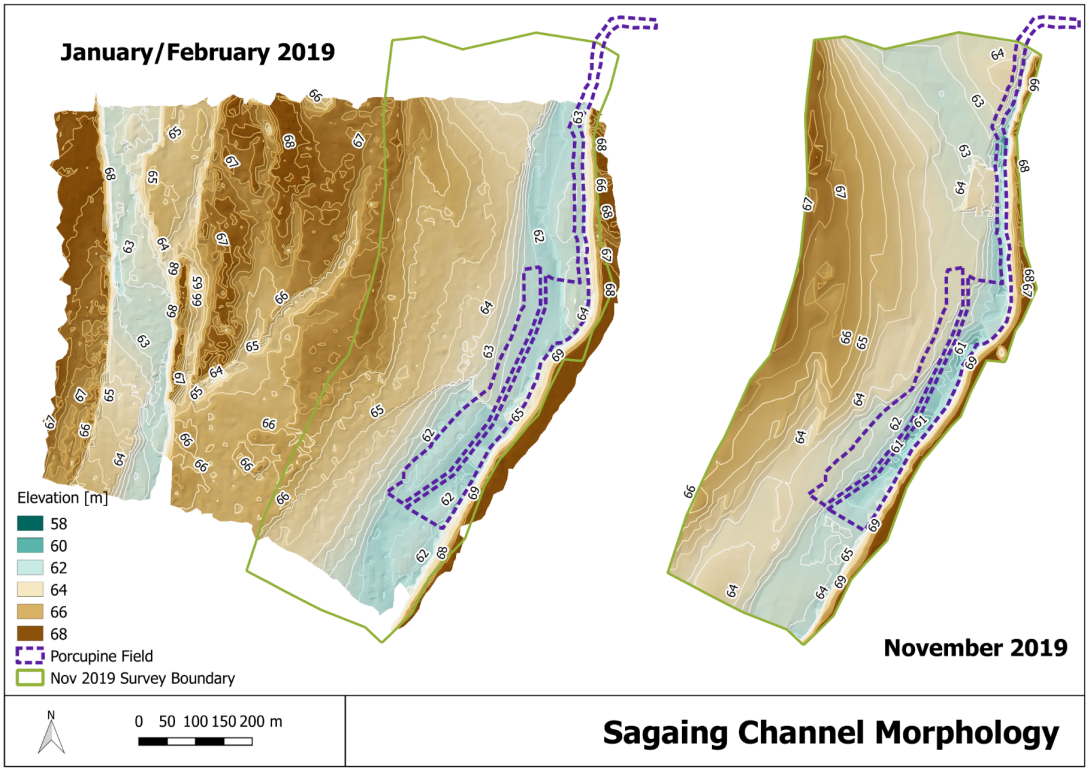

Figure 4.8: Morphology evolution of Sagaing Channel: January 2019 versus November 2019 (Note: New Channel is shown the left [survey in February 2019] and Sagaing Channel [survey in January 2019] is shown on the right.)

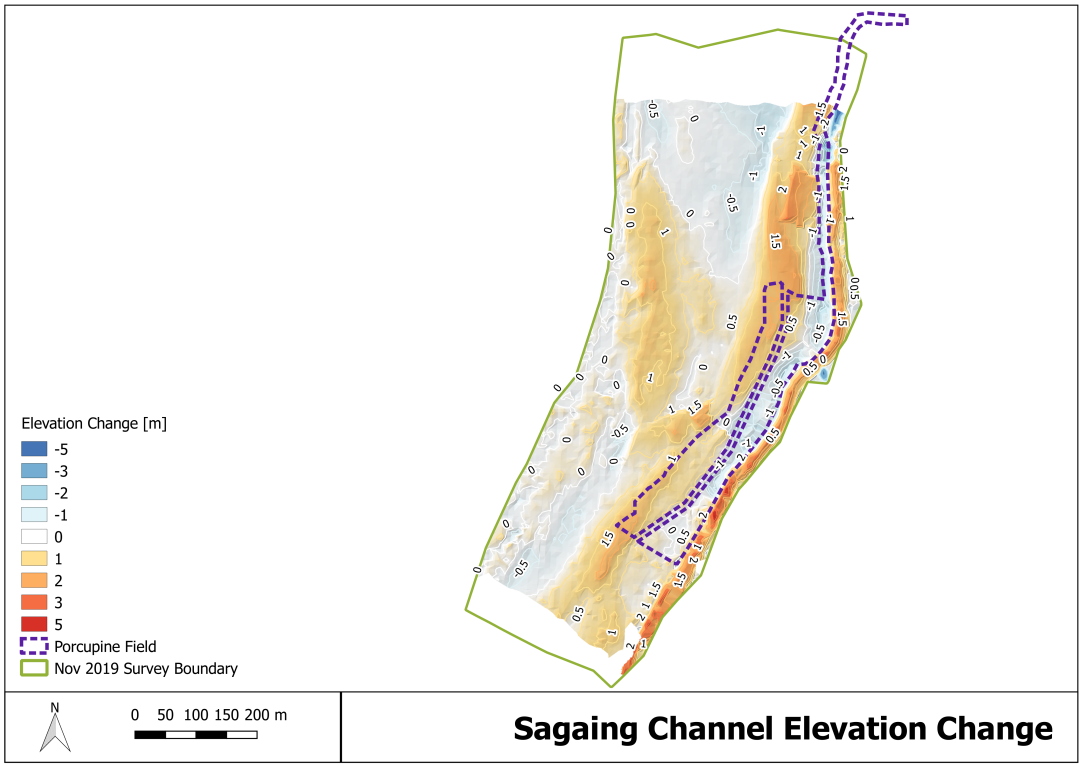

Figure 4.9: Differential Topography of Sagaing Channel: Elevation changes from January 2019 to November 2019

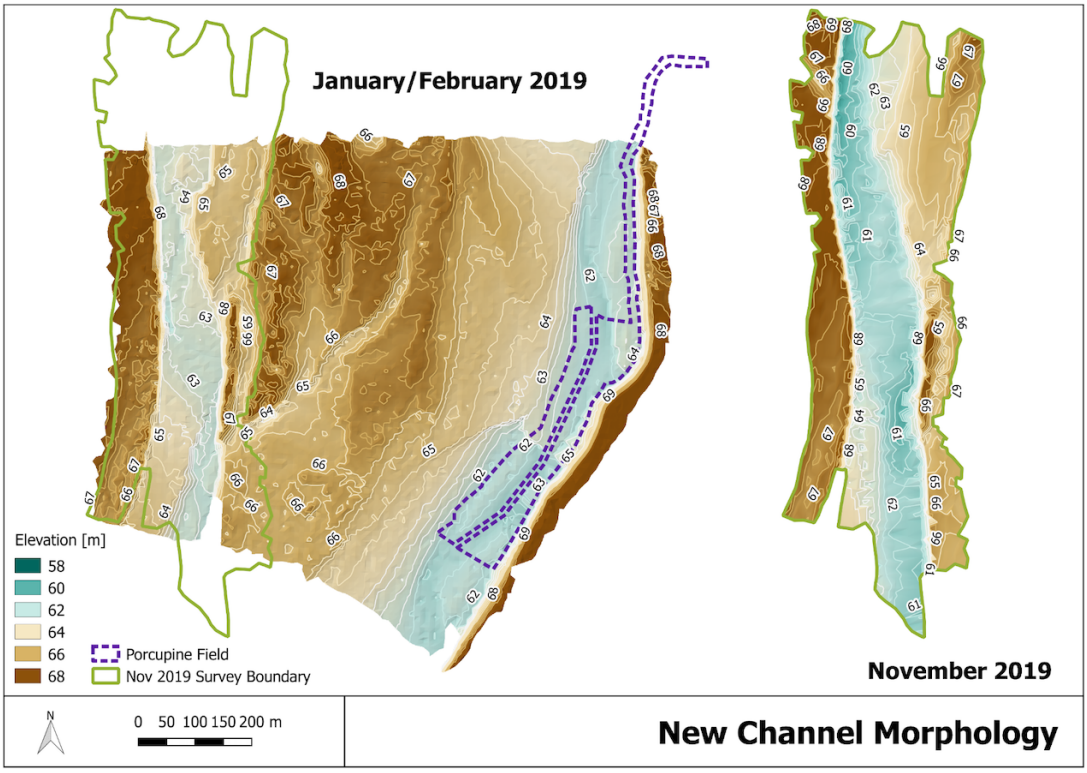

Figure 4.10: Morphology evolution of New Channel: February 2019 versus November 2019. (Note: New Channel is shown the left [survey in February 2019] and Sagaing Channel [survey in January 2019] is shown on the right.)

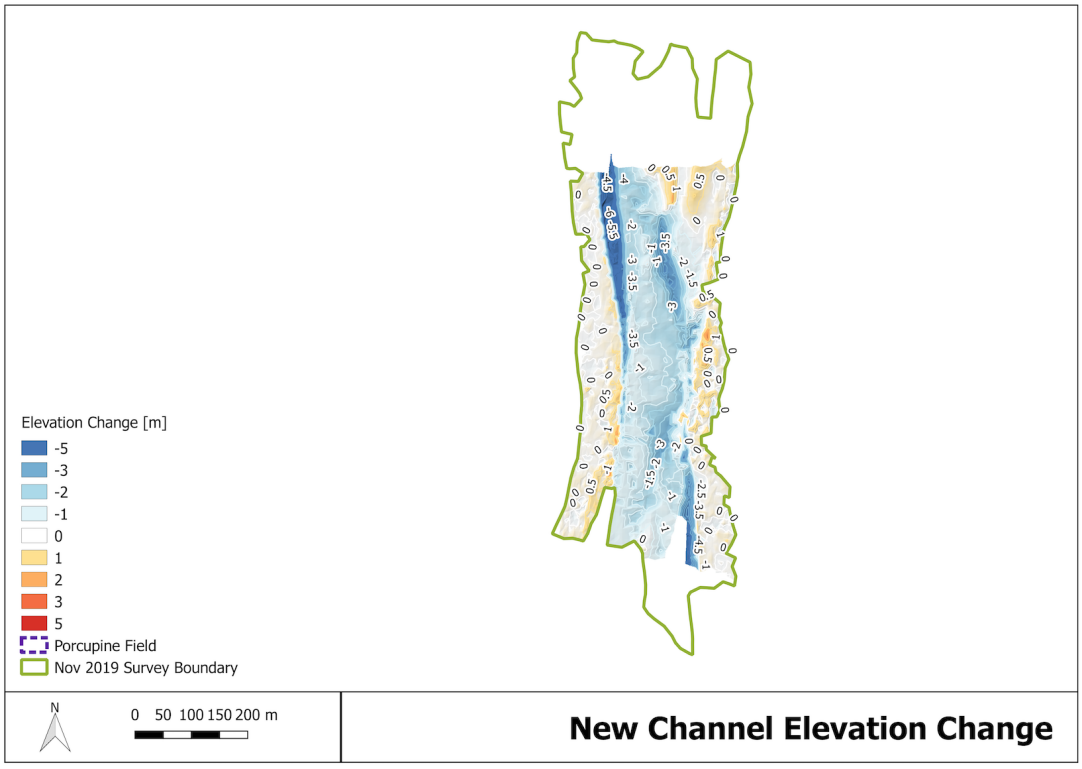

Figure 4.11: Differential Topography of New Channel: Elevation changes from February 2019 to November 2019

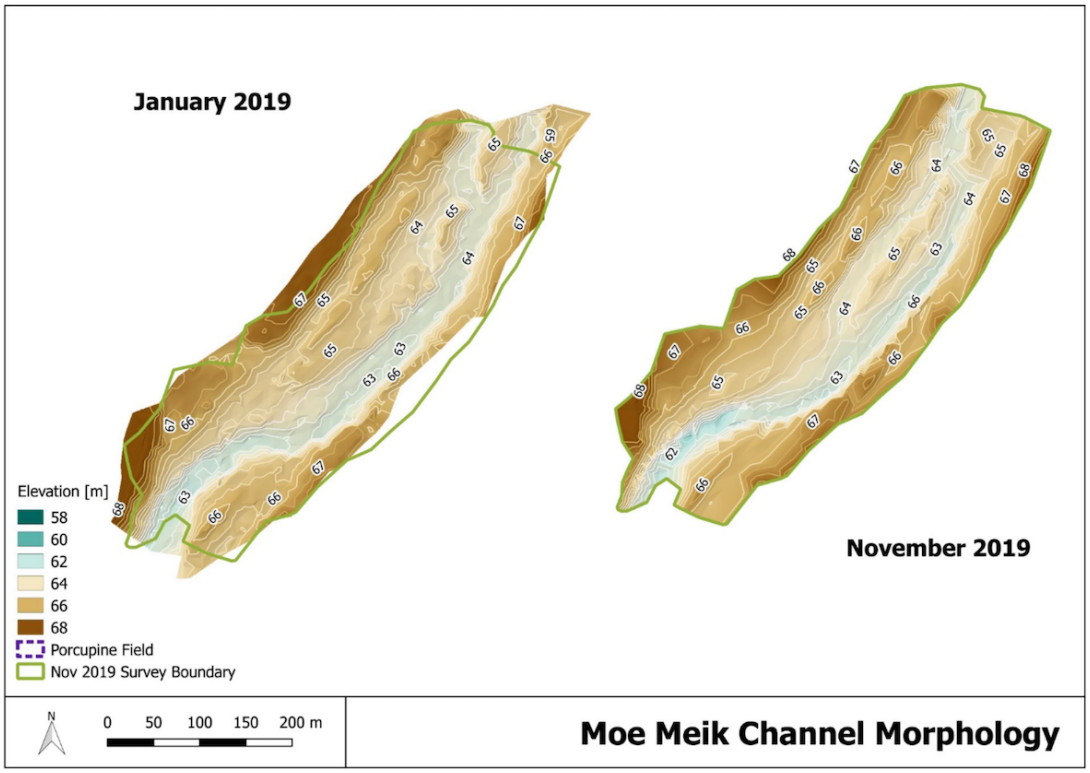

Figure 4.12: Morphology evolution of Moe Meik Channel: January 2019 versus November 2019

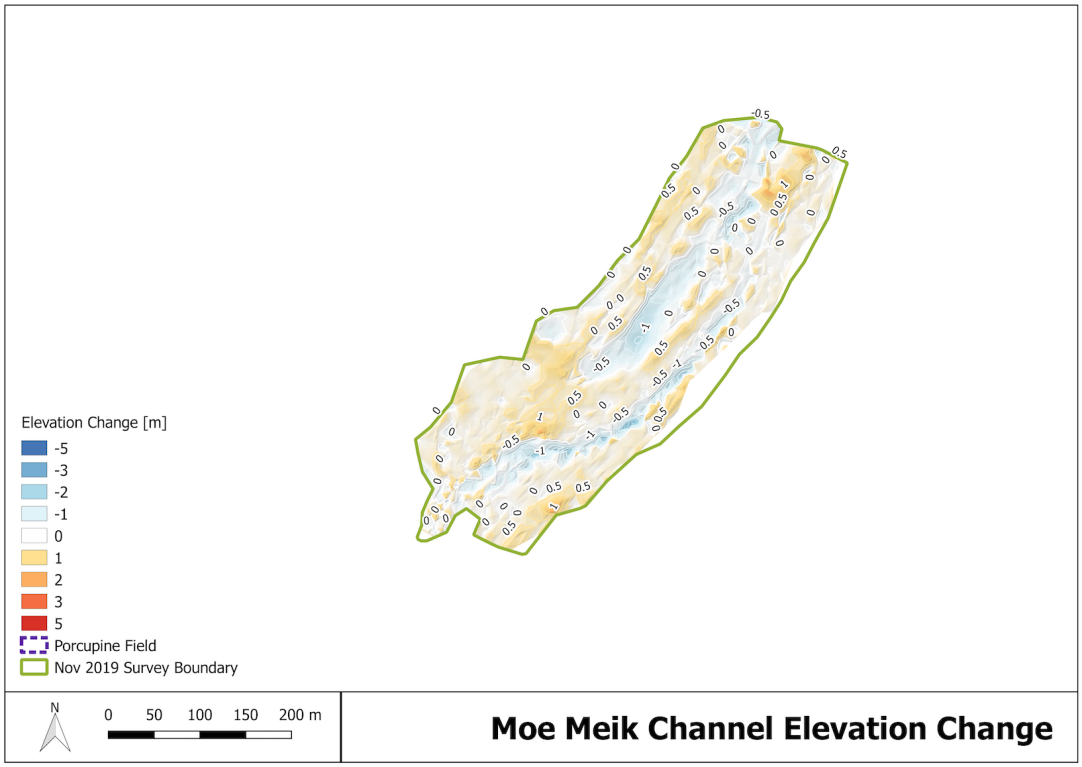

Figure 4.13: Differential Topography of Moe Meik Channel: Elevation changes from January 2019 to November 2019

4.5.2 Photographic Evidence

Photographs of the final porcupine installation (1st and 2nd dry season porcupines together) were taken by RHDHV personnel in February 2020. 2nd dry season porcupines can be distinguished from 1st dry season porcupines because they are generally all firmly lying on the top of the bed and do not show water staining (1st dry season porcupines are darker in color than the 2nd dry season porcupines).

Middle Channel

Figure 4.14 shows photographs from Middle channel. Porcupines installed during the first dry season have sunk significantly into the bed; although the bed level changes within the porcupine field were generally on the order of +/- 1 m. This can indicate that porcupines were sinking into the bed, rather than only sedimentation occurring within the porcupine field, although it can also indicate erosion followed by deposition. Bank erosion is observed next to the large scour hole. Debris is observed in some porcupines. Significant amounts of debris caught in porcupines can reduce their permeability and increase their resistance.

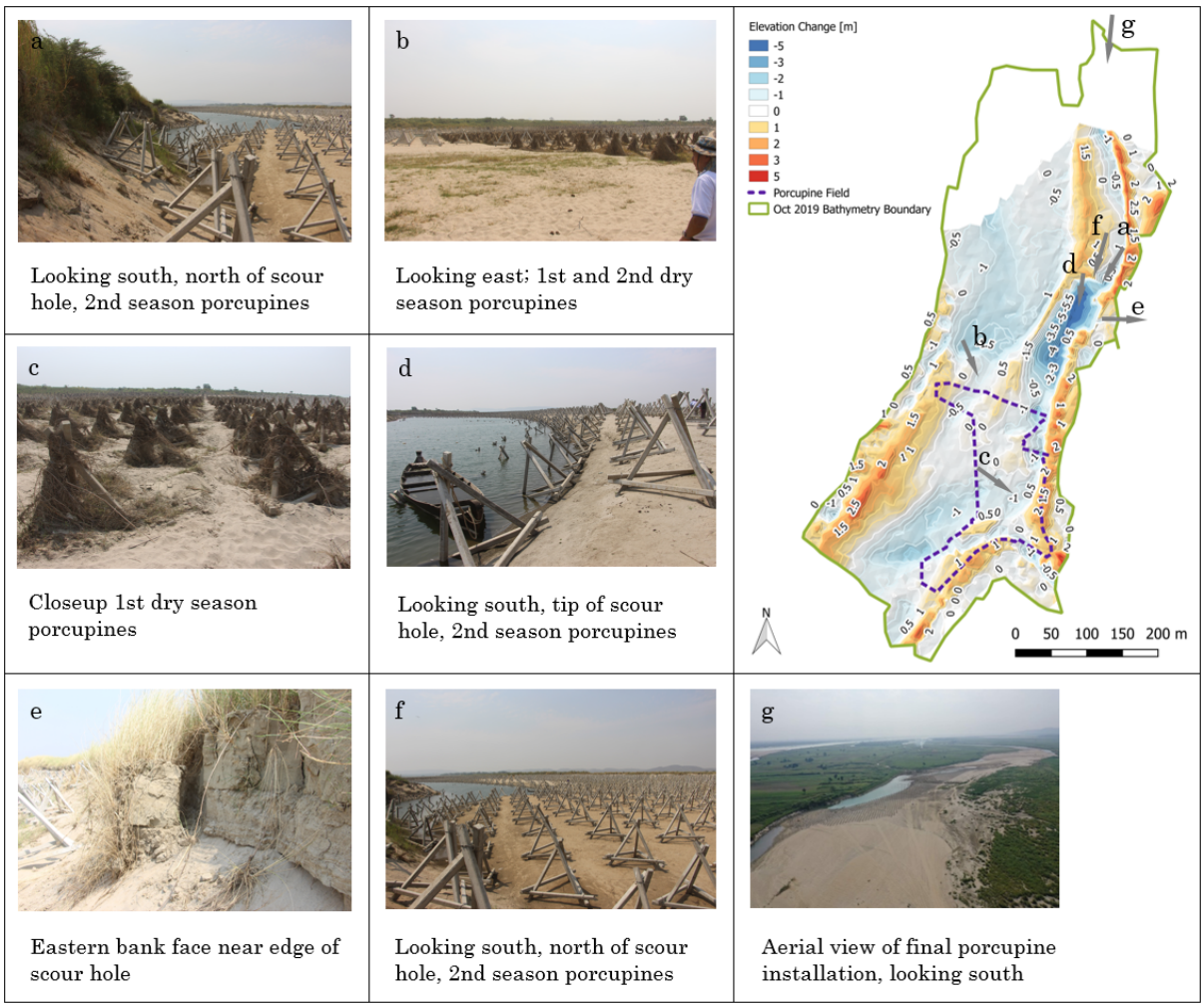

Figure 4.14: Site photographs of porcupine installation in Middle Channel, February 2020. Grey arrows indicate approximate position and direction of photographs. Photograph (g) from [18], (b)-(j) from RHDHV

Sagaing Channel

Figure 4.15 shows photographs of porcupines installed in Sagaing Channel during the first and second dry seasons. The porcupines located toward the center of the channel have been significantly buried. Bed elevation changes in this area are on the order of +1 to +2 m. It is unclear if these porcupines have sunk into the bed or have only had sediment deposit around them. Photograph h shows completely buried porcupines (foreground, right of navigation channel). Porcupines near the bank in photo e experienced approximately 1 m of elevation loss; however, they are still buried above the horizontal bars, indicating that they have sunk significantly into the bed or this area experienced deposition after first being eroded.

Figure 4.15: Photographs of porcupine installation in Sagaing Channel, February 2020. Grey arrows indicate approximate position and direction of photographs. (a) from [18], (b)-(g) from RHDHV

4.5.3 Landsat Aerial Imagery Evidence

Landsat imagery from the study period can be used to asses what factors, external to porcupines, might be influencing the elevation changes observed in the channels. These factors could include sand bars migrating into or across the channel entrances, potentially impacting sediment or discharge distributions; changing water levels; and the physical placement of channels relative to the main channel and to each other. While Landsat imagery could be used to evaluate bank and channel migration in the long-term, over the short study period (May to November 2019), and given the coarse resolution of Landsat data (30 m), only a qualitative comparison is made for now. In addition, the imagery is only available every 5-10 days and is intermittently obscured by clouds (particularly during the heaviest period of the wet season - June, July and August), therefore a detailed analysis of water level changes in the channels is not possible.

Figures 4.16 and 4.17 show Landsat aerial imagery during the study period from April 1, 2019 to December 2, 2019 for the Mandaly region and the pilot study area, respectively. Low water conditions (April and December) can be compared to high water periods (July) and intermediate water levels (e.g. 11/05, 28/09). During the dry season the secondary channels are completely cut off from the main channel. At high water the islands in around the secondary channels are nearly completely inundated.

The images do not clearly indicate external factors that can be influencing the discharge or sediment distribution in the secondary channels, such as bars migration at the channel entrances. That said, at high flows, when we might expect the most channel shifting, movements are obscured from view. We can note a few changes to how water enters the secondary channels from the main channel.

First, we observe that New Channel has deepened. When water levels started rising in April, Sagaing and Middle channels are the first to receive flow; but in December as water levels are receding New Channel still has flow when Sagaing and Middle Channels are cut off from the main channel.

Second we see that in 2019, the entrance angle for both Middle and Sagaing Channels shifted, result in a line of flow directly into the islands on the eastern sides of the channels. In April 2018, the angle from the main channel was sharper, resulting in a gentler approach towards the island edge at the outer bend (at least at low or intermediate water depth). Compare Figure 4.18a (April 2018), and Figure 4.18b (December 2018). The channel shifted angles, and the shift was still present in April 2019 (Figure 4.18c), at the start of the wet season. But by December 2019 (Figure 4.18d), at the end of the study period, the channel has shifted further, to create a very sharp angle directly with the bank of the outer bend. The flow pattern observed in the aerial imagery matches the morphology changes observed in those two channels over the study period. This shift is likely due to upstream morphological influence as opposed to the porcupines; however, it does change how the flow enters the porcupine field. If this channel configuration results in higher velocities as the flow enters the porcupine field, there is potential for higher scour at the leading edge. The changing low flow channel configuration will also alter where the flow enters the porcupine field and can impact porcupine field performance.

Relative to each other, Sagaing and Middle Channel have higher bifurcation angles with the main channel than Moe Meik and New Channels. These two channels also have higher radii of curvature at the channel entrance. New channel might have attracted more flow due to lower resistance from a low entrance angle. The bifurcation angle brings a second consideration. At low and intermediate flows, water entering the secondary channels will be directed through it, in the direction of the channel; however at high flows (e.g. July), part of the water from the main channel can pass over the secondary channel, as the islands are flooded, and potentially lead to sedimentation in the secondary channel which now acts as a sediment trap [39].

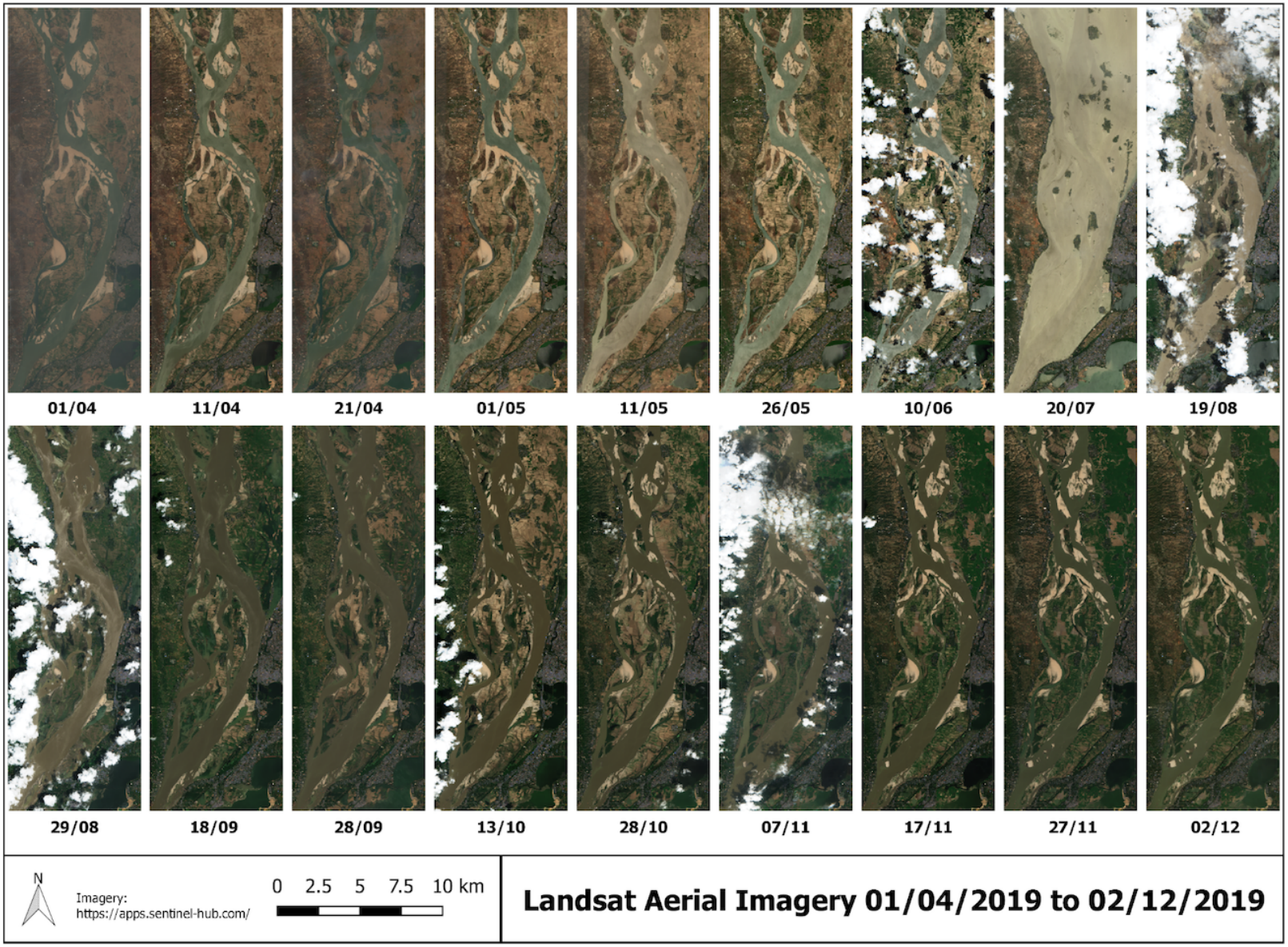

Figure 4.16: Landsat aerial imagery from April 1, 2019 to December 2, 2019

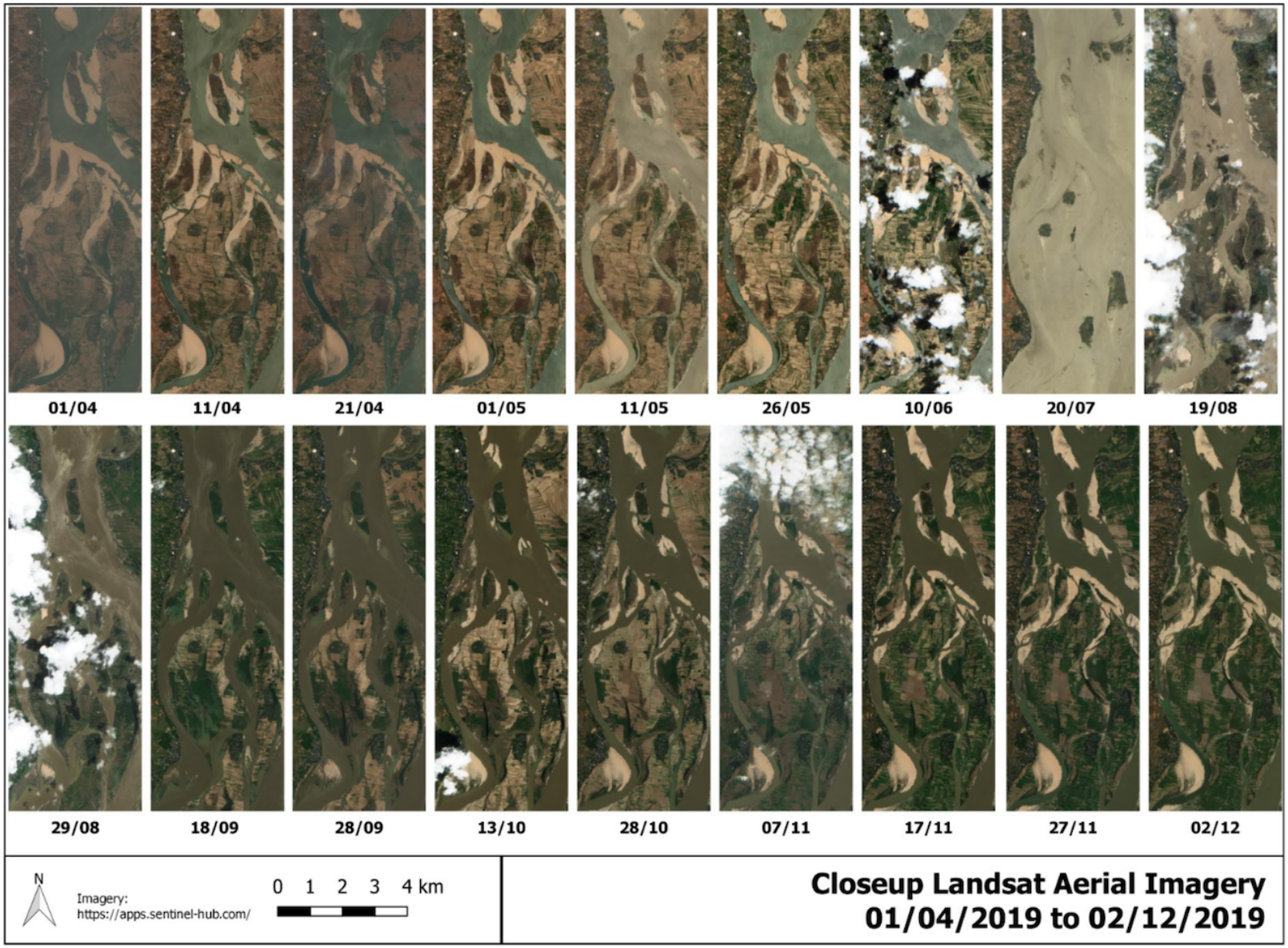

Figure 4.17: Landsat aerial imagery from April 1, 2019 to December 2, 2019, closeup of pilot study area

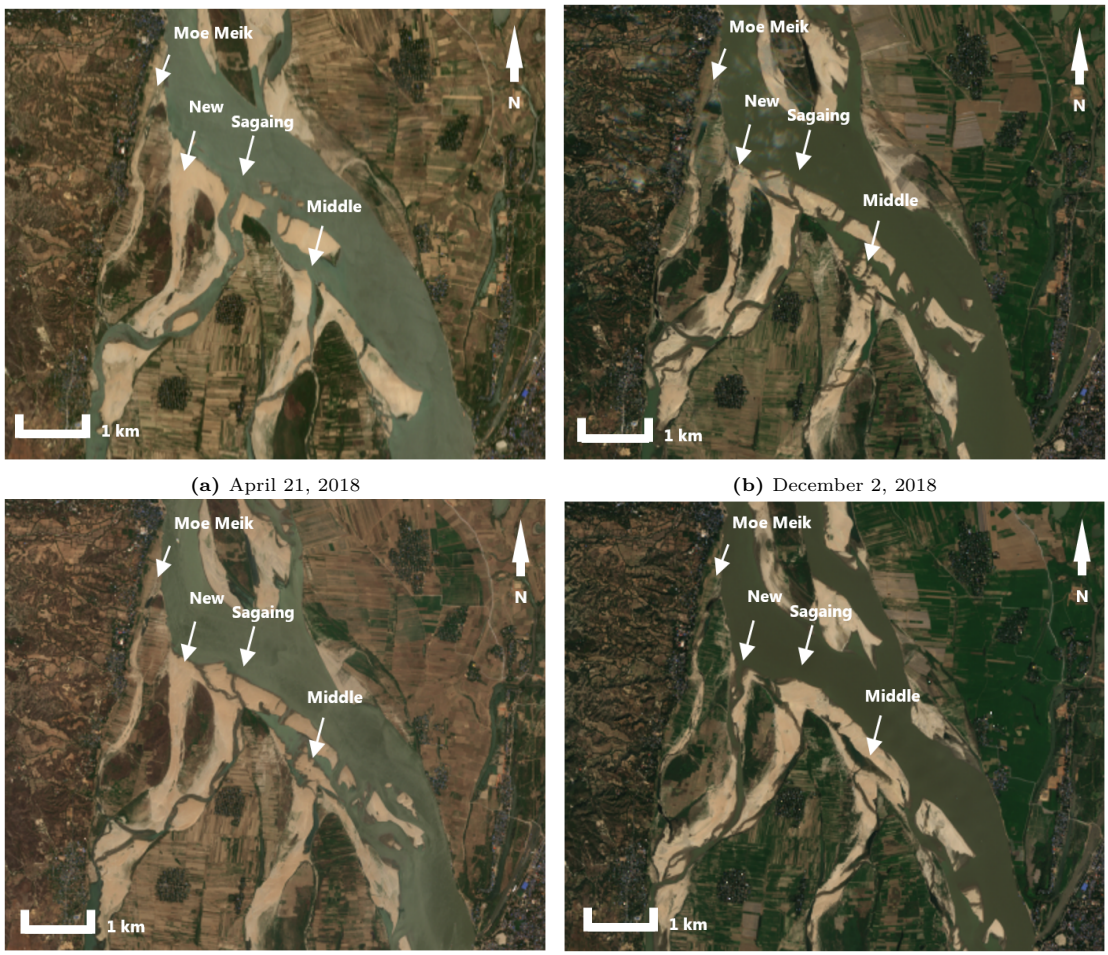

(a) April 21, 2018

(b) December 2, 2018

(c) April 11, 2019

(d) November 27, 2019

Figure 4.18: Angle low-flow channels enter secondary channels (Sagaing and Middle) from the Main Channel shifted from 2018 to 2019, resulting in flow nearly perpendicular to the outer bend. Four images from the start (a), (c) and end (b), (d) of the wet season. Landsat aerial imagery from: http://apps.sentinel-hub.com

4.6 Discussion

This section evaluates possibilities for how the porcupines have influenced the local morphology during the pilot study period; however, there are many external factors that could be influencing the local morphology not related to porcupines. The lack of historical data does not allow us to fully evaluate the changes in morphology compared to typical changes observed during the wet season, or to exclude any factors such as changes in upstream sediment load or changes in discharge or sediment distribution in the secondary channels. These conditions could exacerbate, diminish or otherwise change the expected behavior of the porcupines.

The topography changes in Middle and Sagaing channels showed similar phenomena although lower overall levels of erosion or sedimentation were observed in Sagaing channel compared to Middle channel. The flow appears to be diverted towards the outer bed of the channel. The low-flow channel in the outer bend narrows and deepens. The inner bend erodes slightly, and sediment is deposited in the center of the channel. This was observed in both channels even though, at its widest, the porcupine field in Middle Channel covered the entire channel width whereas in Sagaing channel, the initial porcupine installation only blocked part of the channel width (along the outer bend). This shifting to the outer bend could be due to transverse resistance gradients caused by uniform-height porcupines being placed across a channel

with a higher elevation in the inner bend versus the outer bend. For the same flow, the porcupines in the inner bed will offer more resistance than the porcupines in the outer bend, as resistance is higher for emergent porcupines or for lower submergence ratios. This transverse resistance gradient can push the water upstream to the outer bend.

The exact elevation of the porcupines after one wet season is not known; however, from the photographs, it appears that porcupines located in erosional areas sunk more into the bed than porcupines located in depositional areas. Figure 4.15b (the center of the channel), show 2 m high porcupines sticking out of the bed approximately 30 cm in an area that experienced one to two meters of sedimentation. On the other hand, Figure 4.15e, shows porcupines buried beyond the horizontal bars, even though they were located in an area that experienced 1 to 2 m of elevation loss. However, as stated above, it is unclear how much the porcupines sunk versus deposition that followed erosion. In addition, it is not clear how much of the sedimentation's (or erosion) could have been caused by porcupines versus external morphological influences.

The sinking of porcupines in erosional areas could explain why, in Sagaing Channel, we observe net elevation loss through most of the northern area of porcupine installation. As observed by Nientker in [46], when the velocity in the channel is above the critical velocity, erosion is observed at the leading edge of the porcupine field and the porcupines sink into the bed. Indeed, the Government of India Central Water Commission Handbook on Anti Erosion and River Training Works does not recommend placing porcupines in high energy areas citing ineffectiveness [10].

Once some porcupines have sunk, they loose their effectiveness in reducing velocities and trapping sediment when the approach velocity is too high. As upstream porcupines sink, their capacity to reduce velocities diminishes, and downstream porcupines will be subject to higher and higher approach velocities. In this case, it is unclear if the velocities in the channel would have been too high regardless of the porcupine placement, or if the placement of porcupines contributed to the narrowing and deepening the low-flow channel. Indeed, it is possible that the shifting of the thalweg is a natural or unrelated occurrence, as evidenced by the Landsat imagery (Figure 4.18) and without the presence of porcupines erosion in that area would have been worse. However, considering that the phenomena was observed in both Middle and Sagaing channels, with different porcupine setups, the addition of a transverse gradient in downstream roughness in the channel likely contributed to the formation of the narrow, deep outer bend low-flow channel.

Within the porcupine field, net deposition is not observed in either channel. Middle channel shows a neutral field elevation, with small local areas of elevation loss or gain. Sagaing channel tends to show deposition along the side of the porcupine field closer to the inner bend, and slightly downstream. The Middle channel observations are consistent with the behavior we might expect of a 'sparse' field, where velocities are not sufficiently reduced to encourage deposition, or turbulence is able to entrain sediment within the field; however the behavior in Sagaing channel could suggest that the inner porcupines were more effective slowing velocities and retaining sediment, than the porcupines located in the outer bend. However, the upstream sediment supply or the natural variation in velocities across the channel could also have influenced, even strongly, the deposition in those areas. The Sagaing porcupine field was also much longer, which may have helped in reducing velocities and encouraging deposition both within and downstream of the field; however many of the first season porcupines are significantly buried. Therefore it is likely that those porcupines will not be as effective during the coming wet seasons.

Neither Middle nor Sagaing channels show a definite trend of erosion along the lateral edge of the porcupine field, although local erosion along parts of the lateral edges is observed. This could further support the hypothesis that the design porcupines exhibit a 'transitional' or 'sparse' behavior, where the lateral shear is not strong enough to significantly increase shear stresses along the field edges. It is possible that later shear layers were stronger at the start of the wet season, before porcupines had lost elevation or become buried, and that subsequent deposition has hidden any evidence of earlier scour.

Finally, we need to consider that the porcupine fields placed in Middle and Sagaing channels were not the full design configurations. It is possible that more deposition would have be observed in the channels if the fields had been larger. The impact of the erosion at the leading edge and sinking porcupines may have been less in Sagaing Channel. In Middle Channel, the full-size field may have led to more deposition within the field, instead the neutral elevation change observed.

4.7 Conclusions

The existing data are not sufficient to distinguish which morphological impacts can be attributed to porcupines, and which should be attributed to external factors such as variable discharge, upstream changes in channel direction, or upstream sediment supply. Nevertheless, there is evidence that transverse resistance gradients could be pushing upstream flow in both channels towards the outer bend. In addition, there is some evidence that longer or larger porcupine fields may be more effective than shorter installations. The erosion observed with the porcupine fields, particularly along the outer bed suggests that shear stresses at the leading edge, or in high-energy areas, may not be resisted well by porcupines by themselves. Additional measures might need to be considered to improve their effectiveness in areas of high shear stress. The flexibility of the porcupine system design is an advantage here, where after a wet season additional porcupines could be added if necessary. The burial of porcupines over time, particularly through erosion where the base elevation of the porcupine is lost, is a subject that requires further research at it will be key in how the porcupine field will perform, and how its performance can be predicted with models, in the long term.

Chapter 5

2D Numerical Modelling of Porcupine Fields

This chapter evaluates options for 1D or 2D hydrodynamic modelling of porcupine structures in Delft3D. First, an overview is given of how resistance fields, such as vegetation or porcupines (often schematized as rigid cylinders), can be represented in fluid flow equations. Then the options for numerical parameterization of porcupines on the sub-grid level in Delft3D are presented. The performance of these representations concerning flow, turbulence and bed shear stress characteristics are explored in a 2DV model that is calibrated and compared to a flume study of porcupine field hydrodynamics [46]. Next, the performance of these representations in a 1DH model are compared against the same flume study. This comparison can help us characterizing the strengths and limitations of 1DH representations of porcupine fields, and understand if the most influential processes are being captured by the model, to more effectively interpret model results.

Note that there are a number of limitations with this modelling analysis. Several aspects of porcupines' influence on hydrodynamics is not well understood, but falls outside the scope of this thesis. This thesis will focus on 2D models, rather than detailed 3D representations of the flow field; Uncertainties that would require detailed 3D modelling for clarification, such as the detailed flow field through an individual porcupine structure or through a field of porcupines, will not be explored. In addition, porcupines will be represented on the sub-gird level, therefore it will not be possible to examine the difference in orientation of porcupine structures (such as the vertex facing upstream or downstream), even though the orientation could impact the effectiveness of the structure in retarding flow [81]. These elements will not be considered due to time considerations, lack of detailed data for calibration, as well as limitations with the ability of Delft3D-FLOW to accurately model 3D turbulence. All models in this study will focus on the behavior of a field of porcupines, rather than an individual porcupine.

5.1 Flow Resistance

In the previous chapters a conceptual model was developed to describe the likely impacts of porcupine fields on flow hydrodynamics, and their morphological consequences were explored using pilot study data. These impacts are driven by the altered hydraulic resistance offered by porcupine fields. Accurately translating that resistance into a parameter that can be incorporated into numerical models is critical to properly estimating velocities, water levels and other flow conditions that determine both the short- and long-term morphological evolution of the porcupined reach.

Numerous formulas have been developed to describe resistance in uniform (fully-developed) open-channel flow. The simplest methods are the empirically-derived bulk roughness formulations such as Chezy, Manning's n, or Darcy-Weisbach that relate bulk roughness coefficients: C (Chezy parameter), n (Manning's n), or f (Darcy–Weisbach friction factor), to flow conditions including depth-averaged velocity (u), bed slope (i_b) and the hydraulic radius (R). For a typical river the depth (d) is much greater than the width

(B) and $R = d$. The White-Colebrook relation relates the friction factor (c_f), to the Nikuradse roughness length scale (k_s), which is often approximated as $3.5d_{50}$ from empirical evidence. Details of derivations and the range of applicability of each of these methods can be found in [13, 14, 9]. Table 5.1 summarizes these formulations and their dependencies.

Formulation	Expression
Chèzy	$u = C\sqrt{Ri_b}$
Manning	$u = \frac{1}{n}R^{3/5}i_b^{7/2}$
Darcy-Weisbach	$u = \sqrt{\frac{8g}{f}}\sqrt{Ri_b}$
White-Colebrook	$\frac{1}{\sqrt{C_f}} = \frac{1}{\kappa}\ln\left(\frac{12R}{k_s+\frac{\delta}{3.5}}\right)$

Table 5.1: Roughness formulations, where κ is the von Karman constant (generally assumed to be 0.4) and δ is the thickness of the viscous sub-layer (often neglected for rough flow, which we expect in a real river).

These formulations assume a turbulent boundary-layer approach where the roughness of the bed determines the roughness length (z_0) in the logarithmic velocity profile (Equation 5.1).

$$u(z) = \frac{u_*}{\kappa}\ln\frac{z}{z_0} \tag{5.1}$$

Where u_* is the friction velocity ($\sqrt{\tau_t/\rho}$), and κ is the von Karman constant (generally taken to be 0.4). Nikuradse found an experimental formulation for the roughness height in terms of k_s, where where $z_0 = k_s/30$, [48]. This formulation typically applies when the height of the roughness elements is very small compared to the water depth ($k_s/d \ll 1$). For deeply-submerged vegetation ($h/h_v > 10$), the velocity profile can be assumed to follow a logarithmic form and vegetation can be represented using one of the roughness formulations described above [4, 70].

Porcupines, which are typically 2-3 m in height, are unlikely to be deeply submerged, even in the highly dynamic Ayeyarwady River (ten meter stage difference between high and low flows), except when the porcupines sink into the bed and only a small portion of the structure is exposed. When the roughness elements are large compared to the water depth, drag dominates the energy dissipation (resistance) over skin friction at the bed (roughness); the velocity profile is no longer logarithmic (as discussed in Chapter 2, see Figure 2.10), and other resistance formulations are necessary. Note that in addition to bottom roughness or vegetation drag, resistance can come from the channel geometry (irregularities such as bars or scour holes or variations in the cross-sectional shape), the channel alignment (curvature) or other obstructions in the flow. In addition, the resistance can change with time as discharge (water depths) change, or as the makeup of the bed material changes. The local conditions can be taken into account in computing the roughness value for a specific location. For modelling or design purposes, seasonal variations in the roughness value are often not taken into account [13].

More complete methods of representing vegetation resistance use physics-based models with potentially empirically-derived parameters. The majority of these models use the rigid-cylinder analogy, where vegetation is idealized as uniform cylinders with uniform height and spacing, arranged in a staggered, uniform, or random grid [5, 66]. These physics-based models often divide the total shear stress (τ_t) linearly into bed shear stress from bed roughness (τ_b) and vegetation shear stress (τ_v) from vegetation resistance:

$$\tau_t = \tau_b + \tau_v \tag{5.2}$$

Where in uniform, steady flow gravity and frictional forces balance to give a total shear stress of:

$$\tau_t = \rho_w g R i_b \tag{5.3}$$

Where, ρ_w is the fluid density, g is the acceleration due to gravity, R is hydraulic radius, and i_b is the bed slope. For densely vegetated channels, τ_v is generally several orders of magnitude larger than τ_b, and τ_b

can often be neglected [54, 70]; however, the bed friction can be important in sparsely vegetated channels, and neglecting this term in sparse beds can lead to erroneous predictions of sediment transport.The vegetation resistance is often expressed as drag force:

$$F_{\mathrm{d}} = \frac{1}{2}\rho_w C_{\mathrm{D}} \bar{u}^2 A \tag{5.4}$$

Where, C_d is the apparent drag coefficient, u is the velocity approaching the stem, and A is the cross-sectional area. The drag coefficient is not a constant value but a function of the geometric properties of the object in the flow (porcupine beams) and the hydraulic conditions they are subject to (Hygelund, 2003). Characterizing an exact trend is difficult because of the complex geometries and behavior of vegetation under different flow conditions and submergence ratios [66]; however, for vegetation represented as rigid cylinders, which most closely resembles porcupine beams, drag coefficients have been found to decrease as the element Reynolds number (Re_e, Equation 5.5) increases, as the bed roughness increases, and as the element density decreases (for $Re_e < 600$) [62, 23]. For high Reynolds element numbers ($Re_e > 900$) the drag coefficient increases for decreasing density [44, 52].

$$\mathrm{Re}_e = \frac{\bar{u}D}{\nu} \tag{5.5}$$

Where $\bar{u}$ is the depth-averaged velocity, D is the cylinder diameter, and ν is the fluid kinematic viscosity. Drag coefficients measured from studies of vegetation reveal a wide range of values even for vegetation of similar geometric properties and similar element Reynolds numbers [66]. The Nientker (2018) flume study found drag coefficients for a short field of submerged porcupines over a fixed bed in the range of 3 to 5.5, with higher density fields having a higher drag coefficient for the same velocity. For fields of submerged porcupines over a mobile bed the drag coefficient was approximately 1. This result is consistent with [23] and results reported in [12], where the increased bed roughness found in field studies versus flume studies resulted in decreased drag coefficients for similar hydrodynamic conditions and vegetation properties. Nientker did not correct the energy loss for the effects of the sidewalls and base of the flume, therefore the porcupine drag coefficient is likely smaller than the values reported.

Not only is the apparent drag coefficient complicated by the exact physical make-up of the plant or porcupines, but comparing values in the literature to determine an appropriate C_d is complicated because of different equipment setups and experimental techniques, as well as the fact that the presentation of the drag coefficient is not standardized (e.g. C_d is compared to the flow versus element Reynolds number with various alternatives for defining the vegetation- or velocity-related length scales, or the roughness of the bed or flume side-walls is not corrected in the C_d approximation, etc. [66, 12]).

Therefore, determining a universal model for the representation of the drag coefficient is very difficult, and it is unlikely that any single model will be able to represent such a large range of hydrodynamic or physical conditions to be universally applicable. This also implies that porcupines, particularly porcupines in the highly dynamic Ayeyarwady River, with the differences from vegetation noted in Chapter 2, may require singular studies to determine the appropriate drag coefficients under the range of flow regimes they experience; however, depending on the scale of the model and the other inherent model uncertainties and assumptions, a precise value for the drag coefficient (which should change in time if flow conditions and bed roughness changes), may not be critical for long-term modelling analyses. Indeed, many authors studying vegetation, whether real or represented as rigid cylinders, assume a C_d of one or close to one, and still find reasonable agreement between analytical models and experimental data [32, 66, 5].

Ultimately, the goal is to use the drag force (with the appropriate C_d) in the momentum balance to find a global resistance factor (e.g. Chezy value) for the vegetation or porcupine field, to close the combined continuity and momentum shallow-water flow equations. Some of the physics-based models only look at emergent flow conditions, but models that examine submerged flow conditions (take into account a submergence ratio) generally assume two zones of flow: a lower zone through resistance elements (canopy) and a higher zone above (overflow) [27, 60, 64, 68, 22, 6, 77, 11, 80, 70]. Figure 5.1 shows just two examples of how the four-part velocity profile (Figure 5.1a) of a dense vegetation field can be simplified into two layers. Figure 5.1b represents the two-layer model used by the Baptist model implemented in Delft3d-Flow. Note that other simplifications and configurations are possible, where some authors may use three ([70]) or four zones ([6], 'analytical approach').

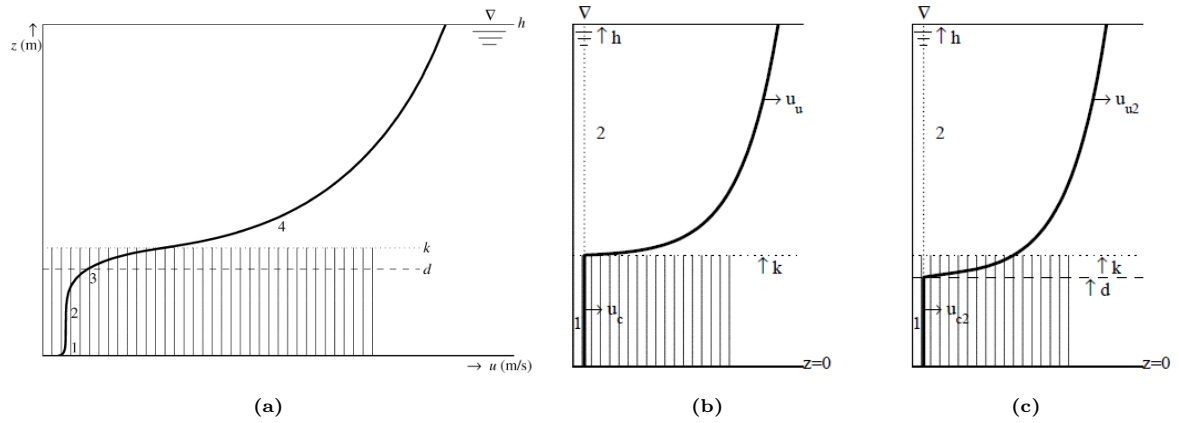

(a) (b) (c)

Figure 5.1: (a) Four zones of the fully-developed velocity profile through dense vegetation. (1) logarithmic boundary layer, (2) uniform canopy zone, (3) exponential profile at top of canopy, (4) logarithmic overflow profile, where k is the cylinder height, d is the depth of penetration of turbulence in the canopy (zero-plane elevation of the logarithmic velocity profile), h is the water depth and u is the velocity. The distance between k and d is equivalent to δ_e in Figure 2.10. Taken from [6]. (b-c) Two simplified 2-layer models of flow through vegetation, where u_c is the velocity through the canopy, and u_u is the velocity in the overflow (a) Uniform flow through the canopy (1) and logarithmic profile through the overflow (2), with a zero-plane displacement at $z = k$, and (b) uniform flow through the canopy (1) and logarithmic profile through the overflow (2), with a zero-plane displacement at $z = d$. Taken from [5].

The models generally differ in the velocity profiles they assume for each zone, the number of zones they include, how they account for the transition from one zone to the next (generally requiring empirical coefficients to satisfy boundary conditions), characterize the turbulence length scale (again often using empirical coefficients) and how the canopy velocity is defined or averaged for input into the resistance formulation. The need to complete the models with empirically-derived coefficients can limit their applicability outside the vegetation (or rigid cylinder) characteristics and hydrodynamic conditions the data used to fit the model were derived from. Details and comparisons of the various models can be found in [4], [20] and [66]. Several models show good agreement to a wide variety of input conditions, with the model of Baptist (2005) generally showing the best agreement to the largest range of conditions (emergent and submerged; real and artificial vegetation; rigid and flexible stems) [66]; however, all models show scatter when comparing theoretically-predicted and experimentally-measured results, particularly for high submergence ratios, that introduces uncertainty into the results obtained. The models used in Delft3D, including the one of Baptist (2005) are presented in more detail below.

5.2 Representing Resistance Elements in Delft3D-Flow

Porcupine structures impact the hydrodynamics of flow by altering the flow resistance. This can be taken into account in a Delft3D 2DV or 1DH numerical hydrodynamic model in several ways. The methods used in this analysis include adjusting the bulk roughness parameter (Chezy), representing porcupines as a permeable structure, and the use of two physics-based resistance models: Baptist and Uittenbogaard. All methods except for Baptist were explored for 2DV flows. The Baptist method and adjusting the bulk roughness parameter were applied in the 1DH model. The following section describes the theory, advantages, disadvantages and potential accuracy of each of each method in 2DV or 1DH. The detailed parameterization of each method in Delft3D-Flow is covered in the Model Setup section (Section 5.3).

5.2.1 Roughness Parameter

First, a very simplified approach to represent resistance would be to increase the bed roughness coefficient (e.g. Chezy, Manning's n, White-Colebrook (k_s) or z_0). This approach should be the least accurate of the four methods for describing flow through shallowly submerged, dense porcupines, because it is not able

to reproduce the correct variation of the velocity profile, including the inflection point at the top of the canopy. Another disadvantage of this method is that an increased roughness coefficient would impact the hydrodynamics as well as the sediment transport, incorrectly increasing sediment transport within the porcupine field when porcupine fields could have the opposite effect. Finally, the roughness coefficient is often used as a calibration parameter in a numerical hydrodynamic models. Many unaccounted for processes are subsumed in the roughness coefficient, besides simply the added roughness of porcupines [75]. Therefore, 'tuning' the roughness coefficient to account for different porcupine configurations may not be straightforward.

However, for high submergence ratios, the resistance of porcupines could simplify to a constant roughness coefficient, as it has been demonstrated to do for vegetation [4]. In addition, at a large scale the global effects of vegetation on morphological changes can be modeled using an increased bed roughness since this method correctly reproduces, to some degree, flow patterns and water depths, even if local morphological impacts are not correctly characterized due to the increased bed shear stress [5]. Therefore, while under typical flow conditions more sophisticated methods may yield better results in predicting local porcupine performance; this method may provide a simple, computationally-efficient estimate of the impact of the porcupine field on the flow, particular for long-term and large-scale morphological impacts. Therefore this method has been retained for consideration; however, for simplicity only one of the four parameters offered by Deft3D is used in this study: the Chezy coefficient.

5.2.2 Permeable Structures

Delft3D-Flow has an option to model permeable structures (porous plates) that induce energy loss on a sub-grid level. This method allows mass and momentum exchange across the porous barrier, but adds a sink term to the momentum equation to induce an energy loss. The porous plate is located at the interface between two computational cells and can be placed along one or more layers in the vertical. Therefore variation in porcupine density with height can be taken into account. A fine grid is required to use the porous plate approximation due to the sudden energy loss. In addition, non-hydrostatic pressure must be assumed. Therefore this method is the most computationally-expensive of the options considered. The energy loss is defined as a quadratic friction term that is added to the momentum equation, M_ξ (see Equation 5.6), where the friction coefficient (c_{loss}) needs to be specified by the user.

$$M_\xi = -c_{loss} \frac{U_{m,n} \left| \vec{U}_{m,n} \right|}{\Delta x} \tag{5.6}$$

An advantage of this method is that the resistance affecting the bed and the resistance affecting the flow is inherently decoupled, since the energy loss in the momentum equation does not impact the calculation of the flow resistance for the bed shear stress, which is defined by the user.

5.2.3 Baptist (2005) - Vegetation Trachytope

In Delft3D-flow, four vegetation-based area trachytopes are available for defining roughness with vegetation at the sub-grid level. The first is based on the work of Klopstra et al. (1997) [27], and the second is a modification to the first by Van Velzen (2003) [68]. These authors define the global flow resistance in terms of the average flow velocity, found by averaging the canopy and overflow velocities. These methods are only applicable to submerged vegetation (as opposed to emergent and submerged conditions that porcupines will experience), and therefore will not be considered further. The last two formulations are both based on the work of Baptist [5], where a momentum balance is applied to a 2-layer model of flow thorough and above a vegetation field represented by uniform, rigid cylinders. The first (as with the Klopstra et al. and van Velzen et al. methods) does not allow for the separation of the roughness impacting flow resistance and the roughness impacting bed roughness. Without this decoupling the increased roughness of the vegetation translates to increased bed shear stress and sediment transport, when dense vegetation has been known to reduce bed shear stress and inhibit sediment transport [7, 32]. Therefore only the second formulation by Baptist [5] (defined as class 154 in Delft3d-Flow) will be considered further. This resistance method has been shown overall to be the best-fitting formulation applicable to a wide range of vegetation and flow conditions (emergent vs submerged vegetation; real vs

artificial plants; varying density and submergence ratios) [66]. Therefore, it is worth looking into how well this formulation can represent the resistance of porcupine fields.

The full derivation of the Baptist method can be found in [5]. I summarize the process but only provide basic and final formulas. The method proposed by Baptist starts with a force balance of the momentum equation where the total shear stress balances the bed shear stress and the shear stress provided by the vegetative drag force, as described in Equation 5.2. Vegetation is parameterized as rigid cylinders. The bed shear stress is equated to the total shear stress multiplied by a 'vegetation reduction factor'. In the process an expression for the emergent and submerged velocities are obtained in terms of the bed roughness and vegetation drag force. For emergent vegetation, the velocity through the vegetation is substituted into the Chezy equation (Equation 5.7), to find an expression for the Chezy value of representative roughness of a vegetated (emergent) channel.

$$\bar{u} = C\sqrt{di} \tag{5.7}$$

This equation is written for normal flow, C is the Chezy coefficient [$m^{1/2}s^{-1}$] and i is the water slope [-].

This vegetated Chezy value is then substituted into a genetically-programmed formula of the representative roughness for vegetated channels developed by Uthurburu [65]. The final formula (Equation 5.8), consists of two parts. One part that represents the contribution to resistance of the flow through the vegetated layer (first term), and one part that represents the contribution to the roughness from the overflow interacting with the vegetated layer (second term). Although with the genetic programming approach, the physical basis behind a derivation of the second part has been lost (see [6] for a description of genetic programming).

$$C_r = \frac{1}{\sqrt{\frac{1}{C_b^2} + \frac{C_{Dnh_0}}{2g}}} + \frac{\sqrt{g}}{\kappa} \ln\left(\frac{h}{h_v}\right) \tag{5.8}$$

Under emergent conditions ($h \leq h_v$), this equation simplifies to just the first term:

$$C_r = \frac{1}{\sqrt{\frac{1}{C_b^2} + \frac{C_D nh}{2g}}} \tag{5.9}$$

This formulation has been modified for implementation in Delft3d-Flow to decouple the resistance felt by the flow and that by the bed [25, 15]. The bed roughness (C_b) is adjusted to remove the portion of the total resistance from the vegetation, shown in Equation 5.10.

$$C_r = C_b + \frac{\sqrt{g}}{\kappa} \ln\left(\frac{h}{h_v}\right) \sqrt{1 + \frac{C_D n h_v C_b^2}{2g}} \tag{5.10}$$

Where κ is the von Karman constant, h is the flow depth, h_v is the cylinder height, g is gravity, C_b is the bed roughess, and n is the cylinder density ($n = mD$ where m is the number of cylinders per square meter and D is the element diameter). Next, to take into account the resistance acting on the flow, the cylinder resistance is added as a sink term to the momentum equation (Equation 5.11):

$$-\frac{\lambda}{2}u^2 \tag{5.11}$$

Where λ is the flow resistance of the cylinders:

$$\lambda = C_D n \frac{h_v}{h} \frac{C_b^2}{C^2} \tag{5.12}$$

Under emergent conditions Equations 5.10 and 5.12 simplify to a fully decoupled bed roughness and flow resistance (Equations 5.13 and 5.14, respectively).

$$C_r = C_b \tag{5.13}$$

$$\lambda = C_D n \tag{5.14}$$

With this method, the hydraulic resistance can be increased without increasing the bed roughness. Cylinders can be applied in multiple layers, to take into account density differences in cylinders (vegetation) that extend to different heights above the bed (and by extension horizontal versus vertical porcupine beams). This formulation assumes homogeneous vegetation represented as stiff cylinders. Parameters that need to be defined include the vegetation height, density, drag coefficient and alluvial bed roughness. Using this formulation to accurately represent porcupine structures which are neither vertical cylinders nor (necessarily) homogeneously distributed, implies adjusting the density and drag coefficient to best represent porcupine structures. For this modelling exercise, the porcupine density was defined once, as described in Section 5.3, and the drag coefficient was left as a calibration parameter.

5.2.4 Uittenbogaard (2003) - Rigid Cylinder Model

The second resistance model used to represent porcupines is the rigid vegetation model, based on the work of Uittenbogaard, 2003 (see [64, 15]). The original work can be consulted for the detailed derivation as well as [49] and [5](Appendix B) for a description of undefined terms and the values of their coefficients not detailed in [64] or [15]. The general method and equations implemented in Delft3D-flow are summarized here.

In the rigid vegetation model, vegetation (and by extension porcupines) are modelled as rigid cylinders. The stems per area and stem width can be defined as a function of depth, therefore vertical variations in porcupine structures can be taken into account. The impact of cylinders on hydrodynamics is incorporated into the momentum equation as a depth-dependent friction force and into the turbulence equations as an extra source term in the turbulent kinetic energy and ϵ (dissipation) equations.

The input to the friction term in the momentum equation include the number of stems per unit area as a function of height ($n(z)$), the stem width as a function of height ($\phi(z)$), and the drag coefficient (C_D).

$$F(z) = \frac{1}{2}\rho_w C_D \phi(z) n(z) |u(z)| u(z) \tag{5.15}$$

Where $u(z)$ is the horizontal flow velocity and ρ_w is the fluid density. The turbulence (k) equation with the vegetation-related source term is given by:

$$\frac{\partial k}{\partial t} = \frac{1}{1 - A_p} \frac{\partial}{\partial z} \left\{ (1 - A_p) \left(\nu + \frac{\nu_t}{\sigma_k} \right) \frac{\partial k}{\partial z} \right\} + T + P_k - B_k - \varepsilon \tag{5.16}$$

Where,

ν = kinematic viscosity

ν_t = turbulent eddy viscosity

$\sigma_k = 1$ (closure coefficient)

P_k = turbulence shear production term

B_k = Buoyancy turbulence production term

And $A_p(z)$ is the horizontal cross sectional area of the plant;

$$A_p(z) = \frac{\pi}{4} \phi^2(z) n(z) \tag{5.17}$$

And $T(z)$ is vegetation turbulence source term, which is a function of the friction force and the horizontal velocity:

$$T(z) = F(z) u(z) \tag{5.18}$$

Here the flow is assumed to be fully turbulent, where the entire plant drag force in converted to tke. For very low Reynolds flow numbers a portion of the energy would be converted to heat by viscous forces

and correction terms would be needed [5]. For this modelling application fully turbulent flow is a valid assumption.

Next the ϵ (dissipation) equation with the vegetation source term (T_τ) is given as:

$$\frac{\partial \varepsilon}{\partial t} = \frac{1}{1-A_p}\frac{\partial}{\partial z}\left\{(1-A_p)\left(\nu + \frac{\nu_t}{\sigma_\epsilon}\right)\frac{\partial \varepsilon}{\partial z}\right\} + T\tau^{-1} + P_\varepsilon - B_\varepsilon - \varepsilon_\varepsilon \tag{5.19}$$

Where,

$\sigma_\epsilon = 1.3$ (closure coefficient)

$P_\epsilon =$ dissipation production term

$B_\epsilon =$ Buoyancy dissipation term

$\epsilon_\epsilon =$ dissipation dissipation term

And τ (the dissipation time scale) is the minimum of τ_{free}, or τ_{veg}:

$$\tau = \min\left(\tau_{\text{free}}\,, \tau_{\text{veg}}\right) \tag{5.20}$$

τ_{free} (the dissipation rate of free turbulence) is given as:

$$\tau_{\text{free}} = \frac{1}{c_{2\varepsilon}}\frac{k}{\varepsilon} \tag{5.21}$$

This corresponds to the intrinsic turbulence time scale and applies at distances sufficiently far from the bed or the top of the vegetation, when turbulence produced in the wake of cylinders is larger than the space available (spacing between the stems).

τ_{veg} on the other hand, is the dissipation rate of eddies between plants, given as:

$$\tau_{\text{veg}} = \frac{1}{c_{2\varepsilon}\sqrt{c_\mu}}\sqrt[3]{\frac{L^2}{T}} \tag{5.22}$$

where $c_{2\varepsilon}$ and c_μ are constants (equal to 1.92 and 0.09, respectively). This time scale applies to the large eddies that are formed in the shear layer above the turbulence that then need to reduce in size to fit between the vegetation stems. Therefore τ_{veg} is a function of the plant geometry, where $L(z)$ is the typical eddy size limited by the stem spacing:

$$L(z) = C_l\sqrt{\frac{1-A_p(z)}{n(z)}} \tag{5.23}$$

The C_l coefficient converts the length scale to the volume-averaged turbulence length scale. This allows the size of the eddies to be reduced for calibration purposes [49]. For cylinders this value can be 1 [6]. For vegetation a value of 0.8 has been found to be applicable [15]. Therefore, this model takes into account the differences between the turbulence production in the wakes of stems and the turbulence generated in the shear layer between the canopy and overflow transferred to the canopy layer.

5.3 Model Setup

The numerical model is calibrated using data from the 2018 porcupine flume experiment. A brief summary will be given below. The data available from the flume experiment is not enough for full calibration, validation and verification of the 2DV and 1DH models. Only a calibration will be performed and even then, the data is not enough for a full calibration. Nevertheless, the analysis is a good starting point to evaluate qualitatively and quantitatively how well the models can predict porcupine impacts to the flow field and what are the most important processes captures (or not captured) by the models. To prevent numerical complications, the numerical models are based on a version of the flume experiment that has been scaled to a prototype version 10 times the original size. The details of the scaling analysis are presented in Appendix A. This section presents a brief summary of the 2018 flume experiment, and then describes the 2DV and 1DH model setups.

5.3.1 Calibration Data

The model was calibrated using data from a porcupine flume experiment [46]. A summary of the experimental setup is presented below, as well as a discussion of data quality.

Flume Setup and Experiments

A flume with a concrete bottom and wooden sides (12 m long and 0.8 m wide) was used with a a recirculating pump to control the discharge and a weir at the downstream end of the flume to control the water level. Porcupines were constructed of square brass beams 10 cm long and 7 mm thick with an effective height of approximately 8.7 cm. A field of staggered porcupines 0.5 or 0.7 meters long across the full flume width was placed approximately 6.5 meters from the upstream end of the flume, where the vertex of the porcupines (side of the porcupine with a single beam) were facing downstream. An overview schematic is shown in Figure 5.2.

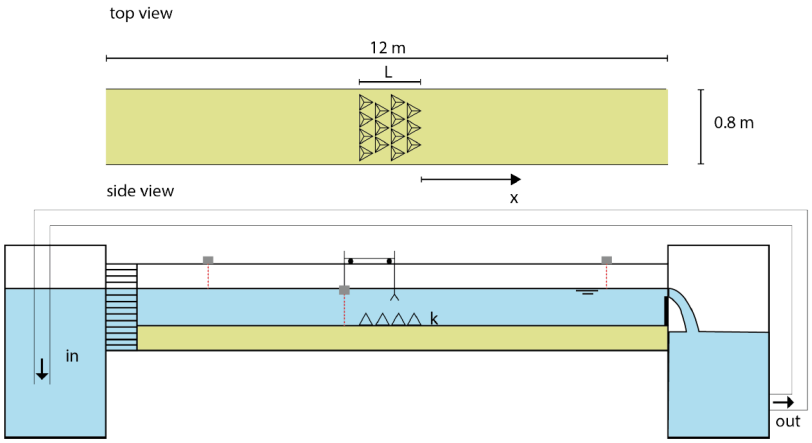

Figure 5.2: Overview of experimental flume setup, not to scale. Taken from [46].

Both fixed-bed and mobile-bed experiments were conducted; however only fixed-bed experiments will be analyzed in this chapter. A portion of the data from the flume experiment was lost, therefore only two of the fixed-bed bed experiments are analyzed, as summarized in Table 5.2.

	Flow					Flume		Porcupines							
Run	h	Q	u	Fr	Re	L_f	B	L_p	s	b	ΔS_x	ΔS_y	L	λ	h/s
9	0.173	0.033	0.23	0.18	1,642	12	0.8	0.1	0.082	7	0.1	0.1	0.5	0.84	2.1
13	0.173	0.033	0.23	0.18	1,644	12	0.8	0.1	0.082	7	0.14	0.1	0.7	0.17	2.1

Table 5.2: Flume experiment parameters

Velocities were measured with an ADV (acoustic doppler velocitmeter) along 8 (Run 9) or 9 (Run 13) longitudinal locations. Only experiment 13 included a measurement location inside the porcupine field. A water level laser was used to record water levels. The measurement equipment was mounted on cart moving along rails that permitted measurements between 3.5 and 8.5 meters from the upstream end of the flume; however, a portion of the water level data was lost and therefore water levels beyond approximately 8 meters from the upstream end of the flume are not available.

Experiments 9 and 13 are identical except for the number of sampling locations and porcupine spacing: $\Delta S_x = 11$ cm for Experiment 9 and 15 cm for Experiment 13. The cross-sectional spacing (ΔS_y) was equal for both experiments (11 cm). Experiment 9 will be referred to as 'less dense' and Experiment 13 will be referred to as 'more dense'. Note that 'less dense' and 'more dense' is relative and, here, does not imply a 'dense' field as described in Chapter 2; however, if the 'sparse' and 'dense' criteria hold for porcupines as for vegetation, both experiments should exhibit transitional behavior, with Experiment 9

($\lambda = 0.84$) closer to dense behavior than experiment 13 ($\lambda = 0.17$). Therefore a transitional or dense behavior is expected of the velocity profile.

Data Quality

The flume experiment was run with a concrete-bottom wooden-sided flume, giving it a roughness higher than typical flume experiments that might use glass sidewalls and a smooth bed. In addition, portions of the bed were uneven, including from a previous experiment that cut out and then replaced a piece of concrete from the bed. Deviations of up to 2 cm along the bed were observed. The effect of this is not only an increased roughness compared to a smooth-sided flume, but the water level, with or without porcupines, showed a sudden increase in the water level a short distance upstream of the porcupine field location. In addition, downstream of the porcupines, the water level increases, and continues to increase to the end of the flume. This was due to the backwater effect of the control weir at the end of the flume, and was present for all runs.

When calibrating the model, it was not possible to match both the water level and the velocity. Therefore the calibration was performed matching velocities over water levels, since there were doubts about the accuracy of the water level measurements due to deviations that could not be incorporated into the model.

Two considerations should be taken into account with the velocity measurements. First, deviations in the velocity profile are observed, where the velocity decreases higher in the water column instead of following a logarithmic profile for locations presumed to experience normal flow (see Figure 3.15 in [46]). This is a result of a decreasing measurement accuracy at the limit of the working range of the instrument, and likely affects all velocity measurements whether the flow is normal, decelerating or accelerating.

The second consideration is that velocity measurements were taken only at one cross-sectional location, along the central axis of the flume. The velocity profile through a resistance field will be highly heterogeneous due to the interaction of the flow with the individual porcupine beams and the subsequent interactions between wakes. For vegetation studies (where vegetation is typically represented as rigid cylinders), a double averaging method is often employed, as described in Chapter 2, to capture an 'average' velocity profile shown in Figure 2.10. Therefore the velocity measurements from the porcupine flume experiment located just upstream, within and just downstream of the porcupine field are likely slightly biased and may not be representative of the average velocity profile.

5.3.2 Model Scaling

The numerical models were based on a version of the flume experiment scaled to 10 times the physical size to prevent numerical complications from parameters that fall below default values in Delft3D-Flow. Details of the scaling analysis are presented in Appendix A. Table 5.3 below presents the scaled model parameters.

	Flow					Flume		Porcupines							
Run	h	Q	u	Fr	Re	L_f	B	L_p	s	b	ΔS_x	ΔS_y	L	λ	h/s
9	1.73	10.24	0.74	0.18	1,642	120	8	1	0.82	70	1.0	1.0	5	0.84	2.1
13	1.73	10.24	0.74	0.18	1,644	120	8	1	0.82	70	1.4	1.0	7	0.17	2.1

Table 5.3: Flume experiment parameters

5.3.3 2DV Model Setup

A 2DV model was created in Delft3D that analyzes three methods of representing vegetation: increased roughness parameter ('increased roughness'); permeable structure ('porous plate'), and the Uittenbogaard rigid vegetation model ('rigid cylinder'). The primary objective of this model is to compare how well the porcupine impacts on hydrodynamics can be simulated using resistance formulations typically used for vegetation.

Domain

The model represents a flat (no slope) channel 120 m long, 8 m wide, with a water depth of approximately 1.7 m, represented by a grid of 600 x 20 cm grid cells in the longitudinal direction and a 1 x 8 m grid cell in the cross-sectional direction with 10 vertical layers (each approximately 17 cm thick). The porcupine field was 5 or 7 meters long implemented at 62.5 m (7 m field, 'less dense') or 64.5 m (5 m field, 'more dense') from the start of the flume.

Boundary Conditions

The upstream boundary condition is discharge (Q), and the downstream boundary condition is the control depth (h).

Physical Parameters

A Chezy value of 45 has been selected for the bed roughness. This value is high compared to typical Chezy values for flumes; however it was appropriate for this analysis for the reasons described in Section 5.3.1. The wall roughness is free-slip. The k-ϵ turbulence model is used for all model runs. While accurately representing turbulence is very important to predict porcupine behavior, in a 2DV model the turbulence modelling will be approximate, therefore the performance of different turbulence models was not evaluated. The background horizontal eddy viscosity was set to 3.1x10$^-$5, as computed from the scaling analysis (Appendix A).

Vegetation Resistance

The porcupines represented had an effective height of approximately 0.87 m and a beam width of 0.07 m. The field of porcupines should represent 5 rows of porcupines with a center-to-center longitudinal spacing (ΔS_x) of 1 m (more dense field, run 9), or 1.5 cm (less dense field, run 13), as described above. Note that 'field' is used in this Chapter even though, as discussed earlier, the 'field' used in the flume study is not long enough to form fully-developed flow, and therefore 'patch' may be a more appropriate description. 'Field' is maintained to not generate confusion over whether the porcupines occupy the entire width of the flume or not.

The resistance due to porcupine is represented on the sub-grid level. Therefore the first step is to define the grid cells occupied by the porcupine field, which correspond to the porcupine field location. Next, for each resistance approximation, the relevant parameters are altered to represent porcupines, as described below.

Increased Roughness To represent porcupines as increased bottom roughness, the Chezy value over the domain of the porcupine field was decreased (Figure 5.3). The value of the Chezy parameter within the porcupine field was adjusted for model calibration.

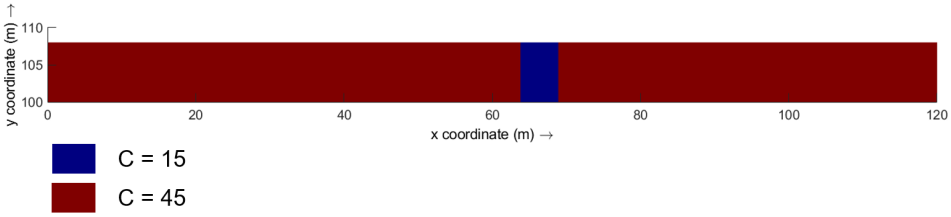

Figure 5.3: Bottom roughness changed over an area of the flume representing the porcupine field. Here the bottom roughness outside the porcupine field is C=45 and inside the porcupine field is C=15, and the porcupine field is 5 m long.

Permeable Structure Porcupines were translated to porous plates by defining two layers of plates: a lower layer of higher resistance ($c_{loss\ down}$), representing the vertical beams up to the horizontal beam height and the horizontal beams; and an upper layer of lower resistance ($c_{loss\ up}$), representing the portion

of vertical beams above the horizontal beams. The vertical layers each plate occupies is defined by the layers representing the height of the two zones. Five sets of plates are used with each pair representing one row of porcupines. For numerical reasons the two plates are displaced by one grid cell. Figure 5.4 shows a schematic (not to scale) of the porous plate representation of porcupines.

Figure 5.4: Porous plate representation of porcupine field. Darker plates represent the zone of higher resistance and lighter plates represent the zone of lower resistance (not to scale).

The coefficient c_{loss} was initially estimated from the Q-H relation across a hydraulic structure (Equation 5.24),[15]:

$$g\frac{\zeta_u - \zeta_d}{\Delta x} = c_{\text{loss}}\frac{U_{m,n}\left|\vec{U}_{m,n}\right|}{\Delta x} \tag{5.24}$$

Where ζ_u is the upstream water level, ζ_d is the downstream water level, Δx is the width of the hydraulic structure and $U_{m,n}$ is the computed velocity at the location of the hydraulic structure. This formula is intended for use with a computational output; however values from the flume experiment were used to get in initial estimate of c_{loss}, for porcupine field of 0.3.

For this exercise, the 'configuration' of the porcupine field is kept constant, and the resistance of the two layers (upper and lower) is adjusted to calibrate the model.

Uittenbogaard (2003) Rigid Cylinder Model For implementation in Delft3D-Flow, the C_l coefficient was set to 0.8. Then the porcupines were defined by their depth-dependent geometry (vertical plant structure). At each relevant elevation, the stem diameter and number of stems can be changed, and the drag coefficient can also be varied with depth. To represent the porcupines as 'rigid cylinders', the porcupines have been divided into two zones. A lower zone of higher density, representing the bottom of the vertical beams and the horizontal beams, and a higher zone of lower density representing the vertical beams above the horizontal beams. Porcupines were translated into cylinders in the upper zone by dividing them into three'tall' cylinders with a diameter equal to the beam width (vertical beams), and in the lower zone by dividing them into many small cylinders equal to the beam width divided by its length, multiplied by three (for the three horizontal beams), as shown in Figure 5.5.

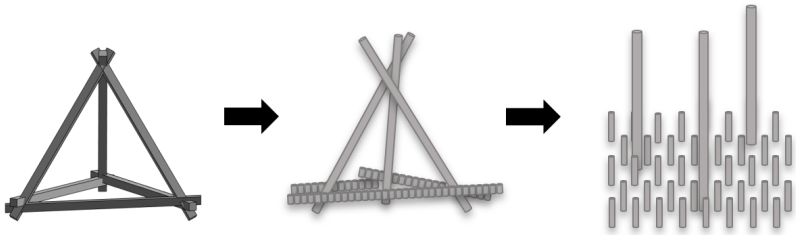

Figure 5.5: Translation of porcupine beams into rigid cylinders to determine cylinder diameter and number of cylinders per area.

Table 5.4 outlines the parameters used.

The translation of the horizontal beams into cylinders is problematic because it places many small cylinders (with a small turbulence spacing), as opposed to three larger beams with a larger spacing. For simplicity this characterization was kept for the evaluations against the flume data and only the drag coefficient was used as a calibration parameter (however, the drag coefficient was kept constant for all layers). The sensitivity of the vertical plant structure is examined later. Note also that the Rigid

Parameter	Unit	Vertical (High) Beams	Horizontal (Low) Beams
h_v range	[m]	0 to 0.82	0.1 to 0.31
D	[m]	0.07	0.07
n	[-]	1	1
C_d	[-]	calibration coefficient	calibration coefficient
Number of plants	[# plants/m^2]	3	45
C_l	[-]	0.8	

Table 5.4: Uittenbogaard Porcupine Parameterization

Cylinder model, as well as the Baptist Trachytope model presented below, represent vegetation as round cylinders, where the porcupine beams are square. In theory, this difference can be accounted for with the adjustment of the drag coefficient; however the volume fraction occupied by the porcupines will also be slightly off compared to the cylinder representation.

Model Runs

The model is run for experiments 9 and 13, as presented in Table 5.3.

5.4 1DH Model Setup

The 2DV model was simplified to a 1DH model by eliminating the vertical layers. Two methods of representing vegetation are explored: increased roughness parameter ('increased roughness') and the Baptist vegetation trachytope model ('Baptist').

The primary objective of this model is to compare how well porcupine impacts on hydrodynamics can be represented in a simplified model. This evaluation will allow us to examine if the 1DH model captures the main processes of porcupines impacting flow and will help us to better interpret where the model does or does not perform well. The same setup and runs are used for the 1DH model as the 2DV model, with the exception that the 1DH model has only one layer and does not use a turbulence model. The only additional description included in this section is the parameterization of the Baptist vegetation trachytope, which could not be used for the 2DV model.

Vegetation Resistance

Baptist (2005)- Vegetation 'Trachytope' The Baptist trachytope method requires defining classes of vegetation based on stem diameter and density. Multiple kinds of vegetation (represented by cylinders) can be specified each with their own height, diameter and number of stems; however, unlike the rigid cylinder method, the vertical plant structure cannot be varied (e.g. number or size of stems changing over the vertical). In addition, the vegetation types need to be specified as a density (# of stems per m^2) and an area fraction (% of grid cell occupied by each vegetation type), rather than simply the number of plants per m^2.

Porcupines were first translated to cylinders using the same approach as the Rigid Cylinder method (Figure 5.5); however the parameters were adjusted to match the Baptist trachytope input files, shown in Table 5.5.

To define multiple kinds of vegetation (and therefore vegetation of different heights), the area fraction of each kind of vegetation needs to be specified. In the case of porcupines the short (horizontal beams) and tall (vertical beams) of the porcupine occupy the same footprint. Therefore, to define these beams in the same grid cells, the number of cylinders per area (m) is doubled, and the area fraction of each is specified as half of each grid cell where porcupines are present.

This method of translating porcupines into cylinders is not completely accurate, as described above, because the turbulence length scale represented by three large horizontal beams will not translate to the

Parameter	Unit	Tall Cylinder	Short Cylinder
h_v	[m]	0.82 ($\sqrt{6}/3 \cdot L_p$)	0,21 ($3 \cdot b_m$)
m	[# stems/m^2]	$3 \cdot 2$	$42.3 \cdot 2$
D	[m]	0.07	0.07
n	[1/m]	0.42	5.92
C_d	[-]	1.05	1.05
C_b	[m$^{1/2}$/s]	45	45
Area fraction	[-]	0.5	0.5

Table 5.5: Baptist Porcupine Parameterization

same turbulence length scale represented by many short cylinders. The sensitivity analysis explores the sensitivity of the density representation on the final results.

This vegetation configuration was left the same for all model runs, and the drag coefficient (kept the same for both layers), was used as a calibration coefficient.

5.5 Summary of Resistance Calibration Parameters

The four resistance formulations outlined above will be presented in the results using acronyms and with the final values of their calibration coefficients, summarized in Table 5.6.

Representation	Abbreviation	Coefficient	Units
Increased Roughness	IR	C	[m$^{1/2}$/s]
Porous Plate	PP	$c_{loss\ up}$; $c_{loss\ down}$	[-]
Rigid Cylinder	RC	C_d	[-]
Baptist Trachytope	B	C_d	[-]

Table 5.6: Calibration coefficients for resistance representations.

5.6 Performance Criteria

The performance of the modelled porcupine fields are compared against data from the 2018 porcupine flume experiment [46]. Qualitative and quantitative criteria are used that differ according the complexity of the model (2DV versus 1DH). The following sections describe the qualitative and quantitative criteria used to evaluate the model performance for the 2DV and 1DH model. Then, a subsequent section describes how each criteria is defined, approximated, normalized and compared.

5.6.1 2DV Model

This modelling study first evaluated a 'detailed' 2DV representation of porcupines. The velocity, turbulence, and Reynolds stress profiles are compared against the flume data and the expected profiles for a transitional or dense vegetation field. Then, model output is compared against against the water level, depth-averaged velocity and bed shear stress measurements from the flume experiment, as well as performance criteria for braided river channel control defined below.

The primary application of porcupines in this study is for channel control in a braided river. Channel control is achieved by maintaining a certain discharge distribution at an upstream bifurcation. Porcupine structures can contribute to this discharge distribution in two ways. First, the additional roughness provided by the porcupines can push up the flow, creating a backwater curve upstream of the porcupine

field. Secondly, the porcupine fields may reduce velocities within the field and for a certain distance downstream of the field, encouraging sediment deposition if the local bed shear stress is also maintained at low enough levels to prevent or minimize scour. If sediment deposition can be encouraged the bed level will rise, attracting less flow to the secondary channel. Since this modelling effort focuses on hydrodynamics, sedimentation will not be considered; however velocity reduction and changes to bed shear stress can be used as proxies for potential sedimentation. Therefore the performance criteria of the model are related to both its ability to accurately reproduce the flow-field characteristics, and on a larger scale accurately predict the ultimate parameters of importance for braided river channel control. The following criteria are evaluated between the 2DV model and the flume data:

Qualitative criteria:

1. Direction of flow field
2. Shape and evolution of velocity, turbulence, and Reynolds stress profiles
3. Evolution of water level
4. Evolution of bed shear stress

Quantitative criteria:

1. Height of upstream backwater curve
2. Predicted energy loss over porcupine field
3. Predicted depth-averaged velocity at porcupine height
4. Predicted bed-shear stress

5.6.2 1DH Model

The evaluation of the 1DH model is simplified because of the lack of profile information. As described above, it is not possible to estimate depth-averaged velocity from the flume experiment. Instead, only the predicted and measured water level and bed shear stress can be compared to the flume experiment, as indicated below.

Qualitative criteria

1. Evolution of water level
2. Evolution of bed shear stress

Quantitative criteria

1. Height of upstream backwater curve

5.6.3 Model Predictions versus Flume Measurements

Delft3D-Flow solves the Reynolds-averaged Navier-Stokes Equations to make predictions of the flow field characteristics; while the flume experiment relies on measurements of velocity, turbulence characteristics and water levels. The comparison of certain parameters, such as velocity, are straightforward, while other need to be approximated. This section discusses the comparison of model and flume measurements, and the limitations of certain measurements.

Because the model was scaled up from the flume experiment, direct comparisons of these criteria cannot be made. Instead, all measurements are normalized, and comparisons are made between the normalized values. For each quantitative criteria, the values used for normalization are described below.

Height of Backwater Curve The height of the backwater curve is measured from the difference in the water surface elevation with porcupines versus without porcupines for the same hydrodynamic conditions. This height is measured from the relative flume position where measurements were started in the flume experiment (x = 3.5 m for the experimental flume, and x = 35 m for the model flume). This height is normalized by the control depth (h) of the experiment.

Energy Loss The energy loss over the porcupine field is predicted from Bernoulli's Equation (Equation 5.25), where changes in the bed elevation are not taken into account since the flume does not have a slope:

$$\frac{\bar{u}_{up}^2}{2g} + H_{up} = \frac{u_{down}^2}{2g} + H_{down} \tag{5.25}$$

Where 'up' and 'down' refer to locations just upstream or just downstream of the porcupine field (x/L = -1 and x/L = 0, respectively). The energy loss is normalized by the downstream control depth of the experiment (h)

Velocity Comparison The depth-averaged velocity is compared for two measurements heights, (1) the depth up to the height of the porcupines, and (2) the depth up to the measurement height of the instrument, as shown in Figure 5.6.

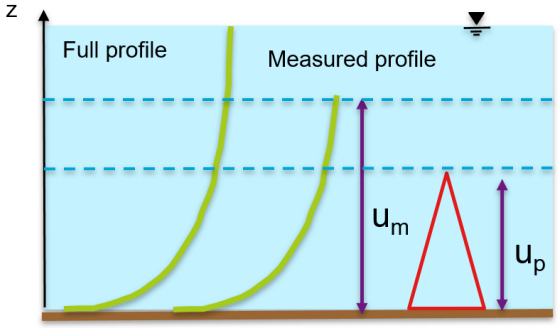

Figure 5.6: Depth-averaged velocities were calculated to two levels: the maximum depth of the ADV measurements (u_m), and the depth up to the height of the porcupines (u_p).

The ADV is not able to measure velocities up to the water surface level. As will be shown below, the flow over and through the porcupine field is accelerating and decelerating (not uniform, normal flow), and therefore a depth-averaged velocity could not be estimated or extrapolated from the measured velocity profile. Therefore, the velocity from the model was averaged to two elevations: the maximum measurement height the height of the porcupine field (where velocities are expected to reduce, a opposed to above the field where velocities could accelerate). The velocities are normalized by the theoretical experiment velocity determined by the experiment boundary conditions and flume dimensions ($\bar{u} = Q/hB$). Detailed velocity and bed shear stress measurements were taken at 8 or 9 locations in the flume experiments. The root mean square difference between the measured and predicted velocities for all locations is used to estimate the error in the approximation, as given by Equation 5.26.

$$RMSE = \sqrt{\frac{1}{n}\sum_{i=1}^{n}\left(x_{f_i} - x_{m_i}\right)^2} \tag{5.26}$$

Where the subscripts 'f' and 'm' refer to the flume measurements and the model predictions, respectively.

Eddy Viscosity, Reynolds Stress and Bed Shear Stress Comparison The bed shear stress in the flume experiment was estimated using the Reynolds stresses at the bed (approximately $h \leq$ 1cm). The Reynolds stresses are approximated from the decomposed velocity signal as:

$$\tau_{xy} = -\rho_w \overline{u'w'} \tag{5.27}$$

Where u' and w' represent the fluctuations of the longitudinal and vertical velocities, respectively. This is not the most accurate approximation of the bed shear stress because the measurements are taken 1 cm from the bed, rather than directly at the bed. (Accurate) closer measurements are not possible with the ADV; however, considering the alternatives, this is a good approximation.

First, the total shear stress can be approximated from Equation 5.3, and the vegetation shear stress can be subtracted (Equation 5.4), to find the bed shear stress; however this method is prone to large errors because the vegetation shear stress is generally an order of magnitude larger than the bed shear stress [79, 78], and the parameters controlling the vegetation drag (e.g. C_d) are not necessarily known. Next, the Reynolds stress at the bed can be approximated from a linear interpolation of the shear stress profile to the bed; however, this only works for uniform flow, which is not the case for nearly all of the sampling locations, where the Reynolds stress profile shows deviations due to the porcupines rather than a linear decrease to the bed. Finally, the bed shear stress can be approximated by fitting a Law of the Wall profile, however this requires both measurements close the bed and a logarithmic velocity profile (e.g. uniform flow) [43, 31], which we already decided was not the case the majority of the sampling locations. Therefore, the closest Reynolds stress measurements to the bed were retained to approximate the bed shear stress. While acknowledging the imprecisions, the method is used by other researchers for the same reasons [78, 7]. A more detailed discussion of the issue can be found in [79].

The Reynolds stress profile for the model was approximated from combining the eddy-viscosity concept (Boussinesq hypothesis) and Prandtl's mixing length hypothesis. First, the eddy viscosity is defined from a characteristic length scale and velocity scale. Equation 5.28 shows the implementation Delft3D-FLow.

$$\nu_t = c'_\mu L\sqrt{k} \tag{5.28}$$

Where, c'_μ is an empirical constant (0.09 for the k-ϵ model), L is the turbulent mixing length, and k is the turbulent kinetic energy.

For the $k-\epsilon$ turbluence model Delft3D-Flow approximates the turbulence length scale as:

$$L = c_D \frac{k\sqrt{k}}{\varepsilon} \tag{5.29}$$

Where c_D is a constant and ϵ is dissipation. Eddy viscosity profiles are normalized by the molecular kinematic viscosity of water ($\nu_{molecular}$), which is approximately 10^-6 m^2/s for water. Note that eddy viscosity is numerical artifact and is not approximated for the flume experiment.

Next, we assume that the shear stress is proportional to the velocity gradient where the eddy viscosity is constant of proportionality, since (as Prandtl postulated), the turbulent velocity scale is related to the turbulent length scale multiplied by a velocity gradient (Equation 5.30).

$$v_\mathrm{T} = \ell_\mathrm{m}^2 \left| \frac{\mathrm{dU}}{\partial \mathrm{y}} \right| \tag{5.30}$$

The end result is Equation 5.31:

$$-\overline{\mathrm{u'v'}} = v_\mathrm{T} \frac{\partial \mathrm{U}}{\partial \mathrm{y}} \tag{5.31}$$

However, this approximation underestimates the shear stress at the bed. Rather, Delft3D-Flow approximated τ_b as:

$$\vec{\tau}_{b_{3D}} = \frac{g\rho_0 \vec{u}_b \left|\vec{u}_b\right|}{C_{3D}^2} \tag{5.32}$$

Where horizontal bed velocity ($\vec{u}_b$) in the first layer above the bed is given as:

$$\vec{u}_b = \frac{\vec{u}_*}{\kappa} \ln\left(1 + \frac{\Delta z_b}{2z_0}\right) \tag{5.33}$$

Assuming that Δz_b is the distance from the bed to the grid point closest to the bed. Finally, the 3D Chezy coefficient (C_{3D}) is defined in terms of the roughness height (z_0):

$$C_{3D} = \frac{\sqrt{g}}{\kappa} \ln\left(1 + \frac{\Delta z_b}{2z_0}\right) \tag{5.34}$$

This gives a better approximation of the bed shear stress; however, coarse vertical layers can lead to inaccuracy in the model bed shear stress computations. The model runs presented use 10 vertical layers for computational efficiency and because the accuracy of the Reynolds stress measurements used for comparison did not necessarily justify better model approximations; however, the sensitivity analysis explores the effect on the results when additional layers are used, particularly thinner layers near the bed and top of the porcupines, where capturing the shear stress profile is most important.

The Reynolds stresses and bed shear stress for the flume measurements and model were normalized by $\rho\bar{u}^2$, where ρ is the density of water (1000 kg/m^3).

Turbulence and Dissipation Measurements The turbulent kinetic energy for the flume experiment is approximated as one-half the average of the horizontal velocity fluctuations:

$$\mathrm{k} = \frac{1}{2}\overline{\mathrm{u'u'}} \tag{5.35}$$

For the full turbulent kinetic energy, the average of the fluctuations of velocity in all three directions are summed; however the horizontal fluctuations are much greater than the fluctuations in the other directions and they can be neglected.

For the model, the turbulent kinetic energy is approximated from the $k - \epsilon$ turbulence model with the Boussinesq and Prandtl mixing length hypotheses, as described above. Both the turbulence and dissipation are estimated using transport equations. Details can be found in [15], section 9.5.3.

The turbulence measurements were normalized using the total velocity squared ($\bar{u}^2$) for the flume or model respectively.

Dissipation in general can be approximated as:

$$\epsilon = u^3/\ell \tag{5.36}$$

Where u is the local velocity and ℓ represents the integral turbulence length scale. Deft3D-Flow approximates ϵ with a transport equation ([15], section 9.5.2). The dissipation measurements were normalized by $\bar{u}^3/b$, where b is the width of the porcupine beams. Note that ϵ is only approximated from the model and is not available for the flume experiment.

Distance Measurements The distances used to define the position along the flume have been normalized using the length of the porcupine field to allow for comparison between the flume and model data and between runs with differing porcupine field lengths. Distances are expressed as x/L, where x is the longitudinal distance from the end of the porcupine field, and L is the length of the porcupine field, as shown in Figure 5.2. Therefore $x/L = 0$ corresponds to the end of the porcupine field, and $x/L = -1$ corresponds to the start of the porcupine field.

5.7 2DV Model Results

First, each porcupine resistance representation is compared visually against plots of velocity vectors from the flume experiment to understand how each representation alters the flow field compared to each other and the flume experiment. Next, the flow field profiles are examined in detail for each resistance representation, to understand where the model is or is not performing well in mimicking the porcupine's impacts on hydrodynamics. Then, the resistance representations are compared against the predicted water level, velocities and bed shear stress values to understand if the models represent well, globally, the influence of porcupines. Finally, the performance of each representation is quantified using the performance criteria outlined in Section 5.6.

5.7.1 Velocity Vectors

Figures 5.7 and 5.8 show the velocity vectors for runs 9 and 13 respectively. All representations are able to reduce velocities within or downstream of the porcupine field; however the rigid cylinder approximation perform best in capturing the velocity reductions and evolution of the velocity profile; however, it does not capture well the diversion of water upward in front of the porcupine field and downward at the end of the porcupine field, clearly seen in the flume experiment. The porous plate approximation has the second best fit; however the profile returns to logarithmic too quickly. The increased roughness profiles do not match the flume experiment well, as the velocity profile returns to logarithmic very quickly and the vertical velocities are too strong.

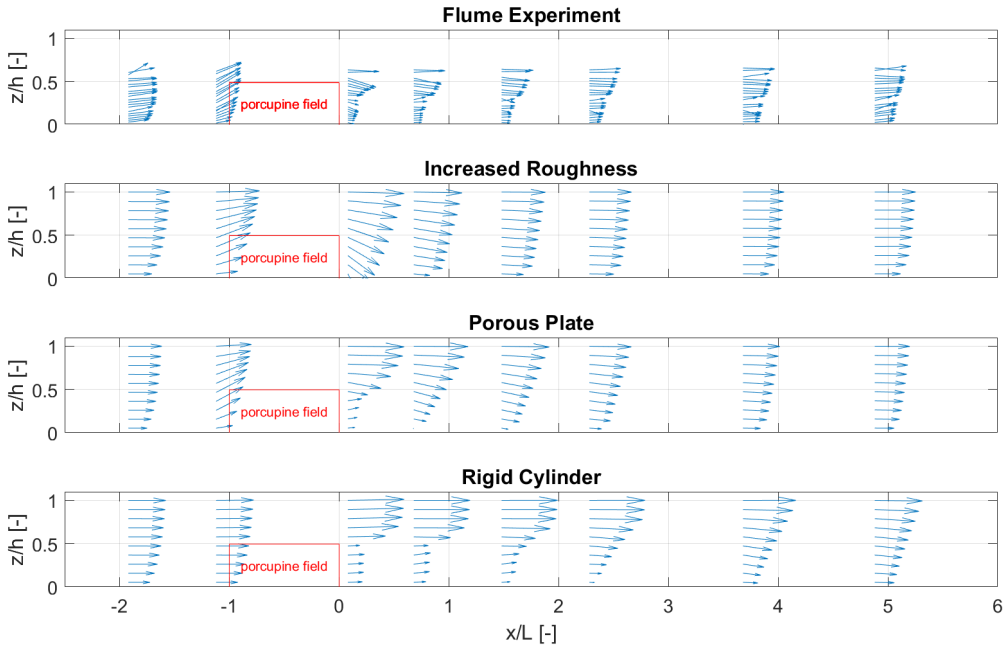

Figure 5.7: Velocity Vectors: Experiment 9. Vertical velocities exaggerated by a factor of 10.

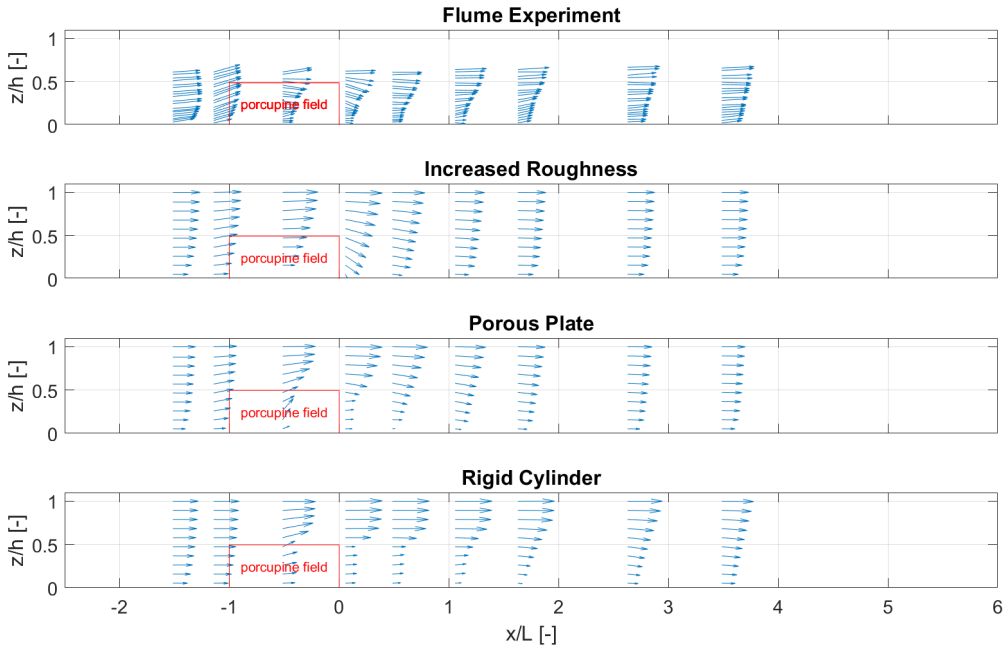

Figure 5.8: Velocity Vectors: Experiment 13. Vertical velocities exaggerated by a factor of 10.

5.7.2 Qualitative Comparison

Velocity, eddy viscosity, Reynolds stresses, turbulence and dissipation profiles are presented for each resistance representation with the flume experiment results. The results are normalized to allow for direct comparison between two setups, as described in Section 5.6.3. Note that only model results are available for the eddy viscosity and dissipation; while only flume results are available for the Reynolds's stresses except for the Rigid Cylinder model.

Increased Roughness

The increased roughness representation for runs 9 and 13 are presented in Figures 5.9 and 5.10 respectively. The more dense fields required a higher Chezy value for calibration, as can be expected. This representation does not accurately reproduce the vertical flow field profiles. The velocities at the porcupine height are retarded too much and the velocities above the porcupines are accelerated too much. The velocity profile returns to normal too quickly and this method overestimates the amount of turbulence produced within and downstream of the porcupine field.

Porous Plates

The porous plates representing the more dense field required higher c_{loss} coefficients than for the less dense field, as expected. $c_{loss\ up}$ was 1 for both experiments (higher than this lead to numerical instabilities), but $c_{loss\ down}$ was 4 for run 9 and 2 for run 13.

The porous plates are able to reproduce the flume velocity profiles relatively well; however the velocities appear to be slightly underestimated (for example location x/L = -2). This was common to all methods, and likely results from a combination of the normalization method, measurement errors, scaling effects and the model approximations.

The porous plate method tends to capture the the trend of the turbulent kinetic energy profile; however, the relative magnitude is higher than predicted from the flume measurements.

Rigid Cylinder

The Rigid Cylinder model calibrated with a drag coefficient of 5 for run 9 and 3 for run 13. This is very close to the drag coefficients predicted by Nientker in [46], where he found a drag coefficient of 5.5 for run 9 and 3 for run 13 by balancing the total shear stress (Equation 5.3) with the the porcupine drag force.

The Rigid Cylinder method performs the best of the three methods in capturing velocity, turbulence and Reynolds profiles, although a 'lag' is noticed where, in particular the Reynolds stresses, do not start to take the form expected from a vegetated bed (Figure 2.11) for a certain distance downstream of the porcupine field, even when the flume measurements are already indicated this characteristic profile (where the Reynolds stresses increase linearly to the top of the porcupine field, then decrease non-linearly to the bed); however, the Reynolds stress profiles do match well at a distance of approximately $x/L = 4$.

Interestingly, the Reynolds stress profiles for both run 9 and run 13 ($\lambda = 0.8$ and 0.2, respectively) are both very similar in profile; however the magnitude of the shear layer is clearly less for the less dense porcupine field.

Overall, while the Rigid Cylinder method did well at representing both the more dense and less dense porcupine field; it performed the best for the less dense field. This could suggest that at higher density the behavior of porcupines shows more deviations from vegetation represented as rigid cylinders, or it could be an indication of increased measurement error for the higher density run, where the bias in the velocity measurements due to the lack of spatial averaging, is greater.

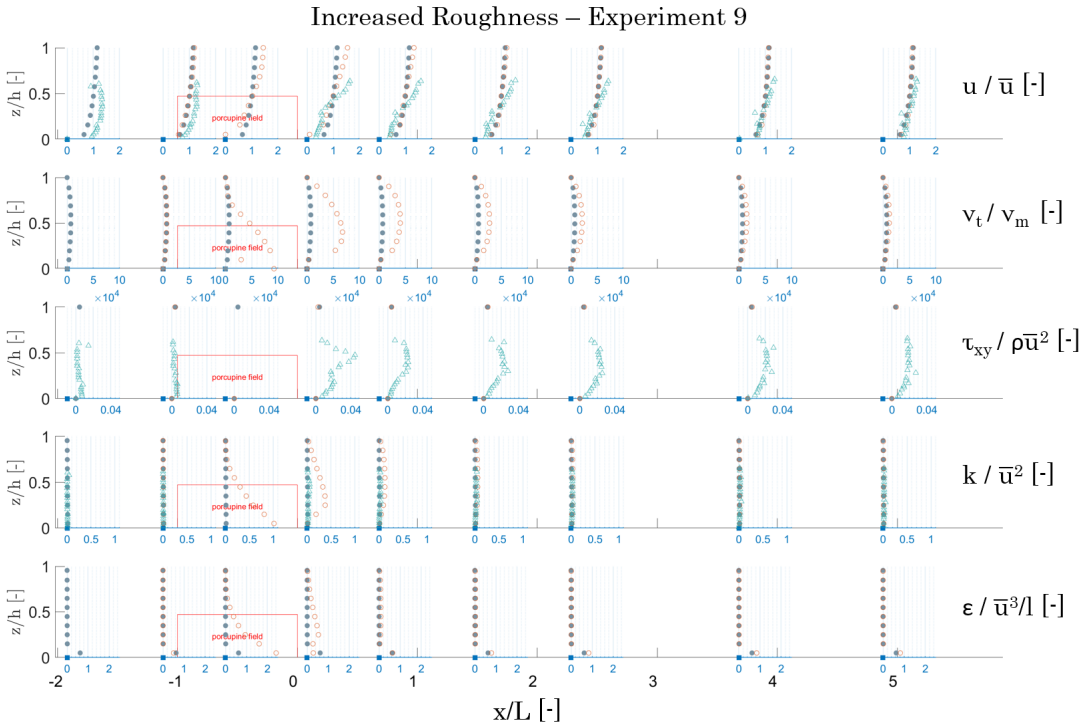

Figure 5.9: More dense field: Increased Roughness (C_b= 45; $C_{b,porc}$ =6). Dark circles = upstream model profile; open circles= current model profile; triangles = flume experiment.

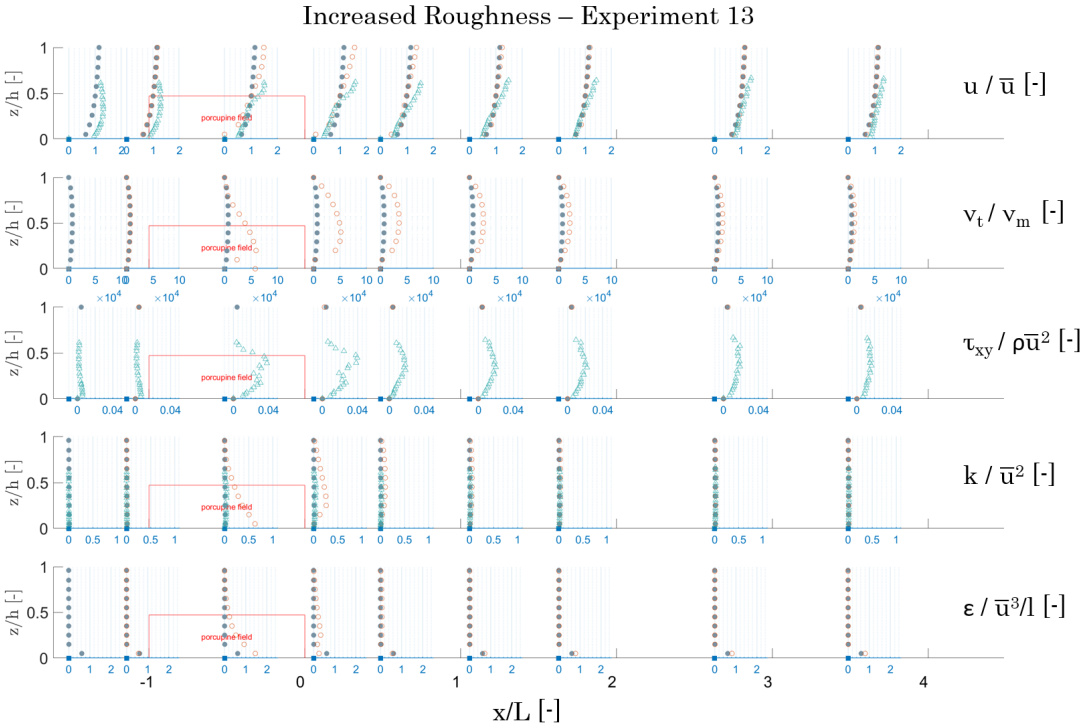

Figure 5.10: Less dense field: Increased Roughness (C_b= 45; $C_{b,porc}$ =7). Dark circles = upstream model profile; open circles= current model profile; triangles = flume experiment.

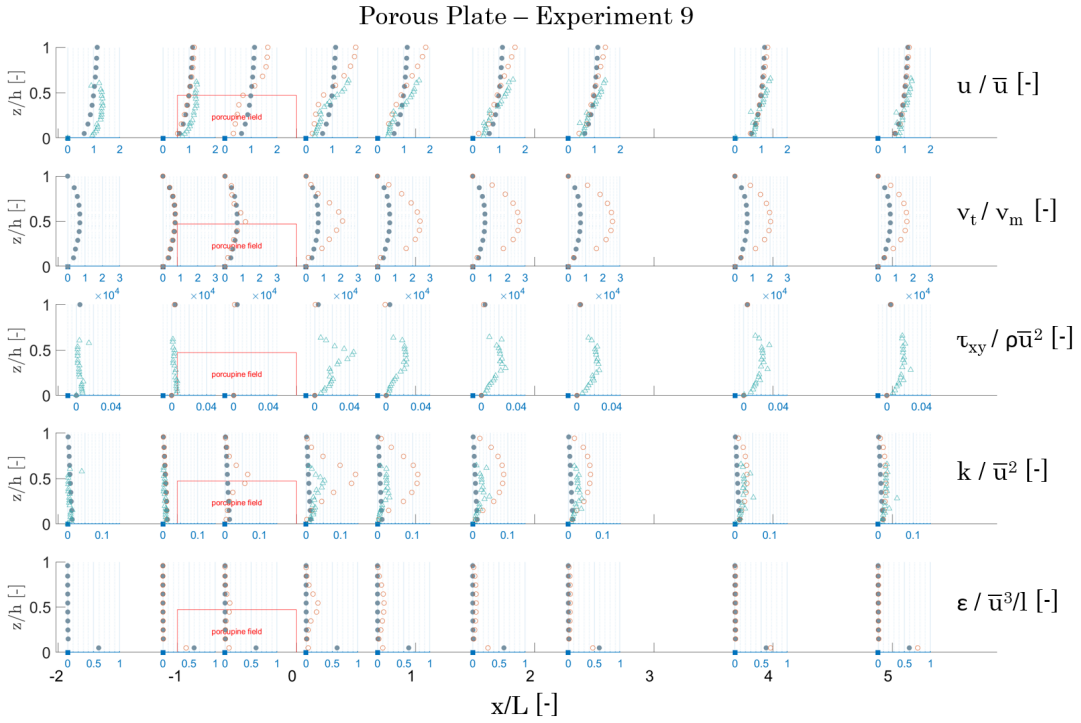

Figure 5.11: More dense field: Porous Plate ($c_{loss\ up} = 1; c_{loss\ down} = 4$). Dark circles = upstream model profile; open circles= current model profile; triangles = flume experiment.

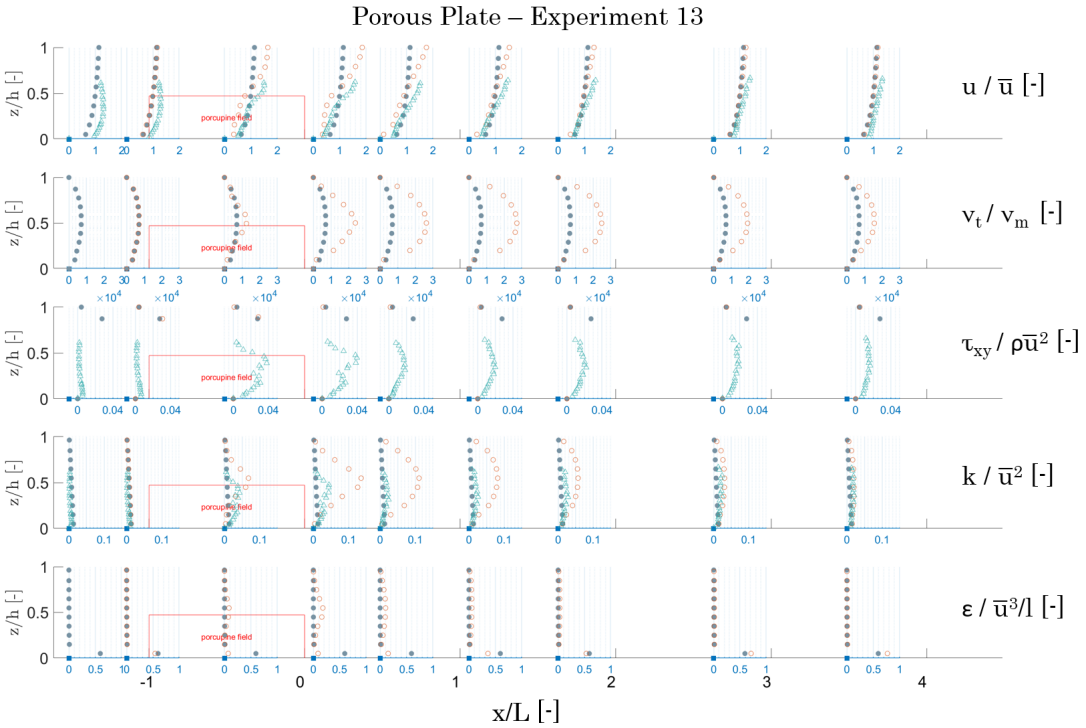

Figure 5.12: Less dense field: Porous Plate ($c_{loss\ up} = 1; c_{loss\ down} = 2$). Dark circles = upstream model profile; open circles= current model profile; triangles = flume experiment.

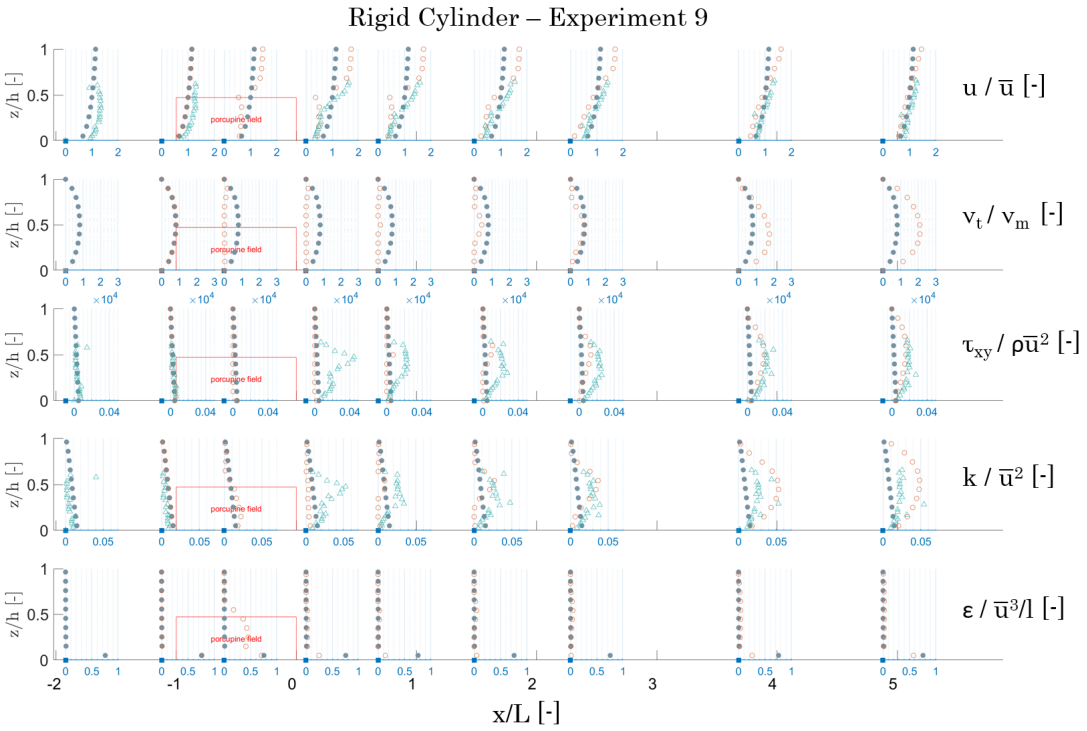

Figure 5.13: More dense field: Rigid Cylinders ($C_d = 5$). Dark circles = upstream model profile; open circles= current model profile; triangles = flume experiment.

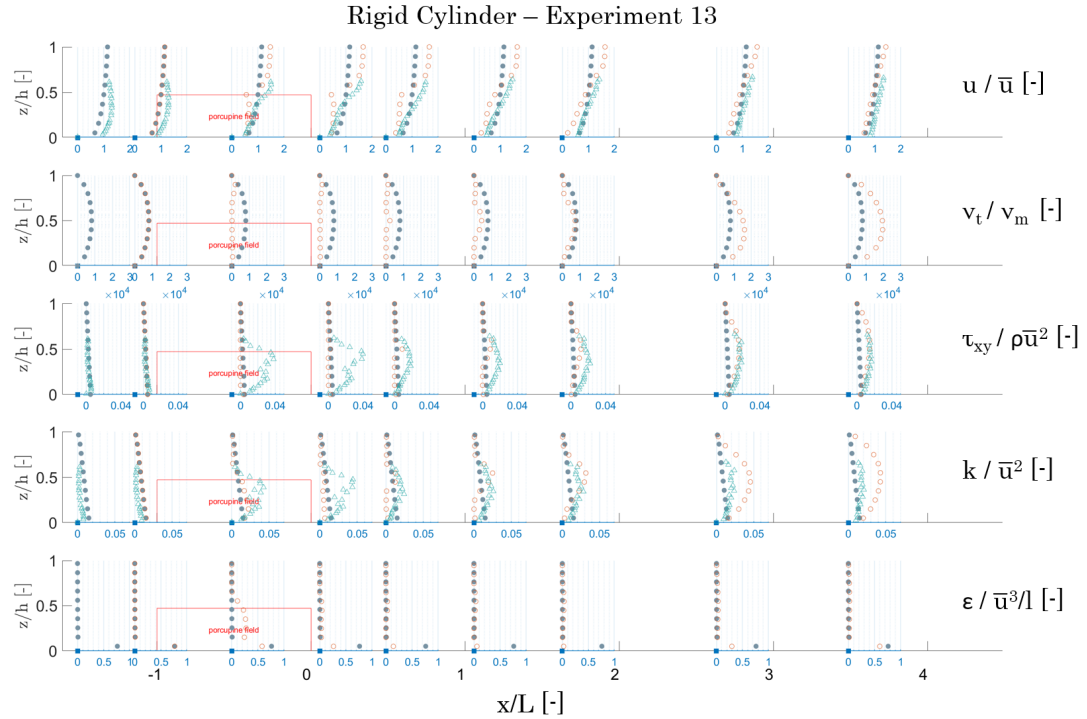

Figure 5.14: Less dense field: Rigid Cylinders ($C_d = 3$). Dark circles = upstream model profile; open circles= current model profile; triangles = flume experiment.

5.7.3 Quantitative Comparison

The behavior of each of the resistance representation is compared to each other, and relative to the measured flume data, as shown in Figures 5.15 and 5.16 for runs 9 (more dense) and 13 (less dense) respectively. The water level, velocities and bed shear stress are normalized against the value at the location upstream of the porcupine field (x/L = -2), estimated to be experiencing normal flow conditions (η_0, u_0, and $\tau_{b,0}$, respectively). Note that the depth-averaged velocity is shown for the model, even though a depth-averaged velocity is not available for the flume experiment. This was to show what could be expected for the evolution of the depth-averaged velocity. First, the three representations are compared relative to each other. Then the strengths and weaknesses of each representation is evaluated.

Overall, all methods show a decrease in water level, as expected, due to the energy lost from turbulence generated in the porcupine field. All three representations show a decrease in velocities, with a greater decrease when averaged up to the porcupine height compared to over the measurement height, as the velocity above the porcupine field is accelerating, as indicated previously. The depth-averaged velocity increases over the porcupine field and downstream of the porcupine field relative to the upstream location, due to the reduction in water depth. The bed shear stress also increased downstream of the porcupine field, relative to the upstream location, even though it is reduced within and just downstream of the field for the porous plate and the rigid cylinder representations. In the long-term, increased velocities and bed shear stress downstream of the porcupine field might lead to increased sediment transport and degradation; however, this is dependent on the exact velocity increase, the sediment supply and the sediment grain size distribution. Now, each representation will be discussed in more detail.

Increased Roughness

The increased roughness representation was calibrated to match the water level, since it was not physically possible to increase the porcupine field roughness enough to match the velocities. Therefore, this model is not able to replicate the measured velocities. As mentioned earlier, due to inconsistencies with the water level measurements, the models were generally calibrated using the velocity measurements rather than water levels. This model also greatly increases the bed shear stress within the porcupine field; however, significant variation is observed. Note that the scale of the bed shear stress for the increased roughness representation is two orders of magnitude greater than the other representations. Even though velocities within and just downstream of the field are reduced, this model will greatly enhance the sediment transport within the porcupine field.

Porous Plate

The porous plate representation underestimates the velocities downstream of the porcupine field, even though it does seem to capture well the velocity drop across the porcupine field. The bed shear stress also increased too quickly downstream of the porcupine field.

Rigid Cylinder

The Rigid Cylinder approximation performs the best of three representations, as may be expected based on the results of the previous sections; however the bed shear stress does not appear to be decreased strongly enough within and just downstream of the porcupine field. This could be due to the 'delayed' effect of the Rigid Cylinder model observed earlier.

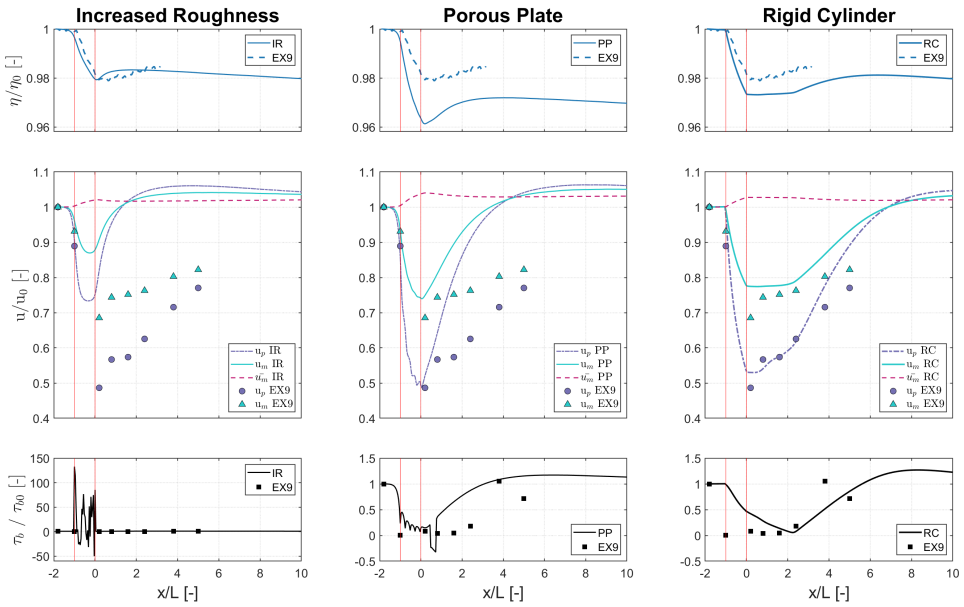

Figure 5.15: More dense field (run 9): Measured and predicted water level, velocities and bed shear stress. Red lines delineate porcupine field location. u_p= depth-averaged velocity to porcupine height; u_m = depth-averaged velocity to measurement height; $\bar{u}_m$ = depth-averaged velocity (only for model); IR: Increased Roughness; PP: Porous Plate; RC: Rigid Cylinder; EX9: Experiment 9

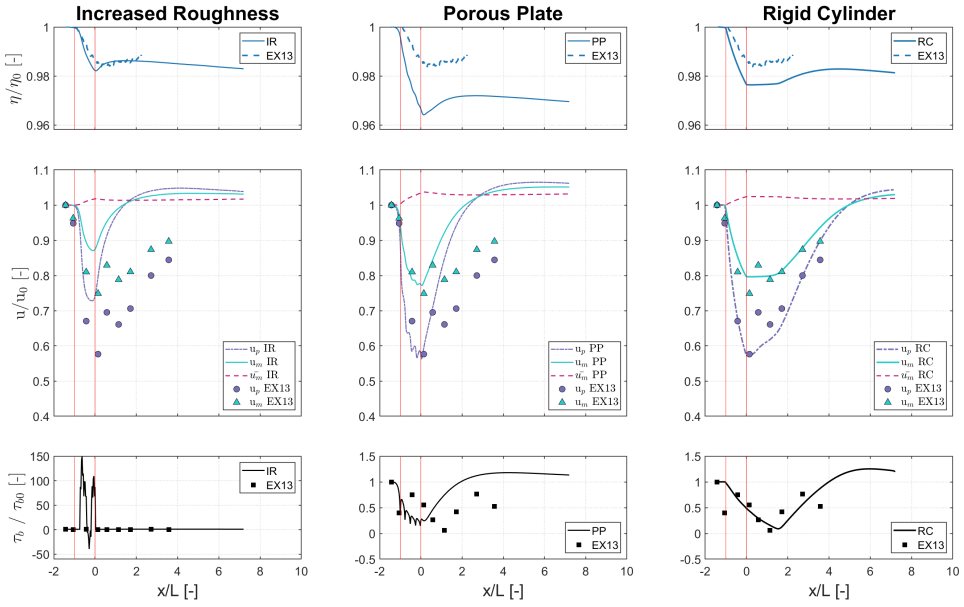

Figure 5.16: Less dense field (run 13): Measured and predicted water level, velocities and bed shear stress. Red lines delineate porcupine field location. u_p= depth-averaged velocity to porcupine height; u_m = depth-averaged velocity to measurement height; $\bar{u}_m$ = depth-averaged velocity (only for model); IR: Increased Roughness; PP: Porous Plate; RC: Rigid Cylinder; EX13: Experiment 13

5.7.4 2DV Model Performance Criteria Evaluation

The performance criteria for each resistance model is shown in Table 5.7. The performance of these models for each of these criteria could be largely interpreted from the figures presented, except for the prediction of the height of the backwater curve.

Run	Model	% diff h_{bw}	%diff ΔE	RMSE u_p	RMSE τ_b
9	Friction	-6	51	0.32	0.73
9	Porous Plate	-77	5	0.19	0.18
9	Rigid Cylinder	-8	12	0.06	0.36
13	Friction	17	74	0.23	222,555
13	Porous Plate	-78	5	0.15	0.16
13	Rigid Cylinder	4	62	0.05	0.08

Table 5.7: Performance Criteria for 2DV Model. Note: diff = difference.

The rigid cylinder method is best able to predict the upstream backwater height, despite calibrating the model to velocities rather than water levels; however, the increased bed roughness, which was calibrated to the water level, showed reasonable agreement to the predicted backwater height, despite not matching the predicted velocities. None of the models were able to predict the energy loss across the porcupine field well. This is most likely due to the measurement errors that did not allow for the model to calibrated to both velocity and water levels. The porous plate model was able to best predict the velocity retardation across the porcupine field; however, if we look at all velocity measurements the rigid cylinder clearly performs the best with the lowest RMSE for the velocity (measured up to the porcupine height). Examining the RMSE for the bed shear stress reveals how important it is to get measurements from within the porcupine field for accurate modelling, when we see the unreasonable value for the Experiment 13 RMSE bed shear stress using the friction model.

5.7.5 2DV Model Sensitivity Analysis

The 2DV model sensitivity analysis aims to explore which parameters are most sensitive model performance. In addition, certain anomalies observed in the results are explored to eliminate factors, such as the grid size or number of vertical layers, in accurately representing the porcupine field. For simplicity, only the rigid cylinder model is explored since the other two models have been eliminated from consideration for further use due tor accuracy (increased roughness) or computational reasons (porous plates).

The sensitivity analysis explores both model parameters (grid size, number of layers, bed friction and background viscosity [ν_t]) as well as parameterization of the porcupines into 'rigid cylinders' (C_d, relative density of each layer). Each will be explored separately.

Figure 5.17 shows the results of altering model parameters. Increasing the background bed roughness (C_b) reduces the deceleration of velocities and reduces the strength of the energy loss within the porcupine field. Therefore, as the bed roughness increases, the effect of the porcupines diminishes. Increasing the background bed roughness leads to stronger deceleration and energy loss; however the effect is minimal. Porcupines, as they influence the bed around them, can locally alter the roughness by inducing the creation of bed forms, which can in turn affect their roughness relative to the bed and the resistance they offer the flow.

Altering the background viscosity ($\nu_{H,back}$) has no effect on the results until a value of 0.01 is reached; however the difference is negligible. This value is orders of magnitude larger than what would be typical for a model this size; therefore the model is not very sensitive to horizontal background viscosity within several orders of magnitude of the value calculated from the scaling analysis.

The grid presented uses grid cells of 20 cm. The grid was refined to 10 cm cells, and coarsened to 50 cm cells. Coarsening the grid cells did not show a significant difference in the predicted and measured

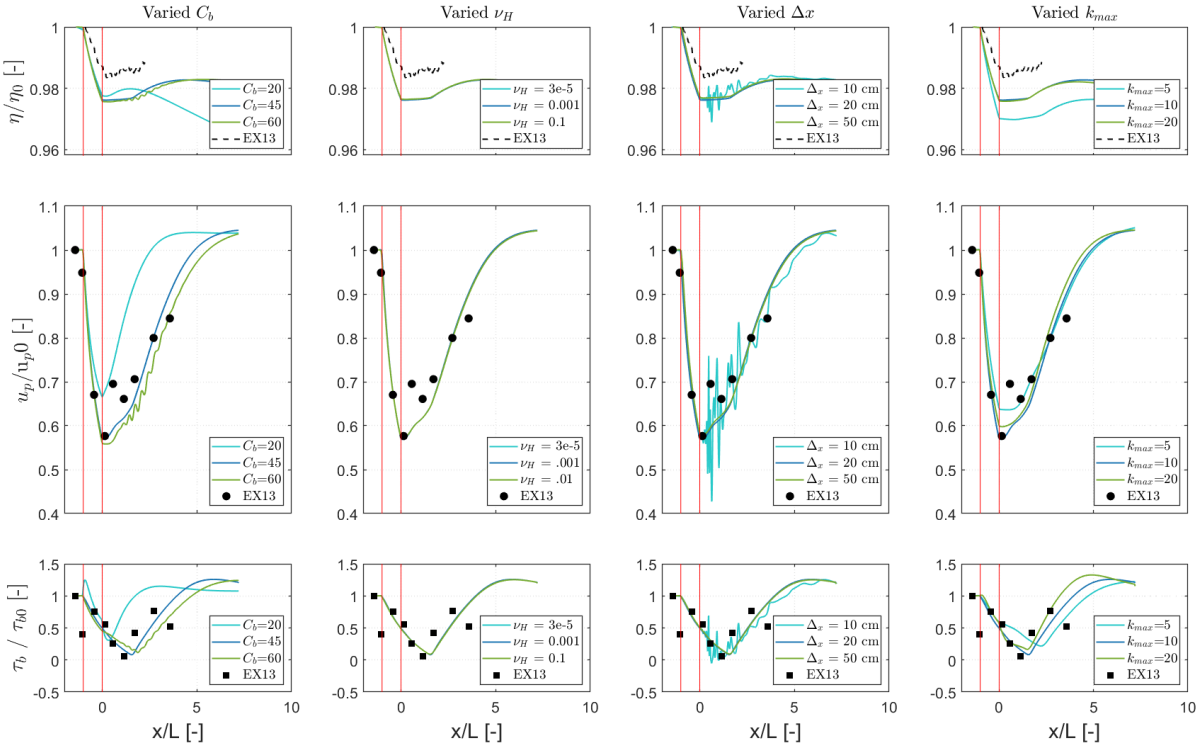

Figure 5.17: Sensitivity analysis for rigid cylinder vegetation model; experiment 13. u_p= depth-averaged velocity to porcupine height; EX13: Experiment 13. Red lines indicate location of porcupine field.

results. Refining the grid resulted in an unstable model. The time step will need to be reduced, which will even further increase the computational cost.

Increasing the number of layers should, in theory, lead to increased accuracy, in particular when the layers near zones of strong shear (the bed and the top of the porcupines) are made thinner, to more accurately capture the strength of the shear zones. Here, we observe that increased layers (20 versus 10) does not improve the accuracy of the predictions. Only 5 vertical layers shows large inaccuracies. This suggests that 10 vertical layers may be sufficient.

Figure 5.18 shows the results of altering the parameterization of porcupines. Altering the turbulence length scale coefficient (C_l) had no impact on the model. This is likely indicates the porcupines are too sparse for the turbulence length scale to switch to the spacing between 'stems'. The vegetation parameterization was changed from two layers (one short, more dense layer and one taller less-dense layer), to just one tall layer of average density. The results show that the higher layers contribute significantly to velocity reductions; however higher vegetation also leads to instability in the model. The time step will need to be reduced to clear the numerical oscillations. In addition, the velocity and bed shear stress could not be matched together, a they could for the 2-layer version. This demonstrates that porcupines parameterized as one unit, without differentiating between the low and high beams, may lead to an inaccurate solution and a more arbitrary process of calibrating the model; rather than characterizing the density based on geometry and tuning with the drag coefficient; however alternative configurations of porcupines or alternative flow conditions may be more conducive to calibration with just one unit.

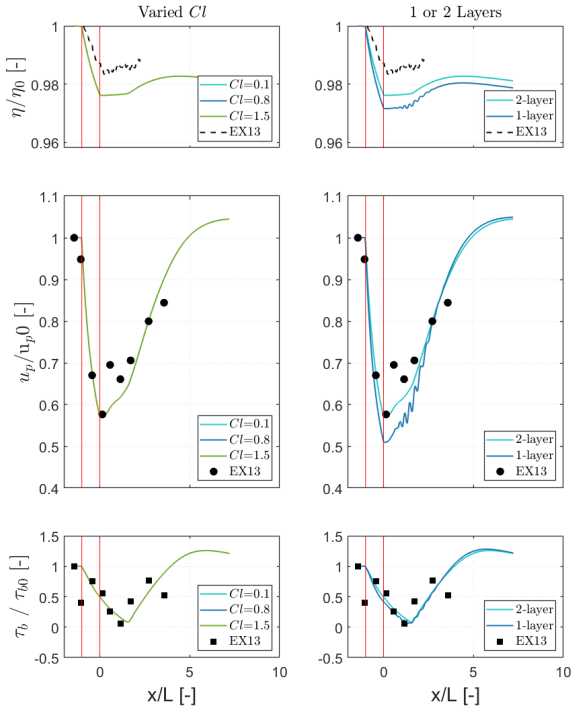

Figure 5.18: Sensitivity analysis for rigid cylinder vegetation model; experiment 13. Red lines indicate location of porcupine field.. u_p= depth-averaged velocity to porcupine height; EX13: Experiment 13. Note that there is no variation in results with varying Cl, therefore the three lines plot one on top of the other.

5.7.6 2DV Model Discussion

Comparison of Resistance Representations

The rigid cylinder resistance representation, although derived to describe rigid cylinder resistance, does a reasonable job of reproducing the hydrodynamic effects of porcupines on the flow field for the one low-density experiment. Of all of the models it was able to most closely reproduce all of the performance criteria, including the velocity reduction, energy loss, and upstream elevation of the water level; however, while the velocities and bed shear stress within and downstream of the field are appropriately reduced, the model shows a certain lag in reproducing the turbulence structure. This phenomena was also observed by other researches [59]. This model is the most flexible of the three considered, since it allows for a completely description of the vertical plant structure and leaves the drag coefficient to be adjusted as a calibration coefficient.

The porous plate representation was able to correctly reproduce the velocity reduction within the porcupine field but did not retard the velocities long enough downstream of the field. When the velocities were matched the bed shear stress too strongly reduced. This was particularly evident for Experiment 13, which had a measurement inside the porcupine field; however, the inaccuracy of the bed shear stress estimations from the flume experiment may be large. The porous plate representation was the most computationally expensive of three models, and it does not allow for a detailed description of the resistance elements beyond the generic loss coefficients, which are also the only parameters available for calibration. Therefore, while this model showed promise as a simple representation of porcupines, with an inherently-decoupled bed shear stress, it is not recommended for a detailed representation of porcupines for design evaluation purposes.

The increased roughness representation did not represent the detailed effects of porcupines well. It was not able to reproduce the velocity reduction across the porcupine field, or correctly reproduce the

evolution of the bed shear stress. Nevertheless, this option may still be of use in representing the porcupine field in the 1DH simulation.

Field Density Behavior Differences

The performance of the less dense porcupine field performed was captured reasonably well by the rigid cylinder model, where the more dense porcupine field showed less agreement. There are two possible reasons. First, since the Uittenbogaard model was derived for rigid cylinders, the this could suggest that porcupine behavior can be well-approximated as rigid cylinders at low densities, but at higher densities the 'configuration' of cylinders selected needs to be adjusted, particularly to take into account the changes to the turbulence length scales. The second reason could be measurement errors in the flume experiment data, related to the ADV, or to the lack of cross-sectional spatial averaging that has biased the results of the higher density field (with greater flow perturbations), more than the results of the lower density field. Further investigation is needed to clarify if this is a measurement issue, or if the rigid cylinder model will not represent porcupines well at high densities without modification to the formulation, such as modifying closure coefficients.

Comparison to Pilot Study and Literature Observations

During the pilot study analysis, significant literature was reviewed to estimate the impacts of porcupines on the local morphology. This revealed that for higher-density resistance patches, a zone of high shear stress should be observed at the leading edge of the patch, where the turbulence intensities are increased but the increased turbulence has not yet retarded flow velocities. This result was indeed observed in the 2018 flume study. The 2DV modelling results do not show this increased shear stress just inside the porcupine field. In addition, measurements were not collected from that location either. Instead, with measurements only on either end, or in the middle of the field, a false impression is given that the shear stress should only decrease from the upstream to the downstream end of the porcupine field. Therefore, not only does this need to be considered when interpreting modelling results, but experimental investigations should target measurements in this area to understand how porcupine field designs and configurations can place these leading porcupines at risk for scour. The pilot study and mobile-bed flume experiments suggest that sinking of porcupines can expose the porcupines further downstream to high velocities, causing a chain reaction.

5.8 1DH Model Results

Only a quantitative comparison is performed for the 1DH model results due to lack of profile information. The predicted water level and bed shear shear stress values are compared against the flume measurements. Only the increased roughness and Baptist resistance methods are compared.

5.8.1 Quantitative Comparison

Figure 5.19 and 5.20 show the results for experiments 9 and 13 respectively. The water levels and bed shear stress are normalized by the value of the water level or bed shear stress at the undisturbed normal-flow location upstream of the porcupine field ($x/L = -2$). Despite the uncertainty in the water levels, the models were calibrated to match the water level and bed shear stress levels, since the depth-averaged velocity was not available.

Unlike for the 2DV model, the increased roughness resistance model can be calibrated to the water level, with a reasonable Chezy value for the porcupine resistance. The same calibration method was followed as for the 2DV model: increasing the bed roughness in the grid cells where the porcupine field is located. While the bed shear stress values are much higher than those predicted with the Baptist method, they are an order of magnitude less than those predicted with the 2DV model. This demonstrates the ability of simply increasing the roughness of the bed in predicting reasonably well the influence of vegetation on water levels, even if the local bed shear stress is incorrect.

To calibrate the Baptist method, the porcupines were broken into rigid cylinders, as described above, and the drag coefficient was altered to match the water levels; however, it was not possible to match

water levels and bed shear stress using a reasonable value of the drag coefficient. While there is much variability in the possible drag coefficients for porcupines or vegetation, the upper limit of recorded values in the literature is approximately 15. Therefore, the drag coefficients were kept at 3 and 5 (the values found through the 2DV model calibration for experiments 13 and 9 respectively), and the vegetation density was increased. For experiment 13, calibration was achieved when the density in both layers (lower- horizontal beams, and upper - vertical beams), was increased by a factor of 10. For experiment 9, calibration was not possible, even with unreasonable densities or drag coefficients; however, above a density increase of 100 or a drag coefficient of 5, the additional reduction in water level or bed shear stress was negligible. Therefore, displayed is a vegetation density increased by 100 and a drag coefficient of 5. The difficulty in calibrating this model is likely the same reason it was difficult to calibrate for the 2DV version: the water level measurement error. On the other hand, the issue could indicate that the Baptist might not work well for less dense fields of porcupines, or otherwise require additional analyses to determine the best method of parameterizing porcupines as rigid cylinders.

The Baptist method tends to overestimate the bed shear stress reduction within the porcupine field. This is likely due to the fact that the method has been derived and calibrated using vegetation data that is largely 'dense' [5]. If additional data sets of 'sparse' vegetation were included in the genetic programming, or if data sets of only 'sparse' vegetation were used, a different formulation may have been obtained.

Downstream of the porcupine field, the Baptist method predicts an immediate increase of the bed shear stress, which could lead to the model predicting erosion and sediment transport in that location, when the flume experiment showed deposition for the mobile-bed experiment run with the same hydrodynamic conditions as Experiment 9. Nevertheless, the Baptist method can still used to predict long-term impacts in reaches were porcupines have been implemented. The following section will clarify which of these two large-scale methods (Baptist or increased bottom roughness) will do a better job in predicting upstream water level changes and the energy loss over the porcupine field.

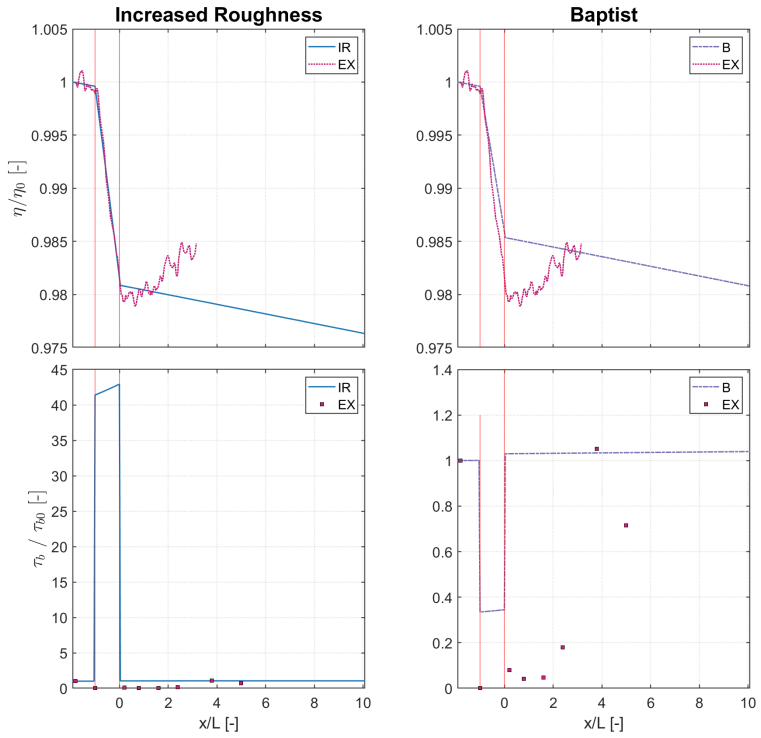

Figure 5.19: More dense field (run 9): Measured and predicted water level, and bed shear stress, normalized by the upstream value at $x/L = -2$. Red lines delineate porcupine field location. IR: Increased Roughness (C_b= 45; $C_{b,porc} = 7$); B: Baptist ($nx100$; $C_d = 5$); EX9: Experiment 9

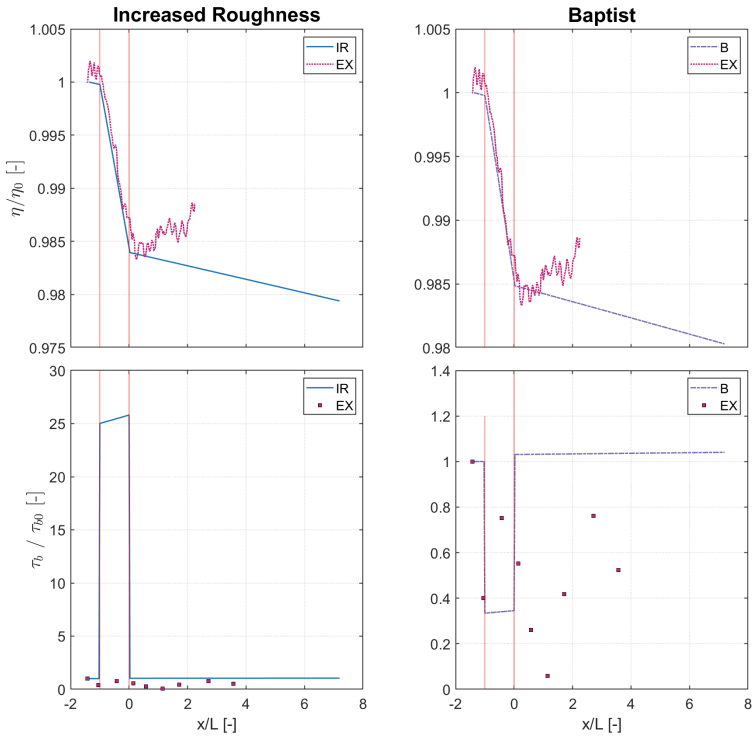

Figure 5.20: Less dense field (run 13): Measured and predicted water level, and bed shear stress, normalized by the upstream value at $x/L = -2$. Red lines delineate porcupine field location. IR: Increased Roughness(C_b= 45; $C_{b,porc} = 9$); B: Baptist ($nx10$; $C_d = 3$); EX13: Experiment 13

5.8.2 1DH Model Performance Criteria Evaluation

Table 5.8 shows the difference between the measured and predicted relative height of the backwater curve upstream of the porcupine field. The results demonstrate that overall both models are able to accurately predict the height of the upstream backwater curve to withing approximately 6%; however given the concerns over the water level data, and the fact that the Baptist method predicts the height of relative backwater curve to within 6%, despite being poorly calibrated to the water levels, these numbers may not reveal the true accuracy of the models, and should be verified with further experiments.

Run	Model	% diff h_{bw}
9	Baptist	5.7
9	Friction	-4.4
13	Baptist	2.2
13	Friction	-4.1

Table 5.8: Performance Criteria for 1DH Model. Note: diff = difference.

5.8.3 1DH Model Discussion

The results of the 1DH modelling analysis indicate that the impact of porcupines on hydrodynamics and bed shear stress may be represented using the method of Baptist if the input parameters are modified; however, a much larger data set it required to see if the method will work for various densities of fields and hydrodynamic conditions.

It is assumed that the results of Experiment 13 are reasonably accurate, given the good calibration achieved for both the 2DV and 1DH models. Therefore, based on the Experiment 13 model, this study found that the density, as calculated translating porcupine beams into cylinders, needs to be increased by a factor of 10 to accurately represent porcupines with the method of Baptist. In addition,for the 1DH model the drag coefficient needs to be tuned first using a more appropriate model, or directly calculated from flume measurements. This is an interesting result, considering that the rigid cylinder model did not require any modification to the porcupine density as originally calculated when translating the porcupine beams in to cylinders. However, under real (mobile bed) conditions, the drag coefficient will likely approach one, and the sensitivity of the drag coefficient in determining the final results may not be as important. However one experiment is not sufficient to draw real conclusions. The parameterization should be tested with more data sets.

Neither the method of Baptist nor the increased bottom roughness representation will completely accurately predict local changes to morphology. The increased roughness method will likely predict erosion and sediment transport within the porcupine field, where the Baptist method will overestimate deposition within the field and the overestimate erosion downstream of the field. A more detailed analysis, including morphology, is required to determine which method will, in the long run, better predict morphological changes within the reach; however, since both methods do a reasonable job of predicting impacts to local flow conditions (water levels) it could be estimated that the method of Baptist will ultimately be a better representation of porcupine roughness, since deposition within the field is a potential performance objective.

5.9 Conclusions

This chapter has examined a 2DV and a 1DH model for representing the impacts of porcupines on local hydrodynamics. The models were calibrated against data from a porcupine flume experiment, and the expected and actual results were compared. Data was not available for full calibration and validation of the models; nevertheless the results provided a necessary first step for exploring numerical modelling of porcupine fields further.

For the 2DV model, the rigid cylinder did a reasonable job of reproducing the porcupine performance,

particularly for the less dense experiment. This could indicate that translating porcupines into cylinders for use in this model is limited to low-density porcupine fields; or the weak calibration could be a result of measurement error. Further studies, with replicate experiments, are required for the full range of validity of the Rigid Cylinder model in representing porcupines. An area of open debate is the ability of this model to predict an increase in shear stress at the upstream end of the porcupine field, as was observed during the flume experiment. This discrepancy needs to be considered when interpreting the model results.

For the 1DH model, both increased roughness and the method of Baptist are able to reproduce the local water levels with reasonable accuracy; however, neither method is able to entirely predict local changes to morphology. The Baptist method under-predicts the shear stress within the field, and over-predicts the downstream shear stress; where the increased roughness method greatly overestimates the bed shear stress within the field, and overestimates the downstream shear stress as well. The method of Baptist assumes fully-developed flow, and therefore does not accurately take into account the transition zones upstream and downstream of the field; however, comparing the order of magnitude of the under and overestimates, the Baptist method will likely do a much better job than increased bottom roughness of estimating the long-term morphological impacts of porcupine since at least the bed shear stress is correctly reduced within the porcupine field. The modeled porcupine field is very short. For a longer field, the distance over which the Baptist method incorrectly reproduced the bed shear stress will be less important. Finally, like in the 2DV model, using the Baptist method one needs to be careful interpreting the results for local morphological impacts. For a dense porcupine field, there will likely be an increase in shear stress just at the upstream end of the field, which is not captured with the Baptist method.

More experimental data is required to better quantify the expected uncertainty using either the Uittenbogaard or Baptist methods for representing porcupines in large-scale numerical models. It is uncertain if these models can be used to predict hydrodynamic impacts of more dense porcupine fields, or under variable flow conditions. Alternate parameterizations of porcupines into rigid cylinders may improve results. In addition, adding morphology, as examined briefly in Appendix B, will greatly complicate the model, requiring even further experiment data for thorough calibration and validation.

Chapter 6

Recommendations for Porcupine Field Design, Modelling and Analysis

This chapter brings together the insights obtained from analysis of field and experimental porcupine data, numerical modelling of porcupine fields and literature review of hydrodynamic and morphodynamic impacts of resistance elements to make recommendations for the design of porcupine systems, 2D numerical modelling of porcupine fields, and the effective design of future experimental setups targeting critical data gaps in our understanding of porcupine field behavior. Cautions are given for the limitations of the recommendations due to areas of porcupine behavior that are least understood.

6.1 Design of Porcupine Systems

Insights gained from this thesis lead to recommendations in several areas of porcupine system design. Porcupine systems are considered to be any configuration of porcupines acting together in a river reach. First, the primary observation of porcupine systems are summarized. Next, considerations for the local system are discussed. Then, alternative design configurations of porcupine field or patches that target issues in current designs are elaborated. Finally, suggestions are given for alternative designs of the porcupines themselves. Note that porcupine systems can have multiple objectives including bank protection, sedimentation, local bed elevation increase, or, as in the case of the Ayeyarwady River pilot study, increased roughness to raise the upstream water level and maintain bifurcation discharge distributions.

In examining the performance of porcupine systems, two primary observations are made that may impact the expected performance. When porcupines are subjected to high velocities or limited sediment supply, they may scour and sink into the bed, particularly at the leading edge. Once that elevation has been lost, it will not be regained. This has implications for both the long-term expected impact of the system, and accurately modelling long-term performance. Potential scour will not necessarily lead to design criteria not being met; however it can, and it is perhaps the most poorly understood aspect of porcupine systems. Therefore, until more detailed studies can clarify the exact impact of potential sinking on performance, it must be carefully considered in designing porcupine system.

The second consideration is that the porcupine system can behave very differently if its influence on the hydrodynamics can be considered ‘sparse’ or ‘dense’. Sparse fields will likely scour less at the leading edge or lateral edges, assuming sediment supply is not an issue and velocities are not too high. At the same time, if maximum resistance is desired, more dense fields should considered - to a point. If the porcupines will be submerged for a significant portion of the wet season, the increased density will at some point cease to increase the resistance of the porcupine field, because water will be pushed above or around the field rather than through it. Therefore, a balance is necessary to find the optimal density of the field given the local conditions and primary design objectives. The available is not enough to give concrete

recommendations about what impacts could be expected for what field densities. The pilot study and the 2018 flume experiment suggest that at a $lambda_p$ of approximately 0.2 a porcupine field could be expected to show a 'transitional' behavior, that may trend to 'sparse' as porcupines loose elevation or become buried; while, at a $lambda_p$ of about 0.8 the behavior is more dense; however, significantly wider data sets and porcupine field configurations need to be tested and evaluated to establish more robust design criteria.

Note that all of the recommendations given in this section are based on analysis and interpretation of the existing data; however any changes to designs should be considered with experimental and/or numerical analyses to confirm their predicted impacts and applicability to the local system.

6.1.1 Location

The design of porcupine systems needs to be aligned with both the local conditions and the primary objectives of the system. The pilot study analysis, experimental data and literature review of porcupine systems and vegetation fields suggest that when sedimentation (and potentially associated bed level increases) are the primary design objective, placing porcupines in low-energy areas will enhance their performance. In high-energy ares porcupines may simply not be able to reduce velocities sufficiently to encourage deposition, and, if the velocity and sediment supply conditions are such that the first rows of porcupines scour and sink, the rows behind will be even more vulnerable to erosion and sinking, leading to an ineffective area of porcupines. Therefore, if porcupines are needed to protect high-energy areas, or it is otherwise desired to place porcupines in high-energy areas, the design of the porcupine system needs to be modified so the leading (and potentially lateral) edges of the porcupine system are either protected from scour, or designed in way that they maintain their original elevation, in spite of scour, or those areas simply need to be targeted for maintenance on a regular basis. Suggestions for achieving this protection are given in the next section.

The second consideration for location in design of porcupine systems, is that the local sediment supply is key a factor in how the porcupine system might perform. Therefore, if detailed information on the variability of the local sediment supply is not available or cannot be collected, then at least in designing the system, cases of sedimentation or erosion waves entering the system should be considered.

The final key considerations is that the flexibility inherent in porcupine systems is a major advantage that should not be overlooked. River systems are dynamic and this can influence porcupine systems in unforeseen ways. For example, new channels forming can increase or reduce flow in porcupined areas. Natural channel widening can change velocities or shift the channel away from a porcupine field. The presence of the porcupines could potentially enhance or inhibit these processes. Given the natural variability inherent in any river system and the uncertainties associated with any river training design, monitoring and maintenance will be key to a successful long-term design. For example, to date placement of porcupines in high energy areas is generally not recommended. The final design may need to incorporate regular monitoring and maintenance of these areas, if effective alternative designs are not found.

6.1.2 Alternative Porcupine Field and Patch Designs

From the pilot study data, it is postulated that transverse resistance gradients may have pushed the water in Sagaing and Middle channels towards to the outer bed of the river, narrowing and deepening the low-flow channel and shifting the thalweg towards the outer bend (although the change in the direction of the low-flow channel at the channel entrance could be partly responsible for the shift). Increased flow along an outer bend can lead to higher velocities and potentially bank erosion. If protection of that bank is desired, alternative configuration of porcupines across the main channel, described below, may help to maintain the designed resistance while alleviating pressure on the outer bank.

Lateral Variations in Porcupine Height or Density

Porcupine systems can be designed to minimize transverse resistance gradients by placing taller or more dense porcupines at lower elevations, and shorter or less dense porcupines at higher elevations. The change in density or height of the porcupines reduces resistance differences at low and/or high flows,

compensating for varying water levels across the channel width. At the same time, transverse gradients can be specifically encouraged in the porcupine field design to encourage flow in desired areas and away from non-desired areas (e.g. towards the center of the channel and away from the banks).

Additional Porcupines to Protect the Bed

In the center of a sparse or transitional porcupine field under submerged conditions, the bed can be exposed to large turbulent eddies from the overflow. The placement of smaller porcupines between larger porcupines can help to alter the local field field near the bed, protecting it from large eddies and scour. In addition, the porcupines design could be altered such that the porcupines maintain their frontal area but have a wider base and shorter vertical beams. This would reduce the effective height of the porcupine giving it higher submergence ratios for the same flows compared to porcupines with equal-length beams. High submergence ratios will reduce the effective resistance of the field. Therefore the design criteria and local flow conditions need to be considered to evaluate if this option might be effective.

Gradual Density Increase for Leading or Lateral Edges of Porcupine Field

If a dense porcupine field is desired, but high scour at the leading and trailing edge of fields is a concern, the density of the field could be gradually increased from the leading edge inwards, to allow for a slower development of the velocity profile. Once velocities at the leading edge have been reduced enough, the additional density deeper in the field will be less likely to induce high shear stresses that may lead to scour.

Fixed Elevation at Leading or Trailing Edges

Another alternative to protect the leading or trailing edges would be to design porcupines in those areas such that they maintain their elevation, even if the beams are scoured. This could mean driving poles (at least two per porcupine) into the bed, deep enough that they can't be scoured without the porcupine sinking. This may hamper the flexibility of the system if movement of the porcupines might be desired; however, porcupines that have sunk or become buried into the bed are likely not very easy to move anyway. In addition, in highly dynamic rivers where large bed elevation changes over the course of the season may be expected, this option might simply be infeasible.

Adding Resistance to Porcupines

To increase the resistance offered by porcupines (effectively increasing the blockage or density), additional branches could be wrapped around the porcupine structure or placed inside the porcupines. This can be used to increase their resistance in targeted areas, or potentially to protect the leading edge of the porcupine field. A very high resistance at the leading edge will reduce velocities more quickly, protecting the porcupines behind from high velocities; however this high resistance at the leading edge will also likely cause high scour and sinking of these porcupines, if their elevation is not fixed. Therefore, these 'dense' porcupines could also incorporate a method to fix the elevation, as described above, or they could be designed to sustain just one wet season, and be targeted for regular maintenance. Debris may already naturally accumulate in porcupines; however branches can be placed proactively in areas where large amounts of debris are not expected or to have increased resistance from the initial installation. Of course, for some systems the increased resistance may not be desired.

Many Patches as Opposed to One Field

It has been demonstrated that for the same blockage many patches of vegetation can offer more resistance than a single field across the entire channel width, because the effective perimeter of shear layers is increased (lateral and vertical shear layers create a longer total area of strong shear layers than one vertical shear layer alone); however, this method will only work for fields that are 'dense' enough to develop strong shear layers. Therefore, if maximizing resistance is the design goal, patches of dense fields can be considered. Further analyses would be need to evaluate optimal configurations and examine what the implication of the additional shear would be for scour along the leading and lateral edges, and in the

channels between the patches. It is possible, or likely, that this alternative would not be well-suited to all systems, particularly when high flow velocities are expected and potential sinking of porcupines is a concern.

6.1.3 Porcupine Design

Potential scour and sinking of porcupines is a critical aspect of the porcupine field design. Scour or sinking will not necessarily lead to poor performance - that depends on the exact design objectives of the system; however, if porcupines need to be placed in high-energy flows, or if the performance design requirements will be hindered by porcupines sinking, then the design needs to be adapted to minimize scour.

A detailed study of the mechanisms and parameters influencing the scour around porcupine beams was not studied in detail; however, the scour will generally increase with increasing beam width, increasing velocities and decreasing sediment grain size. Two alternative porcupine designs proposed below potentially address the issue of scour by using thinner beams. In addition, they use more beams per area, for a higher density. As has been well-established, high densities and scour are related, therefore these designs, while offering some advantages, would need more careful analyses to determine their exact effectiveness in different kinds of systems.

Teepee Porcupines

Teepee porcupines are composed of many slender poles arranged in a cone configuration, attached at a central location near the top of the poles (see Figure 6.1. This design eliminates the horizontal bar, which has been shown to (1) be critical to high density (and thus high resistance) of a porcupine, and (2) easily become buried. This design, even if the porcupine beams scour and sink, maintains a higher density for the same elevation loss. In addition, the thinner beams may produce a lower scour depth than the thicker traditional porcupine beams, depending on the exact diameter of the poles used.

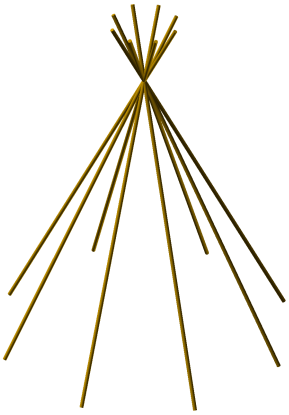

Figure 6.1: Example of a 'teepee' porcupine configuration

Mangrove Porcupines

The next design option mimics the root system of mangroves, as shown in Figure 6.2. This design also eliminates the horizontal beams and can include thinner beams than traditional porcupines for the same overall density. The two alternatives are very similar; however the mangrove root porcupine has the advantages of a higher density within the porcupine itself, as opposed to the the rather empty 'inside' of the teepee, if the configuration of the poles are left as one large circle. This design might be more stable under high flow conditions, since it the weight is evenly distributed from the center to the edges.

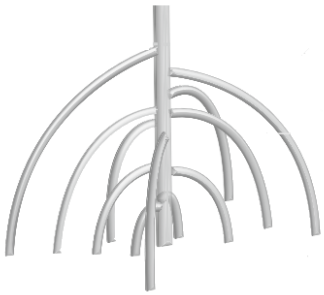

Figure 6.2: Example of porcupine design that mimics mangrove roots. Adapted from [50].

6.2 Numerical Modelling of Porcupine Fields

Accurately modelling the short- and long-term impacts of porcupine fields will be critical to effectively designing porcupine systems, as long-term experimental analyses are not practical. As demonstrated earlier, these models can be more detailed (2DV), and used to evaluate design elements of porcupines or porcupine systems; or they can focus on the large-scale impacts (2DH or 1DH) as would be necessary for designing porcupine systems for real rivers. Insights and recommendations collected from this thesis are elaborated below.

6.2.1 Modelling Long-term Performance

To model the long-term impacts of porcupines, it will be critical to take into account potential sinking of porcupines, as that may reduces their ability to resist the flow. To achieve this, criteria need to be established for when porcupines might be expected to sink (such as high flow velocities near the bed for a critical period of time). Then, when those criteria are reached, the porcupine height or density can be updated. Establishing these criteria will involve a combination of expert judgement and experimental analyses to better understand the rate and condition of scour around porcupine beams.

In addition, porcupines will not grow if sedimentation occurs, therefore the model needs to be updated when sedimentation or erosion occurs so the height of the porcupines is always relative to the initial installation elevation (assuming no scour has occurred). The dynamic vegetation module in the Delft3D Flexible Mesh Suite, or something similar, may be an option for incorporating such effects.

One issue encountered in this study was parameterizing porcupine fields into rigid cylinders for input into the Baptist vegetation model. The rigid cylinder density estimated from the porcupine geometry needed to be increased by a factor of 10 to calibrate the model. Additional data sets are needed to determine the best parameterization of porcupine fields when represented as rigid cylinders, particularly for the Baptist model.

In this study, the formulations found to best represent porcupines in 2DV or 1DH models were frameworks designed for vegetation, where vegetation is schematized as a series of rigid cylinders. These formulations, such as the Uittenbogaard (2003) rigid cylinder vegetation model, use empirical coefficients to satisfy boundary conditions to close turbulence models. They will work best for predicting the behavior of systems similar to the data used (experimental setup and range of of hydrodynamic conditions) for the original calibration of the coefficients. Therefore, when using this, or similar, models for porcupines, results may be improved if the coefficients are calibrated to porcupine data.

6.2.2 Detailed Modelling of Local Porcupine Impacts

The models explored in this study were not able to capture local effects of porcupine fields, particularly for flow development at the leading and trailing edges of porcupine fields. Other, potentially more complex models should be explored that can capture these effects, such as 3D CDF models; however detailed experimental data would be require to calibrate these models.

In addition, parameters that can be used to incorporate the effects of porcupines into numerical models, such as the drag coefficient developed from experimental setups or field data may be limited to a narrow range of flow regimes, porcupine design parameters, or flow conditions used in the tests. These parameters should be understood for the range of conditions that may be feasible to encounter in the location of interest.

6.2.3 Interpretation of Modelling Results

The numerical models examined in this thesis have shown reasonable performance in predicting water level changes, energy loss, velocity reductions and the general trend of the bed shear stress evolution for a very limited porcupine field data set; however, several processes are not well-captured. In general, the results show that these models may work better for estimating fully-developed flow conditions in porcupine fields, or large-scale impacts, as opposed to local or short-term impacts.

First, the porcupine flume experiment clearly demonstrated scour and sinking of porcupines at the leading edge of the porcupine field for higher density fields ($\lambda_p = 0.8$), due to the initial increase in turbulence intensity and as the flow enters the field, before velocities could be reduced. The pilot study data also seemed to confirm this trend for the porcupines placed in high-energy areas; however, the resistance representations in neither the detailed 2DV or 1HD models were able to correctly capturing this initial increase in turbulence intensity and increased bed shear stress. The rigid cylinder model, while reasonably accurately capturing other processes, shows a delay in the impacts to turbulence and Reynolds stresses. The model of Baptist, used in 1DH flows, assumes fully-developed flow, and is not able to capture the details of flow development at the leading edge. Therefore, when interpreting model results, local scour may need to be anticipated at the leading or lateral edges, that the model does not predict. Quantifying the expected impact of this scour will likely require additional experimental analysis.

Second, the shear stresses in these models are not fully captured at the downstream end of the porcupine field. The rigid cylinder models does seem to accurately capture a reduce in bed shear stress downstream of the porcupine field for the less dense porcupine field (experiment 13); however it underestimates the predicted bed shear stress in the more dense field. This could be because the rigid cylinder model was derived for cylinders rather than porcupines, and something about porcupines leads to increased bed shear stress more quickly downstream of the porcupine field compared to cylinders. Or, this could result from a combination of measurement error, and the fact that the bed shear stress was estimated from Reynolds stresses measured 1 cm from the bed, instead of directly at the bed. Further experimental analyses, with more accurate measurements of bed shear stress, will be needed to quantify the expected error in using these models to predict the bed shear stress.

The Baptist model predicts an immediate increase in bed shear stress downstream of the porcupine field, which will not be the case. For large porcupine fields and long-term models, the velocity retardation length is likely not long enough to significantly alter results if it is neglected. Therefore, this model may capture well the general long-term trends in water level changes; however, it should not be used to make assumptions about the local or short-term impacts of porcupine fields.

6.3 Experimental Analyses of Porcupine Systems

Experimental analyses will be key to filling data gaps related to our understanding of porcupine systems and their performance. This thesis has identified a number of considerations that should be incorporated into future experimental designs to maximize the benefit of the results. The section is not intended to provide a complete sampling plan; however considerations that have been missing from previous studies will be mentioned.

6.3.1 Target Measurements

Previous studies of porcupines (and vegetation), generally targeted measurements from fully-developed flow at the center of a resistance field, or outside the field altogether (particularly for studies of porcupines); however, successful design of porcupine systems must take into account the potential for increased

bed shear stresses at the leading and lateral edges of a porcupine field. Therefore, when possible, measurements should be taken at the leading and lateral edges (for patches not occupying the entire channel width) to understand how the shear stress and turbulence profiles should evolve when modelling porcupine fields, and to obtain data that can be use to quantify the potential severity of this scour so the system design can be adapted accordingly.

Next, a large data gap is understanding under what density the porcupine fields will transition from a sparse to a dense behavior. Therefore, accurate measurements from inside the porcupine field, where the flow is fully-developed, are critical; however these measurements need to be laterally averaged to capture the true average profile, rather than taken from a single position from the center of the flume, because the local velocities within the field are highly heterogeneous. For experiments using rigid cylinders to represent vegetation, four measurements have been found to be satisfactory in identifying the average profile [74]. For porcupines, this number may need to be more given that that the pyramid structure introduces additional irregularities compared to a field made up of identical single cylinders.

6.3.2 Experimental Setup Design

The experimental setup can be modified in several ways to facilitate comparison of results between experiments and translating those results to design or modelling analyses. Comparing experimental results is greatly facilitated when one value - such as the velocity, is held constant while the other parameters are changed (e.g. density, submergence ratio). Changing too many parameters between runs makes the results harder to interpret or translate to modelling exercises.

Finally, the experimental setup, when possible, should include the full range of hydrodynamic conditions that the porcupines might experience, including velocities and submergence rations, as discussed above. This is is necessary to accurately parameters porcupines for modelling studies, as well as define design criteria such as expected shear stresses or scour.

Chapter 7

Conclusions and Future Work

This thesis has explored how the hydrodynamic impacts of porcupines can be incorporated into 2D numerical models through analysis of field data, laboratory data, numerical modelling, and extensive literature review. The hydrodynamic impacts of porcupine systems were reasonably-well modelled for in 2D using methods traditionally used for modelling vegetation resistance; however, certain processes are not well captured, including the transitional flows at the leading and trailing edges of porcupine fields. These impacts will require special attention when interpreting modelling results. In addition, the models were tested against an extremely limited data set. Therefore much further work is needed to determine the exact performance of these vegetation models in predicting porcupine field performance. This section elaborates the conclusions drawn from each chapter (research question) of this thesis, and then proposes areas of future work.

7.1 Conclusions

First, the physics of porcupines was examined. The existing literature on porcupines is sparse, particularly for detailed measurements of the flow field. Therefore, porcupines were hypothesized to be a special kind of vegetation, and use was made of an analogy between how vegetation impacts hydrodynamics and morphology and how that response might differ for porcupines. The most important finding is that the velocity profile and turbulence characteristics can be very different for 'sparse' or 'dense' resistance fields, where dense fields generally reduce velocities and shear stresses inducing sedimentation; and sparse fields may experience erosion. In addition, the leading, trailing and lateral edges of a field or patch can have a different response than the center (fully-developed) flow area, where increased shear stresses are generally observed at the edges, before velocities can be reduced. Therefore the density and location of the field or patch is critical in estimating its influence on the flow field and in turn velocities and shear stresses near the bed, which dictate morphological responses.

The Ayeyarwady River pilot study was analyzed for the short-term local morphological response of the porcupine fields over their first wet season. While a lack of site data makes it very difficult to distinguish between what changes were induced by porcupines versus local morphological influences, several observations could be hypothesized. It was observed that the design porcupines likely exhibit transitional or sparse behavior of the flow field, where significant scour at the lead and lateral edges was not evident; however porcupines located in high-energy areas did show significant scour and sinking, where the porcupines were not able to reduce flow velocities sufficiently. In addition, it seems likely that transverse resistance gradients have helped to push the flow in Sagaing and Middle channels towards the outer bend. This analysis demonstrated that understanding the behavior of porcupines at the field edges, the range of hydrodynamic conditions the porcupines might experience, and in particular the burial of porcupines over time through scour or deposition are critical aspects that need to be understood and captured in short- and long-term numerical models of porcupine systems.

Next, two models were created to examine how porcupine resistance can be incorporated into large-scale 2D models. The best frameworks were found to be those developed for modelling vegetation resistance;

where vegetation is schematized as rigid cylinders; however, very limited data sets were tested. Data was not sufficient for calibration, let alone validation of the model. Therefore much further work will need to be done with expanded data sets to determine exactly how appropriate these frameworks are for modelling porcupine field impacts. Using the method of Baptist in a 1DH model will likely require adjusting the porcupine density compared to the value estimated from porcupine geometry, as this density had to be increased by a factor of 10 to calibrate the model. Additional studies should confirm this finding. The 1DH model results showed that the method of Baptist was able to reproduce water level changes induced by the porcupine field; however, it does not capture well the change in shear stress at the entrance of the porcupine field, nor the decreased shear stress just downstream of the porcupine field. Therefore, this model may be able to reproduce long-term morphological effects, however, caution should be used when interpreting results where local changes in morphology are concerned.

In 2DV, the Uittenbogaard rigid cylinder model performed reasonably well at replicating porcupine field behavior as a lower field density; however the model showed a lag in reproducing velocity and turbulence structures, related to the short distance of the flume porcupine field (as opposed to a field long enough for flow to fully develop). This suggests that the results may need to be used with caution for short fields. In addition, the model was not able to capture the increased shear stresses at the leading edge of the porcupine field, so the local morphological impacts were not all correctly reproduced. Finally, additional work is needed to confirm if the poor performance in reproducing the results of more dense porcupine fields is related to measurement error, or is a limitation of a model derived for the Uittenbogaard model in representing porcupines.

The insights gained from each of these Chapters has been synthesized into recommendations for porcupine field design, numerical modelling of porcupine fields, and the design of future experimental setups.

The design of porcupine fields must take into account the potential for the field to scour. This includes the density of the designed field and the potential for scour at the leading or trailing edges, as well as location within the channel (high energy or low energy areas). Design alternatives have been proposed for the porcupine system or individual porcupines that address potential performance issues including scour and transverse pressure gradients.

Numerical modeling of long-term performance of porcupine systems will require some special considerations. The models must taken into account burial of porcupines, either through scour or deposition. In addition, parameterization of porcupines needs careful consideration. In 2DV the rigid cylinder model performed well with calculations that directly transformed porcupine beams into cylinders; however the method of Baptist, which uses nearly identical parameters, needed to be multiplied by a factor of 10, as discussed above. The data available for this study was not sufficient to elaborate firm conclusions, therefore, further studies are needed to confirm the optimal parameterization of porcupines when using the rigid cylinder or Baptist resistance models. Finally, the models developed in this thesis were not able to capture the details of the flow response to the porcupine fields in transition areas, Therefore, caution needs to be taken when interpreting model results for potential local morphological responses.

Finally, this thesis identified several considerations related to the design of future experimental setups that will aid in improving numerical models of porcupine fields. First, existing studies show that there is a lack of measurements taken from within the porcupine field, and in particular at the leading edge of the porcupine field. Measurements in these locations will help to improve our ability to predict potential scour of porcupines at the leading edge. When taking measurements from within the porcupine field, multiple measurement across the transverse direction should be averaged, as the velocity within the field will be highly heterogeneous. These measurements can help us understand under what conditions porcupine fields behave as 'sparse' or 'dense', and in verifying that the model is able to correctly reproduce the response. In addition, The following section elaborates suggestions for critical data gaps identified by this thesis and suggestions for expanding the work performed here.

7.2 Recommendations for Future Work

The primary data gap identified in this study related to effectively designing and accurately modelling porcupine systems is understanding how porcupines become buried, including their response to scour, and under what conditions burial or scour may negatively influence design objectives. Criteria need to

be developed for how a morphological model of porcupine systems can be updated to effectively take into account the decrease, or increase in porcupine field density over time with burial and re-emergence of porcupines.

The second data gap related to effectively designing and modelling porcupine systems is understanding when porcupine fields exhibit sparse or dense behavior, and what the optimal balance is between increased density (increased resistance), and potential for increased scour or sinking, as well as potential recommendations for maintenance.

The key to improving numerical models of porcupine systems is additional experimental data; in particular carefully-measured flume data that can be used for model calibration and validation; however, these studies must include collection of the key data points mentioned earlier, to maximize their utility.

This thesis has largely focused on short-term impacts of porcupine systems to hydrodynamics and morphology. Further studies are needed to examine the potential long-term morphological impacts of porcupine systems, which could be different from the initial morphological responses observed here.

I have proposed several alternatives to porcupine field designs that may address considerations revealed during the pilot study analysis, including the issue of leading porcupines that sink into the bed, and transverse resistance gradients that might push water into undesired areas. These alternatives, and others, can be analyzed further for feasibility.

Much more work can be done in examining optimal configuration of porcupine fields, including field density, staggering, and orientation, as well as exploring options of distributed patches versus one large field across the channel width.

The design of individual porcupines can be explored further. I have proposed two design alternatives that might increase the density of the field while reducing risk of sour. These options, or others could be considered for feasibility and potential performance compared to the 'traditional' design.

The porcupine system implemented in the Ayeyarwady River has a primary design of objective of raising upstream water levels to maintain discharge distributions; however porcupine systems can be implemented with other design objectives such as bank protection. In addition, porcupines could be used to simply encourage sedimentation in certain areas for habitat creation or channel control. Many possibilities of porcupine systems, and the implications for their design, can be explored.

Bibliography

[1] M Aamir and N Sharma. "Efficiency of triangular and prismatic Porcupines in capturing sediment". In: *Hydro 2015 International* December (2015), pp. 17–19.

[2] Mohammad Aamir and Nayan Sharma. "Riverbank protection with Porcupine systems: Development of rational design methodology". In: *ISH Journal of Hydraulic Engineering* 21.3 (2015), pp. 317–332. ISSN: 21643040. DOI: 10.1080/09715010.2015.1029544.

[3] Aronne Armanini. *Principles of river hydraulics*. 2018, pp. 1–217. ISBN: 9783319681016. DOI: 10.1007/978-3-319-68101-6.

[4] Denie C M Augustijn, F Huthoff, and E H Van Velzen. "Comparison of vegetation roughness descriptions". In: *Proceedings of River Flow 2008 - Fourth International Conference on Fluvial Hydraulics, 3-5 September 2008 Cesme, Turkey* (2008), p. 9.

[5] M J Baptist. "Modelling floodplain biogeomorphology". PhD thesis. Technische Universiteit Delft, 2005, p. 213. ISBN: 9040725829. DOI: ISBN90-407-2582-9.

[6] M. J. Baptist et al. "On inducing equations for vegetation resistance". In: *Journal of Hydraulic Research* 45.4 (2007), pp. 435–450. ISSN: 00221686. DOI: 10.1080/00221686.2007.9521778.

[7] Sean J. Bennett et al. "Modeling fluvial response to in-stream woody vegetation: implications for strea corridor restoration". In: *Earth Surface Processes and Landforms* 33.890-909 (2008).

[8] T J Bouma et al. "Spatial flow and sedimentation patterns within patches of epibenthic structures: Combining field, flume and modelling experiments". In: *Continental Shelf Research* 27.8 (2007), pp. 1020–1045. ISSN: 02784343. DOI: 10.1016/j.csr.2005.12.019.

[9] Glenn O. Brown. "The history of the Darcy-Weisbach equation for pipe flow resistance". In: *Proceedings of the Environmental and Water Resources History* 40650.January (2002), pp. 34–43. DOI: 10.1061/40650(2003)4.

[10] Central Water Commision. *Handbook for Flood Protection, Anti Erosion and River Training Works*. New Delhi: Central Government of India, Flood Management Organization, 2010.

[11] Nian Sheng Cheng. "Representative roughness height of submerged vegetation". In: *Water Resources Research* 47.8 (2011), pp. 1–18. ISSN: 00431397. DOI: 10.1029/2011WR010590.

[12] Nian Sheng Cheng and Hoai Thanh Nguyen. "Hydraulic radius for evaluating resistance induced by simulated emergent vegetation in open-channel flows". In: *Journal of Hydraulic Engineering* 137.9 (2011), pp. 995–1004. ISSN: 07339429. DOI: 10.1061/(ASCE)HY.1943-7900.0000377.

[13] Ven Te Chow. *Open-Channel Hydraulics*. McGraw-Hill Book Company, Inc., 1959. ISBN: 07-010776-9.

[14] C.F. Colebrook and M. White. "Experiments with fluid friction in roughened pipes". In: *Proceedings of the Royal Society of London. Series A - Mathematical and Physical Sciences* 161.906 (1937), pp. 367–381. ISSN: 0080-4630. DOI: 10.1098/rspa.1937.0150.

[15] Deltares. *3D/2D modelling suite for integral water solutions: Delft3D Hydro-Morphodynamics User Manual*. Tech. rep. Version 11 March 2020, 2020.

[16] Maruf Dustegir et al. "Flow and sediment process around bandal like semi-permeable structure: A case study along a reach of the braided Jamua River in Kazipur". In: *7th Annual Conference on Water and Flood Management-ICWFM*. March. 2019.

[17] DWIR (Directorate of Water Resources and Improvement of River). *Myanmar Ayeyarwady Integrated River Basin Management Project: Draft Environmental and Social Management Framework*. Tech. rep. August. 2014.

[18] Family Nest Company Limited. *Final Report: Project Completion Report - The Project for Ayeyarwady Integrated River Basin Management Project Hydraulic Structure for Sub-Project 1 CW3.3 in Republic of the Unions of Myanmar*. Tech. rep. 2020.

[19] Mark S. Fonseca et al. "The role of current velocity in structuring eelgrass (Zostera marina L.) meadows". In: *Estuarine, Coastal and Shelf Science* 17.4 (1983), pp. 367–380. ISSN: 02727714. DOI: 10.1016/0272-7714(83)90123-3.

[20] Alida Galema. "Vegetation Resistance. Evaluation of vegetation resistance descriptors for flood management". In: October (2009), p. 113.

[21] Zhu Gao et al. "Three-dimensional hydrodynamic model of concrete tetrahedral frame revetments". In: *Journal of Marine Science and Application* 8.4 (2009), pp. 338–342. ISSN: 1671-9433. DOI: 10.1007/s11804-009-8092-2.

[22] Fredrik Huthoff, Denie C M Augustijn, and Suzanne J M H Hulscher. "Analytical solution of the depth-averaged flow velocity in case of submerged rigid cylindrical vegetation". In: *Water Resources Research* 43.6 (2007), pp. 1–10. ISSN: 00431397. DOI: 10.1029/2006WR005625.

[23] Bretagne Hygelund and Michael Manga. "Field measurements of drag coefficients for model large woody debris". In: *Geomorphology* 51.1-3 (2003), pp. 175–185. ISSN: 0169555X. DOI: 10.1016/S0169-555X(02)00335-5.

[24] Deliverable Iii and Frans Hamer. "Protocols for scaling morphodynamics in time Public". In: 654110 (2019), pp. 1–71. DOI: 10.5281/zenodo.2420824.

[25] J de Jonge. "Modelling the influence of vegetation on the morphodynamics of the river Allier". In: September (2005), 104 pp.

[26] Hyung Suk Kim, Ichiro Kimura, and Yasuyuki Shimizu. "Bed morphological changes around a finite patch of vegetation". In: *Earth Surface Processes and Landforms* 40.3 (2015), pp. 375–388. ISSN: 10969837. DOI: 10.1002/esp.3639.

[27] D. Klopstra et al. "Analytical model for hydraulic roughness of submerged vegetation". In: *Proceedings, Congress of the International Association of Hydraulic Research, IAHR* A.January 1997 (1997), pp. 775–780.

[28] Peter Van De Kreeke et al. "Report AIRBM - Component 3 , Engineering , Design , Capacity Building and Construction Supervision for Sub- Project 1". In: 1.February (2018).

[29] Lynn A Leonard and Alexander L Croft. "The effect of standing biomass on flow velocity and turbulence in Spartina alterniflora canopies". In: *Estuarine, Coastal and Shelf Science* 69.3-4 (2006), pp. 325–336. ISSN: 02727714. DOI: 10.1016/j.ecss.2006.05.004.

[30] D Ligthart. *The physical processes influencing morphodynamics in braided rivers*. Tech. rep. 2017.

[31] D. Liu et al. "An experimental study of flow through rigid vegetation". In: *Journal of Geophysical Research: Earth Surface* 113.4 (2008), pp. 1–16. ISSN: 21699011. DOI: 10.1029/2008JF001042.

[32] Fabian Lopez and Marcelo Garcia. "Open-channel flow through simulated vegetation: Suspended sediment transport modeling". In: *Water Resources* 34.9 (1998), pp. 2341–2352.

[33] Fabián López and Marcelo García. "Open-channel flow through simulated vegetation: Turbulence Modeling and Sediment Transport". In: *Wetlands Research Program (US)* August (1998), p. 123.

[34] Jau Yau Lu et al. "Turbulence characteristics of flows passing through a tetrahedron frame in a smooth open-channel". In: *Advances in Water Resources* 34.6 (2011), pp. 718–730. ISSN: 03091708. DOI: 10.1016/j.advwatres.2011.03.003.

[35] Mitul Luhar and Heidi M. Nepf. "From the blade scale to the reach scale: A characterization of aquatic vegetative drag". In: *Advances in Water Resources* 51 (2013), pp. 305–316. ISSN: 03091708. DOI: 10.1016/j.advwatres.2012.02.002. URL: http://dx.doi.org/10.1016/j.advwatres.2012.02.002.

[36] Mitul Luhar, Jeffrey Rominger, and Heidi Nepf. "Interaction between flow, transport and vegetation spatial structure". In: *Environmental Fluid Mechanics* 8.5-6 (2008), pp. 423–439. ISSN: 15677419. DOI: 10.1007/s10652-008-9080-9.

[37] Bruce Melville. "The physics of local scour at bridge piers". In: *Proceedings of the 4th International Conference on Scour and Erosion* 1 (2008), pp. 28–40.

[38] Bruce W. Melville and Arved J. Raudkivi. "Flow Characteristics in Local Scour at Bridge Peirs". In: *Journal of Hydraulic Research* 15.4 (1977), pp. 373–380. ISSN: 00221686. DOI: 10.1080/00221687709499641.

[39] Erik Mosselman. "Morphological development of side channels". In: *CFR Project Report (Netherlands)* August (2001). DOI: 10.13140/RG.2.1.3384.4960. URL: http://agris.fao.org/agris-search/search/display.do?f=./2003/v2904/NL2003000133.xml;NL2003000133.

[40] H. Nakagawa et al. "Hydraulic characteristics of typical bank-protection works along the Brahmaputra/Jamuna River, Bangladesh". In: *Journal of Flood Risk Management* 6.4 (2013), pp. 345–359. ISSN: 1753318X. DOI: 10.1111/jfr3.12021.

[41] V. S. Neary et al. "Effects of Vegetation on Turbulence, Sediment Transport, and Stream Morphology". In: *Journal of Hydraulic Engineering* 138.9 (2012), pp. 765–776. ISSN: 0733-9429. DOI: 10.1061/(asce)hy.1943-7900.0000168.

[42] H. M. Nepf. *Flow Over and Through Biota*. Vol. 2. January 2012. 2012, pp. 267–288. ISBN: 9780080878850. DOI: 10.1016/B978-0-12-374711-2.00213-8.

[43] Heidi M Nepf. "Flow and Transport in Regions with Aquatic Vegetation". In: *Annual Review of Fluid Mechanics* 44.1 (2012), pp. 123–142. ISSN: 0066-4189. DOI: 10.1146/annurev-fluid-120710-101048.

[44] Heidi M Nepf and Evamaria W Koch. "Vertical secondary flows in submersed plant-like arrays". In: *Limnology and Oceanography* 44.4 (1999), pp. 1072–1080. ISSN: 00243590. DOI: 10.4319/lo.1999.44.4.1072.

[45] Heidi M. Nepf. "Hydrodynamics of vegetated channels". In: *Journal of Hydraulic Research* 50.3 (2012), pp. 262–279. ISSN: 00221686. DOI: 10.1080/00221686.2012.696559.

[46] G.E. Nientker. *Porcupines for river training: A study on the near-field effects of porcupines*. Tech. rep. Delft University of Technology, 2018.

[47] Vladimir Nikora et al. "Spatially averaged flows over mobile rough beds: Definitions, averaging theorems, and conservation equations". In: *Journal of Hydraulic Engineering* 139.8 (2013), pp. 803–811. ISSN: 07339429. DOI: 10.1061/(ASCE)HY.1943-7900.0000738.

[48] J. Nikuradse. "Untersuchungen über turbulente Strömungen in nicht kreisförmigen Rohren". In: *Ingenieur-Archiv* 1.3 (1930), pp. 306–332. ISSN: 00201154. DOI: 10.1007/BF02079937.

[49] Arnel T. Oberez. *Turbulence modelling of hydraulic roughness of submerged vegetation*. 2001.

[50] Wataru Ohira et al. "Mangrove stilt root morphology modeling for estimating hydraulic drag in tsunami inundation simulation". In: *Trees - Structure and Function* 27.1 (2013), pp. 141–148. ISSN: 09311890. DOI: 10.1007/s00468-012-0782-8.

[51] J. Peakall, P. Ashworth, and J. Best. "Physical Modelling in Fluvial Geomorphology: Principles, Applications and Unresolved Issues". In: *The Scientific Nature of Geomorphology: Proceedings of teh 27th Bighamton Symposium in Geomorphology*. 1996.

[52] Ana M. Ricardo et al. "Turbulent flow within a random array of rigid, emergent stems: Laboratory characterization of the drag coefficient". In: *Proceedings of 35th ...* June 2013 (2013). URL: http://infoscience.epfl.ch/record/188588.

[53] Jeffrey T Rominger, Anne F Lightbody, and Heidi M Nepf. "Effects of added vegetation on sand bar stability and stream hydrodynamics". In: *Journal of Hydraulic Engineering* 136.12 (2010), pp. 994–1002. ISSN: 07339429. DOI: 10.1061/(ASCE)HY.1943-7900.0000215.

[54] Jeffrey T. Rominger and Heidi M. Nepf. "Flow adjustment and interior flow associated with a rectangular porous obstruction". In: *Journal of Fluid Mechanics* 680 (2011), pp. 636–659. ISSN: 00221120. DOI: 10.1017/jfm.2011.199.

[55] Gerrit J. Schieeck and Henk Jan Verhangen. *Introdcution to Bed Bank and Shore Protection*. 2nd Editio. Delft Academic Press, VSSD, 2019.

[56] Qian Qian Shang, Hui Xu, and Guo Bin Li. "Overview of research on the influence of permeable structures". In: *Applied Mechanics and Materials* 405-408 (2013), pp. 2115–2122. ISSN: 16609336. DOI: 10.4028/www.scientific.net/AMM.405-408.2115.

[57] R. G. Sharpe and C. S. James. "Deposition of sediment from suspension in emergent vegetation". In: *Water SA* 32.2 (2006), pp. 211–218. ISSN: 03784738. DOI: 10.4314/wsa.v32i2.5244.

[58] Jie Shi, Xiaolei Zhang, and Zunxin Huang. "Experimental research on preventing root-stones loss with tetrahedron-like concrete penetrating frames". In: *Advanced Materials Research* 233-235 (2011), pp. 1930–1934. ISSN: 10226680. DOI: 10.4028/www.scientific.net/AMR.233-235.1930.

[59] Dimitris Souliotis and Panayotis Prinos. "Effect of a vegetation patch on turbulent channel flow". In: *Journal of Hydraulic Research* 49.2 (2011), pp. 157–167. ISSN: 00221686. DOI: 10.1080/00221686.2011.557258.

[60] Brian M. Stone and Hung Tao Shen. "Hydraulic resistance of flow in channels with cylindrical roughness". In: *Journal of Hydraulic Engineering* 128.5 (2002), pp. 500–506. ISSN: 07339429. DOI: 10.1061/(ASCE)0733-9429(2002)128:5(500).

[61] Hong Wu TANG et al. "Protection of bridge piers against scouring with tetrahedral frames". In: *International Journal of Sediment Research* 24.4 (2009), pp. 385–399. ISSN: 10016279. DOI: 10.1016/S1001-6279(10)60012-1. URL: http://dx.doi.org/10.1016/S1001-6279(10)60012-1.

[62] Yukie Tanino and Heidi M Nepf. "Lateral dispersion in random cylinder arrays at high Reynolds number". In: *Journal of Fluid Mechanics* 600 (2008), pp. 339–371. ISSN: 00221120. DOI: 10.1017/S0022112008000505.

[63] S Temmerman et al. "Impact of vegetation on flow routing and sedimentation patterns: Three-dimensional modeling for a tidal marsh". In: *Journal of Geophysical Research: Earth Surface* 110.4 (2005), pp. 1–18. ISSN: 21699011. DOI: 10.1029/2005JF000301.

[64] Rob Uittenbogaard. *Modelling Turbulence in Vegetated Aquatic Flows*. 2003.

[65] Javier Rodriguez Uthurburu. *Evaluation of physically based and evolutionary data mining approaches for modelling resistance due to vegetation in SOBEK 1D-2D*. Tech. rep. Delft, The Netherlands: UNESCO-IHE Institute for Water Education, 2004.

[66] Andres Vargas-Luna, Alessandra Crosato, and Wim S J Uijttewaal. "State of Science Effects of vegetation on flow and sediment transport : comparative analyses and validation of predicting models". In: 176 (2015), pp. 157–176. DOI: 10.1002/esp.3633.

[67] Andrés Vargas-Luna et al. "Representing plants as rigid cylinders in experiments and models". In: *Advances in Water Resources* 93 (2016), pp. 205–222. ISSN: 03091708. DOI: 10.1016/j.advwatres.2015.10.004.

[68] E.H. van Velzen et al. *Fluid resistance due to vegetation in floodplains Part 1 (Dutch: Stromingsweerstand vegetatie in uiterwaarden - Deel 1)*. Tech. rep. Arnhem: RIZA rapport 2003.2028, 2003.

[69] Nicholas P Wallerstein et al. "Distorted froude-scaled flume analysis of large woody debris". In: *Earth Surface Processes and Landforms* 26.12 (2001), pp. 1265–1283. ISSN: 01979337. DOI: 10.1002/esp.271.

[70] Jia Mei Wang et al. "Bed morphology around various solid and flexible grade control structures in an unstable gravel-bed river". In: *Water (Switzerland)* 10.7 (2018). ISSN: 20734441. DOI: 10.3390/w10070822.

[71] Jia Mei Wang et al. "The effect of tetrahedron framed permeable weirs on river bed stability in a mountainous area under clear water conditions". In: *Scientific Reports* 7.1 (2017), pp. 1–14. ISSN: 20452322. DOI: 10.1038/s41598-017-04711-8.

[72] Pingyi Wang et al. "Effects of the central bar protection with tetrahedron-like penetrating frames". In: *Procedia Engineering* 28.2011 (2012), pp. 389–393. ISSN: 18777058. DOI: 10.1016/j.proeng.2012.01.738. URL: http://dx.doi.org/10.1016/j.proeng.2012.01.738.

[73] Shaohua Wang et al. "Effect of inclination angles on the local scour around a submerged cylinder". In: *Water (Switzerland)* 12.10 (2020), pp. 1–20. ISSN: 20734441. DOI: 10.3390/w12102687.

[74] Wei jie Wang et al. "Roughness height of submerged vegetation in flow based on spatial structure". In: *Journal of Hydrodynamics* 30.4 (2018), pp. 754–757. ISSN: 18780342. DOI: 10.1007/s42241-018-0060-3.

[75] Catherine Wilson, T Stoesser, and Paul D Bates. "Modelling of Open Channel Flow through Vegetation". In: *Computational Fluid Dynamics: Applications in Environmental Hydraulics* (2005), pp. 395–428. DOI: 10.1002/0470015195.ch15.

[76] World Bank. "Project Appraisal Document on a Proposed Credit in the Amount of SDR 67.5 Million to the Republic of the Union of Myanmar For a Ayeyarwady Integrated River Basin Management Project". In: *Report No. PAD987* (2014). ISSN: 00034983. DOI: 10.1179/136485908X337463.

[77] Weiming WU and Zhiguo HE. "Effects of vegetation on flow conveyance and sediment transport capacity". In: *International Journal of Sediment Research* 24.3 (2009), pp. 247–259. ISSN: 10016279. DOI: 10.1016/S1001-6279(10)60001-7. URL: http://dx.doi.org/10.1016/S1001-6279(10)60001-7.

[78] E. M. Yager and M. W. Schmeeckle. "The influence of vegetation on turbulence and bed load transport". In: *Journal of Geophysical Research: Earth Surface* 118.3 (2013), pp. 1585–1601. ISSN: 21699011. DOI: 10.1002/jgrf.20085.

[79] Judy Q. Yang, Francois Kerger, and Heidi M. Nepf. "Estimation of the bed shear stress in vegetated and bare channels with smooth beds". In: *Water Resources Research* 51.5 (2015), pp. 3647–3663. ISSN: 19447973. DOI: 10.1002/2014WR016042.

[80] Wonjun Yang and Sung Uk Choi. "A two-layer approach for depth-limited open-channel flows with submerged vegetation". In: *Journal of Hydraulic Research* 48.4 (2010), pp. 466–475. ISSN: 00221686. DOI: 10.1080/00221686.2010.491649.

[81] Zhonghua Yang et al. "Experimental Investigation of Flow over a Tetrahedron Penetrating Frame with PIV". In: *Proceedings of 2013 IAHR World Congress* September (2013).

[82] Tao Yu et al. "Study on the beach protection with the tetrahedron like penetrating frame groups". In: *Applied Mechanics and Materials* 90-93 (2011), pp. 2533–2536. ISSN: 16609336. DOI: 10.4028/www.scientific.net/AMM.90-93.2533.

[83] Lijun Zong and Heidi Nepf. "Flow and deposition in and around a finite patch of vegetation". In: *Geomorphology* 116.3-4 (2010), pp. 363–372. ISSN: 0169555X. DOI: 10.1016/j.geomorph.2009.11.020. URL: http://dx.doi.org/10.1016/j.geomorph.2009.11.020.

[84] Lijun Zong and Heidi Nepf. "Spatial distribution of deposition within a patch of vegetation". In: *Water Resources Research* 47.3 (2011), pp. 1–12. ISSN: 00431397. DOI: 10.1029/2010WR009516.

Appendix A

Scaling Analysis for Numerical Model Setup

To avoid complications from numerical constraints of Delft3D-Flow, the 2018 porcupine flume study was scaled by a factor of 10 for implementation in Delft3D. Scaling of fluid flows for the fixed-bed experiments will be described first, followed by scaling of sediment transport processes for the mobile-bed experiments.

A.1 Fixed-Bed Experiments

Scaling of fluid flows must meet three kinds of similarities for the flows to be equivalent: kinematic, dynamic and geometric similitude. For fluid flows, these three conditions will be met when both the Reynolds number (Equation A.1) and the Froude number (Equation A.2) are the same for both the experiment (physical flume model) and the numerical model are the same [51].

$$\mathrm{Re} = \frac{\rho u l}{\mu} = \frac{u l}{\nu} \tag{A.1}$$

Where,

u = velocity

l = characteristic length (porcupine beam width - b)

ρ = fluid density

μ = dynamic viscosity

ν = kinematic viscosity

$$Fr = \frac{u}{\sqrt{gh}} \tag{A.2}$$

Where h is the water depth. It is well-known that in scaling fluid flows that the Froude number and Reynolds cannot both be scaled to similarity if the same fluid (water) is used. The Reynolds number is generally considered less sensitive than the Froude number, and Froude number similarity has been considered the priority [69]. Fortunately, the properties of the fluid can be changed in the numerical model, so we can mimic using a fluid that is 'dissimilar' to water to achieve similarity of both the Reynolds and Froude numbers.

Table A.1 gives the parameters of the model experiment, including the boundary condition (discharge [Q], water depth[h] and characteristic velocity [u]) and the associated Reynolds and Froude numbers. The

flume dimensions are given by the length (L_f) and width (B_f). The porcupine characteristics include the length of the beams (L_p), the effective assembled height (s), the beam width, the longitudinal and cross-sectional spacing (ΔS_x and ΔS_y, respectively), as well as the porcupine field length (L), the roughness density (λ) and the submergence ration (h/s). Finally, the fluid parameters are given as the density (ρ), molecular dynamic and kinematic viscosity, and the background viscosity ($\nu_{background}$) is a numerical parameter.

To scale the model experiment, all physical length scales were scaled by a multiple of 10: h, L_f, B, L_p, b, ΔS_x, ΔS_y and L. Then, the velocity was varied until the Froude numbers for the flume and model experiments matched. This adjusted the discharge. Finally, the Reynolds number was matched by scaling the molecular viscosity. The molecular viscosity cannot be changed in Delft3D-flow, however the background eddy viscosity is a combination of the molecular kinematic viscosity, the viscosity computed by the $k - \epsilon$ turbulence model, and a user-specified background viscosity. Therefore, the molecular viscosity was subtracted from the total viscosity required, and the remaining viscosity was set as the user-specified background viscosity ($\nu_{background}$). The final scaled parameters used as input for the model are show in in Table A.2.

A.2 Mobile-Bed Experiments

A number of dimensionless parameters must be similar to accurately scale sediment movement. For the numerical models considered in this study, a 'best' scaling approach was used [24], which is equivalent to a Froude-number scaled model for sediment transport. The geometric ratios are maintained between the flume experiment and the numerical model, as well as the ratio of sediment density; however the particle-Reynolds number and fall velocity (Rousse number) ratios are relaxed. The conserved ratios are the shields-number (Equation A.3), the relative sediment density (Equation A.4), and the relative submergence (Equation A.5). Non-conserved properties are the Reynolds particle number (Equation A.6), and the Rousse number (or relative fall speed, Equation A.7) [24]. The subscript r indicates the ratio between the model (flume experiment) and the prototype (numerical model).

$$Fr_{*r} = \frac{u_{*r}^2}{(\rho_s - \rho_w)_r \, d_{50,r}} = 1 \tag{A.3}$$

Where,

Fr_* = shields number (densimetric Froude number)

u_* = shear velocity

ρ_s = sediment density

ρ_w = water density

ρ_s = sediment density

ρ_w = water density

d_{50} = mean sediment diameter (50% passing)

$$\rho_{s,r} = 1 \tag{A.4}$$

$$\frac{h_r}{d_r} = 1 \tag{A.5}$$

$$Re_{*_r} = d_{50,r} u_{*_r} = 1 \tag{A.6}$$

Where,

Re_* = Reynolds particle number

$$Rou_{*_r} = \frac{\nu_{s,r}}{u_{*,r}} = 1 \tag{A.7}$$

Where,

Rou_* = Rousse number

ν_s = molecular kinematic viscosity

Geometrically, the numerical model was scaled by a factor of 10 from the flume experiment. The flow parameters were scaled using a non-distorted Froude scale as in the fixed-bed numerical model described above. Considering the conservation of the above ratios, for the same sediment density used in the flume experiment (ρ_s=2600 kg/m^3), the ratios will be maintained as long as the sediment diameter (d_{50}) is increased by the same ratio used for the geometric scaling (10). This results in an experiment where the sheilds number (densimetric Froude number) ratio is conserved, and the particle Reynolds number ratio is nearly conserved. The original flume experiment and scaled numerical model parameters are given in Tables A.3 and A.4 respectively.

Finally, the last scaling item to consider is the time scale of morphological processes, which need to be scaled up with the model. A number of time scales are involved in morphological processes, including the initiation of motion of an individual grain, the movement of grains and the transport rate of sediment [24]. For this model, the time scale we are interested in conserving is the dimensionless transport rate. Since the sediment movement is scaled by maintaining the Sheilds number, the time-scale ratio in Equation A.8 was selected for the time-scaling of this model [].

$$t_{\eta,r} = L_r h_r^{1.5} d_{50,r}^{-7/6} (1-\phi)_r \tag{A.8}$$

Where,

t_η = time scale for vertical bed movement

L = length scale

ϕ = porosity

The numerical model has a length scale, water depth and d_{50} ratio of 10, and a $(1-\phi)$ ratio of 1. Therefore the numerical model should be run 21 times longer than the flume experiment for similarity in the bed evolution.

Run	Flow					Flume		Porcupines								Fluid				
	h [m]	Q [m^3/s]	u [m/s]	Fr [-]	Re [-]	L_f [m]	B [m]	L_p [m]	s [m]	b [mm]	ΔS_x [m]	ΔS_y [m]	L [m]	λ_p [-]	h/s [-]	ρ_w [kg/m^3]	$\mu_{molecular}$ [$Pa \cdot s$]	ν_{total} [m^2/s]	$\nu_{molecular}$ [m^2/s]	$\nu_{background}$ [m^2/s]
9	0.173	0.033	0.23	0.18	1,642	12	0.8	0.1	0.082	7	0.1	0.1	0.5	0.84	2.1	1000	1.001E-03	1.001E-06	1.001E-06	na
13	0.173	0.033	0.23	0.18	1,644	12	0.8	0.1	0.082	7	0.14	0.1	0.7	0.17	2.1	1000	1.001E-03	1.001E-06	1.001E-06	na

Table A.1: Fixed-Bed Flume Experiment Parameters

Run	Flow					Flume		Porcupines								Fluid				
	h [m]	Q [m^3/s]	u [m/s]	Fr [-]	Re [-]	L_f [m]	B [m]	L_p [m]	s [m]	b [mm]	ΔS_x [m]	ΔS_y [m]	L [m]	λ_p [-]	h/s [-]	ρ_w [kg/m^3]	$\mu_{molecular}$ [$Pa \cdot s$]	ν_{total} [m^2/s]	$\nu_{molecular}$ [m^2/s]	$\nu_{background}$ [m^2/s]
9	1.73	10.242	0.74	0.18	1,642	120	8	1	0.82	70	1.0	1.0	5	0.84	2.1	1000	3.155E-02	3.155E-05	1.001E-06	3.05E-05
13	1.73	10.242	0.74	0.18	1,644	120	8	1	0.82	70	1.4	1.0	7	0.17	2.1	1000	3.151E-02	3.151E-05	1.001E-06	3.05E-05

Table A.2: Fixed-Bed Scaled Model Parameters

Run	Flow					Flume		Porcupines								Fluid					Sediment
	h [m]	Q [m^3/s]	u [m/s]	Fr [-]	Re [-]	L_f [m]	B [m]	L_p [m]	s [m]	b [mm]	ΔS_x [m]	ΔS_y [m]	L [m]	λ_p [-]	h/s [-]	ρ_w [kg/m^3]	$\mu_{molecular}$ [$Pa \cdot s$]	ν_{total} [m^2/s]	$\nu_{molecular}$ [m^2/s]	$\nu_{background}$ [m^2/s]	d_{50} [μm]
2	0.165	0.0325	0.25	0.19	1,726	12	0.8	0.1	0.082	7	0.1	0.1	0.5	0.84	2.0	1000	1.000E+03	1.00E-03	1.001E-06	na	260
4	0.178	0.0325	0.23	0.17	1,592	12	0.8	0.1	0.082	7	0.14	0.1	0.7	0.17	2.2	1000	1.000E+03	1.00E-03	1.001E-06	na	260

Table A.3: Mobile-Bed Flume Experiment Parameters

Run	Flow					Flume		Porcupines								Fluid					Sediment
	h [m]	Q [m^3/s]	u [m/s]	Fr [-]	Re [-]	L_f [m]	B [m]	L_p [m]	s [m]	b [mm]	ΔS_x [m]	ΔS_y [m]	L [m]	λ_p [-]	h/s [-]	ρ_w [kg/m^3]	$\mu_{molecular}$ [$Pa \cdot s$]	ν_{total} [m^2/s]	$\nu_{molecular}$ [m^2/s]	$\nu_{background}$ [m^2/s]	d_{50} [μm]
2	1.65	10.09	0.76	0.19	1,726	120	8	1	0.82	70	1	1	5	0.84	2.0	1000	3.100E-02	3.10E-05	1.001E-06	3.000E-05	2600
4	1.78	10.12	0.71	0.17	1,592	120	8	1	0.82	70	1.4	1	7	0.17	2.2	1000	3.124E-02	3.12E-05	1.001E-06	3.024E-05	2600

Table A.4: Mobile-Bed Scaled Model Parameters

Appendix B

Morphodynamic Modelling of Porcupine Systems

This study has focused on numerical modelling of the hydrodynamic impacts of porcupines. A preliminary analysis was carried out with a numerical model that examined the predicted morphological response of the bed to porcupines. The Nientker flume experiment ([46]) carried out both mobile-bed and fixed-bed experiments. Two 2DV mobile-bed experiments were reproduced in Delft3D, using the Uittenbogaard (2003) rigid cylinder approximation to represent porcupines. First, the two mobile-bed flume experiments replicated are described. Then, the numerical model setup, including deviations from the scaling analysis for the sediment transport are described. Finally, preliminary results of the analysis are presented. Ultimately, the flume data was not sufficient for calibration of the model, considering that the model does not correctly reproduce the sediment transport observed; however, why this occurs and next steps for improving the model are discussed.

B.1 Flume Experiment

Two mobile-bed experiments from the Nientker (2018) flume study were analyzed in this study: Runs 2 and 4 which correspond, approximately, to runs 9 and 13 used in the fixed-bed experiments. Runs 13 and 4 have a larger density, or longitudinal porcupine spacing (λ= 0.2) than runs 9 and 2 (λ = 0.8). Table A.3 gives the primary experiment parameters.

The mobile-bed experiments used relatively uniform sediment with a d_{50} of 260 μm. The flume was filled with sand and water, and run for approximately 24 hours without porcupines to obtain an equilibrium bathymetry, which was measured before the porcupines were placed in the flume. Then the experiment was re-started with measurements (water level and bathymetry) carried out approximately every 24 hours, with an additional 5-hour measurement. The details of the experiment setup and measurements can be found in [46]. For this analysis, only the 24 hour bathymetry measurements are used.

B.2 Numerical Morphological Model

The setup of the numerical model is described as well as the input parameters for the sediment transport formulation and deviations from the calculated scaled parameters.

B.2.1 Model setup

A 2DV numerical model was created with Delft3D with additional parameters turned on for sediment transport and morphology. The Uittenbogaard (2003) rigid cylinder approximation was used to represent porcupines, using the same settings found when calibrating the respective fixed-bed experiment (fixed-bed run 9 for mobile-bed run 2, and fixed-bed run 13 for mobile-bed run 4).

The van Rijn (1984) sediment transport formula was used, as outlined in []. This formulation includes expressions for bedload and suspended load (Equation B.1).

$$S_b = \begin{cases} 0.053\sqrt{\Delta g d_{50}^3} D_*^{-0.3} T^{2.1} & \text{for } T < 3.0 \\ 0.1\sqrt{\Delta g d_{50}^3} D_*^{-0.3} T^{1.5} & \text{for } T \geq 3.0 \end{cases} \tag{B.1}$$

Where,

Δ = relative density: $(rho_s - \rho_w)/\rho_w$

d_{50} = mean sediment diameter

D_* = dimensionless particle parameter

T = dimensionless bead shear

The dimensionless bed shear is described as:

$$T = \frac{\mu_c \tau_{bc} - \tau_{bcr}}{\tau_{bcr}} \tag{B.2}$$

Where,

μ_c = efficiency factor current

τ_{bcr} = Shield's critical bed shear stress

τ_{bc} = shear stress (where $\mu_c \tau_{bc}$ is the effective shear stress)

The shear stresses are found from:

$$\tau_{bc} = \frac{1}{8} \rho_w f_{cb} q^2 \tag{B.3}$$

$$f_{cb} = \frac{0.24}{\left({}^{10}\log\left(12h/\xi_c\right)\right)^2} \tag{B.4}$$

$$\mu_c = \left(\frac{18^{10} \log\left(12h/\xi_c\right)}{C_{g,90}} \right)^2 \tag{B.5}$$

Where,

$C_{g,90}$ = grain related Chezy coefficient

$$C_{g,90} = 18^{10} \log\left(\frac{12h}{3D_{90}}\right) \tag{B.6}$$

The Shield's critical bed shear stress is written as:

$$\tau_{bcr} = \rho_w \Delta g D_{50} \theta_{cr} \tag{B.7}$$

Where θ_{cr} is the Sheilds parameter and D_* is found from:

$$D_* = D_{50} \left(\frac{\Delta g}{\nu^2} \right)^{\frac{1}{3}} \tag{B.8}$$

The suspended transport formula is described as:

$$S_s = f_{cs} q h C_a \tag{B.9}$$

Where,

C_a = reference concentration

q = depth-averaged velocity

h = water depth

f_{cs} = shape factor

The shape factor is approximated as:

$$f_{cs} = \begin{cases} f_0(z_c) & \text{if } z_c \neq 1.2 \\ f_1(z_c) & \text{if } z_c = 1.2 \end{cases} \tag{B.10}$$

$$f_0(z_c) = \frac{(\xi_c/h)^{z_c} - (\xi_c/h)^{1.2}}{(1-\xi_c/h)^{z_c}(1.2-z_c)} \tag{B.11}$$

$$f_1(z_c) = \left(\frac{\xi_c/h}{1-\xi_c/h}\right)^{1.2} \ln(\xi_c/h) \tag{B.12}$$

Where,

ξ_c = reference level (bedload layer thickness)

z_c = suspension number

$$z_c = \min\left(20, \frac{w_s}{\beta\kappa u_*} + \phi\right) \tag{B.13}$$

$$u_* = q\sqrt{\frac{f_{cb}}{8}} \tag{B.14}$$

$$\beta = \min\left(1.5, 1 + 2\left(\frac{w_s}{u_*}\right)^2\right) \tag{B.15}$$

$$\phi = 2.5\left(\frac{w_s}{u_*}\right)^{0.8}\left(\frac{C_a}{0.65}\right)^{0.4} \tag{B.16}$$

Finally, the C_a is calculated as:

$$C_a = 0.015\alpha_1 \frac{D_{50}}{\xi_c}\frac{T^{1.5}}{D_*^{0.3}} \tag{B.17}$$

Three parameters need to be specified in Delft3D for the van Rijn transport forumla: Aks (reference height), α (calibration parameter) and w_s (fall velocity). Aks was defined as 3xd_{50}. α was left as one. The fall velocity was calculated with Equation B.18.

$$w_s = \frac{10\nu}{d_{50}}\sqrt{1 + \left(\frac{0.01\Delta g d_{50}^3}{\nu^2}\right)} \tag{B.18}$$

The effect of suspended sediment on the fluid density was not taken into account. To minimize boundary effects the sand concentration at the upstream boundary is set to the equilibrium sand concentration one grid cell inside the boundary. A morphological acceleration factor of 12 was employed for computational efficiency. The model was run to simulate 24 hours of morphological development. Only one sediment transport formulation has been considered.

B.2.2 Scaling Deviations

To avoid numerical complications the flume experiment flow and transport characteristics were scaled by a factor of 10 (geometrically). The scaling analysis is described in detail in Appendix A. Certain deviations from the values calculated with the scaling analysis were required.

The sediment used in the flume experiment had a d_{50} of 260 μm. The scaled mean grain size became 2600 μm; however, it was found that this grain size was too large for initiation of motion. Therefore, a grain size of 2000 μm was used in the model, and the sediment density was reduced to $\rho_s = 2500$ kg/m^3. While the numerical model is not strictly scaled correctly, it is sufficient for an initial comparison of the flume experiment and numerical model results. As will be shown in the following section, the model could not be calibrated anyway, therefore the results can only be used for an initial comparison and additional scaling uncertainty at this stage can be tolerated. The final scaled model parameters are found in Table A.4.

B.3 Results

The cumulative sedimentation (final bathymetry level minus the original bathymetry level) after 24 hours are compared for the flume experiments and numerical models for runs 2 and 4 in Figures B.1 and B.2, respectively.

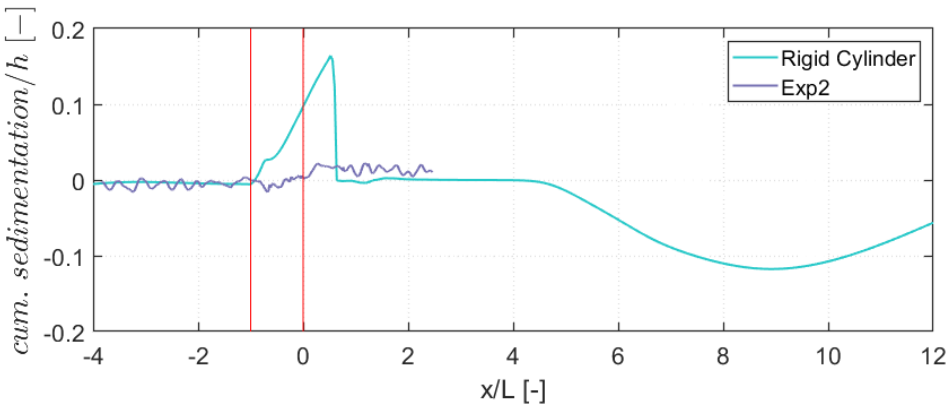

Figure B.1: More dense field (run 2): cumulative sedimentation over 24 hours (end bathymetry minus start bathymetry), normalized by the starting water depth (h=1.65 m). Red lines delineate porcupine field location. cum. = cumulative; L= length of porcupine field (5 m); x = 0 located at downstream end of porcupine field; Exp2: Experiment 2.

For run 2, the model predicts sedimentation in the porcupine field, that is moving downstream of the field, consistent with reduced velocities and bed shear stress found within the porcupine field in the fixed-bed numerical model. Downstream of the field, at a location of approximately x/L = 6-10, erosion is observed. This coincides with the location of increased turbulence in the rigid cylinder model. The flume experiment shows erosion at the leading edge of the porcupine field, deposition at the downstream edge of the field and downstream of the field.

For run 4, the model shows deposition within in the porcupine field and erosion a certain distance downstream of the field, similar to the results of experiment 2 but with reduced magnitudes, consistent with the lowered resistance offered by they less-dense porcupine field. The flume experiment showed deposition within and downstream of the porcupine field, and a small zone of erosion towards the end of the flume.

For both experiments, dunes that formed along the bed in the flume experiment are not reproduced by the model. In addition, the sinking of porcupines into the bed or changed submergence ratio of porcupines as they become buried are not taken into account in these models.

These models were not calibrated. First, the models do not reproduce the sedimentation hump behind

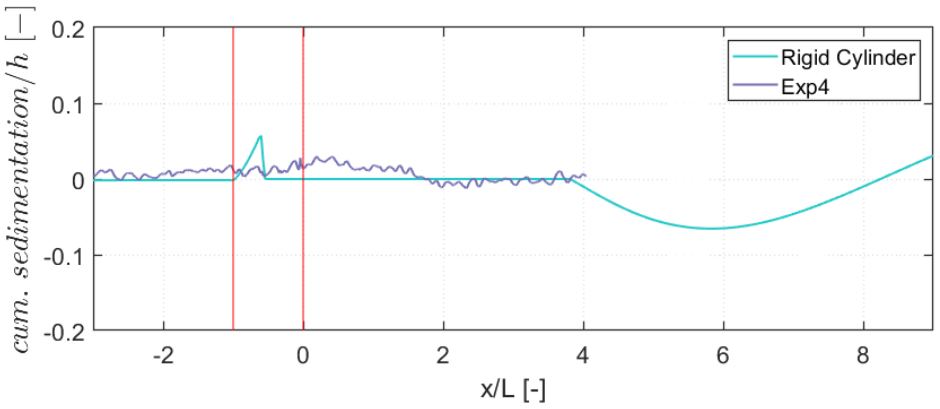

Figure B.2: More dense field (run 2): cumulative sedimentation over 24 hours (end bathymetry minus start bathymetry), normalized by the starting water depth (h=1.78 m). Red lines delineate porcupine field location. cum. = cumulative; L= length of porcupine field (7 m); x = 0 located at downstream end of porcupine field; Exp4: Experiment 4.

the porcupine field. Therefore, calibrating the model based on the celerity of the sedimentation wave is not possible. Calibrating the model based on velocity, water level and bed shear measurements, as was done for the fixed-bed models, was not possible either. The velocity measurements in the mobile-bed experiments had uncertainties largely due to the changing bed elevation under the ADV which lead to velocities being recorded at incorrect heights above the bed, resulting in imprecise velocity profiles and imprecise bed shear stress estimations. In addition, because the model is not reproducing the general pattern of erosion and sedimentation predicted by the flume experiment, the velocity profile and shear stressed predicted by the model will not match those measured by the model, even if precise measurements were available. Finally, because the model is not reproducing dunes along the bed, the bed roughness is underestimated and that is reflected in mis-matched water levels. Therefore, the results should be examined qualitatively, to understand the limitations of this model in predicting the morphological evolution of the bed in the presence of porcupines.

B.4 Discussion

The rigid cylinder vegetation model, while reproducing certain aspects of the hydrodynamics for the experiments examined in Chapter 5, is not able to reproduce shear stresses and turbulence in a way that accurately predicts erosion and sedimentation patterns within the porcupine field, particularly at the leading and trailing edge. This may not be a surprise given the limitation of the hydrodynamic predictions observed in Chapter 5.

However, certain aspects of the model have potential for improvement. As was noted in Chapter 5, the porcupine field studied is too short to allow the flow to fully develop. For the Uittenbogaard rigid cylinder model, a delay in turbulence generation was observed, consistent with findings of other studies using this model to represent short vegetation patches [59]. In Figures B.1 and B.2, this delayed turbulence increase leads to a zone of erosion downstream of the porcupine field, which was not observed in the flume experiment. Therefore, it should be explored if this model can provide useful predictions for longer porcupine fields, where the flow is fully-developed. In addition, the results of run suggest that the model may be capable of capturing deposition downstream of the porcupine field; however, more precise data from mobile-bed experiments would be needed to fully develop, calibrate and validate those models.

B.5 Conclusions and Limitations

Morphological development around a porcupine field was explored with a numerical model using the Uittenbogaard rigid cylinder approximation to represent porcupines. The results were compared against two mobile-bed flume experiments with more dense (experiment 2) and less-dense (experiment 4) porcupine

field. The model could not be calibrated due to insufficient data. Nevertheless, qualitatively, qualitatively, it can be observed that the the model does not reproduce the general erosion and sedimentation pattern observed in the flume experiments. However, part of the discrepancy could be due to attempting to represent a very short porcupine field. The model may provide more useful results for a longer field, where the flow and turbulence are fully-developed. Experimental data from mobile-bed experiments with longer porcupine field configurations would be needed to develop, calibrate and validate such models. At the same time, other modelling softwares, sediment transport formulations, or methods of parameterizing porcupines could all lead to more accurate models. Finally, any future morphological models must be able to take into account the porcupines potentially scouring and sinking into the bed, as well as the changing submergence ratio of porcupines as they become buried, to make accurate predictions of bed level changes.